

R&D6603-EE-03  
vm (2)

AD-A243 427



DTIC  
ELECTE  
DEC 6 1991  
S C D

INTERNATIONAL WORKSHOP ON :

**HYDROGEN MIGRATION AND THE  
STABILITY OF HYDROGEN RELATED  
COMPLEXES IN CRYSTALLINE  
SEMICONDUCTORS**

**HORBEN BEI FREIBURG**  
(FEDERAL REPUBLIC OF GERMANY)

3-6 NOVEMBER 1991

91 12 001

91-17158



## Hydrogen Diffusion in Crystalline Silicon: a First-Principles Molecular Dynamics simulation

Guido L. Chiarotti<sup>(a,b,c)</sup>

(a) *International School for Advanced Studies, 34014 Trieste, Italy*

(b) *Laboratorio TASC, INFN, 34012 Trieste, Italy*

(c) *Int'nal Centre for High Technology and New Materials, 34014 Trieste, Italy*

A detailed microscopic understanding of H diffusion in crystalline silicon, in addition to its interest *per se*, is a basic step to interpret technologically important H incorporation processes [1]. Much of the earlier theoretical effort on this subject has been devoted to study the energetically favoured sites for H at zero temperature on the basis of total energy calculations. In the most notable of these investigations [2] the fully relaxed adiabatic total energy surface for an isolated H impurity was parametrized for all H locations in the unit cell. One of the important results of this study is that  $H^+$  ( $H^0$ ) prefers to sit in regions of high valence charge density (HD) rather than in interstitial low density regions (LD). All the HD configurations are characterized by a large relaxation of the neighbouring Si atoms, in contrast to the LD configurations where only small distortions are induced. In agreement with experimental findings [3], the BC site is the lowest energy configuration. A low energy path connecting adjacent BC sites through the intermediate C [4] site can be traced, lying entirely in the HD region: this was indicated in Ref. [2] as the most likely diffusion path for H in the neutral or the positively charged state. An activation energy barrier less than 0.2 eV can be estimated along this path. In these earlier calculations no attempt was made to compute the diffusion coefficient. Therefore no direct comparison with diffusion experiments was possible.

H diffusion coefficients have been measured with various techniques. At high temperatures ( $T > 1000$  K), Van Wieringen and Warmoltz (VW) [5] found that H diffusion is characterized by a very high mobility ( $D \simeq 2 \times 10^{-4} \text{ cm}^2/\text{sec}$  at  $T \simeq 1470$  K) and a thermal activation barrier of 0.48 eV within a 10% error. At lower temperatures, DLTS spectra [6] of H passivation of deep levels led to estimates of the diffusion coefficient orders of magnitude lower than the Arrhenius extrapolation of the VW data. Recently, however, diffusivity data at low T have been presented [7, 8] that agree with the Arrhenius extrapolation of the VW results. These measurements confirm the high mobility of H in Si and suggest that a single Arrhenius behaviour can be

roughly traced from room up to high temperature ( $T > 1200$  K).

The absence of dynamical simulations, in earlier theoretical studies of H in silicon, can be traced to the difficulty to accurately represent the potential energy surface of the system. We have been able to overcome this difficulty using First Principle Molecular Dynamics [9]. We report here the main results of this investigation [10].

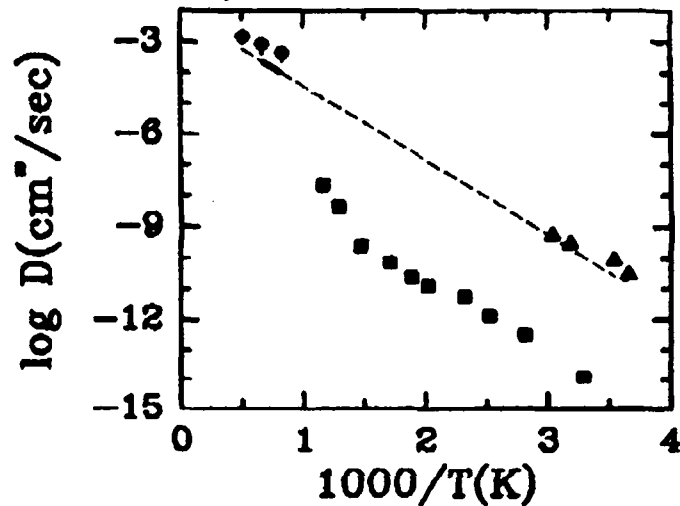


Figure 1: Diffusion coefficient for hydrogen in c-Si as a function of inverse temperature. Solid circles: present calculation for  $H^+$ . Error bars are indicated by vertical bars. Solid line:  $D = 9.41 \times 10^{-3} \exp(-0.48 \text{ eV}/k_B T) \text{ cm}^2 \text{ sec}^{-1}$  as obtained by VW (see text) in the temperature range  $1240 \div 1480$  K; extrapolation outside this range is given by the dashed line. Squares: experimental data from Ref. [6]. Triangles: experimental diffusivity values in Au Schottky barrier sample [7].

In our simulation we focused on  $H^+$  [10] in c-Si. This charge state has been argued to be the dominant one, at least in p-doped material, both experimentally [7, 8] and theoretically [2]. We used a periodically repeated FCC supercell containing 128 Si atoms and one proton. The details of the simulation are reported in ref. [10]. As explained there we have a very accurate description of the  $H^+$  energy surface, which is overall very similar to that of Ref. [2]. In particular, we recover the distinction between HD and LD regions in the  $T = 0$  total energy surface. We have performed several MD runs at different temperatures higher than 1000 K. At these temperatures an H impurity in silicon can travel distances of the order of several bond lengths during a time of few picoseconds. This allows to study the diffusion process with sufficient accuracy using MD techniques. In Fig. 1 we report our results for  $D$  at three different

temperatures, one of which would correspond to an overheated crystal. The agreement with the experimental VW data is remarkable, considering the uncertainties of both theory and experiment in addition to the fact that theory does not take into account presence of defects, possible molecular formation or other factors that could hinder the diffusion process.

An analysis of the diffusive path of the proton in the various MD runs reveals that the diffusion process proceeds via jumps between sites of high symmetry. Both high- and low-density regions are visited by the migrating particle, at variance with the predictions based on zero temperature calculations. More specifically we have detected, as the most likely, a path lying mostly in the HD region, connecting adjacent BC (or M [4]) sites, through tetrahedral (Td) site. In other segments of the trajectory, the proton has been instead observed to follow a path lying completely in the LD region. This path proceeds via jumps between near antibonding (AB) sites (about 1.6 Å from a Si atom) using Td or Hex as crossing sites. These two paths can alternate during the same simulation run and differs not only in the topology but also for the dynamical behaviour of the diffusing proton, as shown by the power spectra of the velocity-velocity correlation function of H [10]. Interestingly, the H diffusion coefficient is, within the error bars, essentially the same in the two paths.

The reason why the proton does not follow the strictly HD path resulting from  $T=0$  calculations, can be traced to the large difference in mass between H and Si. When the  $H^+$  motion is fast, as it is the case at these high temperatures, the heavy Si ions cannot follow adiabatically the proton. Thus the lattice may not have the time to undergo the large relaxation needed for the HD sites to become energetically favourable. When this happens the proton prefers to move through regions of low energy for the undistorted lattice.

Recently Blöchl et al. [11] used static total energy calculations to compute the H diffusion coefficient at any temperature, on the basis of a simplified rate theory approach. At high temperature their values are surprisingly in good agreement with the results of our MD simulations. Rate theory, in facts, neglects dynamical effects and is expected to be correct in the limit of low temperatures. However, the result of Blöchl et al. does not indicate that dynamical effects are not affecting the behaviour of H at high temperatures, but rather that dynamical effects do not appreciably modify the value of  $D$ . This is consistent with our finding that the two observed paths yield very similar diffusion coefficients.

## References

- [1] See, for instance, S. J. Pearton, J. W. Corbett and T. S. Shi, *Appl. Phys. A* **43**, 153 (1987).
- [2] C. G. Van de Walle, Y. Bar-Yam and S. T. Pantelides, *Phys. Rev. Lett.* **60**, 2761 (1988).
- [3] B. Bech Nielsen, *Phys. Rev. B* **37**, 6353 (1988); R. F. Kiefl, M. Celio, T. L. Estle, S. R. Kreitzman, G. M. Luke, T. M. Riseman and E. J. Ansaldo *Phys. Rev. Lett.* **60** 224 (1988).
- [4] M individuates a two-fold coordinated site located in the middle of a straight line segment connecting the bond-center with the nearest hexagonal site; C individuates a site located in the middle of a straight line segment connecting two adjacent M sites.
- [5] A. Van Wieringen and N. Warmoltz, *Physica* **22**, 849 (1956).
- [6] S. J. Pearton, *J. Electron. Mater.* **14a**, 737 (1985).
- [7] C. H. Seager and R. A. Anderson, *Appl. Phys. Lett.* **53**, 1181 (1988).
- [8] A. E. Jaworowski, *Radiation Effects and Defects in Solids* **111&112**, 167 (1989).
- [9] R. Car and M. Parrinello, *Phys. Rev. Lett.* **55**, 2471 (1985).
- [10] F. Buda, G. L. Chiarotti, R. Car, and M. Parrinello, *Phys. Rev. Lett.* **63**, 294 (1989).
- [11] P. E. Blöchl, C. G. Van de Walle, and S. T. Pantelides, *Phys. Rev. Lett.* **64**, 1401 (1990).

*INTERNATIONAL WORKSHOP ON :*

**HYDROGEN MIGRATION AND THE  
STABILITY OF HYDROGEN RELATED  
COMPLEXES IN CRYSTALLINE  
SEMICONDUCTORS**

**HORBEN BEI FREIBURG**  
(FEDERAL REPUBLIC OF GERMANY)

**3-6 NOVEMBER 1991**

Accession For	
NTIS ORNL	<input checked="" type="checkbox"/>
DTIC TAB	<input type="checkbox"/>
Unannounced	<input type="checkbox"/>
Justification	
By <i>Per Form 50</i>	
Distribution/	
Availability Codes	
Dist	Avail and/or
<i>A-1</i>	Special

**Organizers :**

**Bernard CLERJAUD**  
Université Pierre et Marie Curie, Boîte n° 86  
4 Place Jussieu  
F-75252 Paris Cedex 05, France  
Tel : +33 (1) 44 27 44 47  
Fax : +33 (1) 44 27 38 54  
Telex : 200145F (UPMCSIX)  
E-mail : BEC@FRUNIP62.BITNET

**Bernhard DISCHLER**  
Fraunhofer-Institut für Angewandte Festkörperphysik  
Tullastrasse 72  
D-7800 Freiburg, Germany  
Tel : +49 (761) 5159 354  
Fax : +49 (761) 5159 400

**Noble JOHNSON**  
Xerox Palo Alto Research Center  
3333 Coyote Hill Road  
Palo Alto, California 94304, USA  
Tel : +1 (415) 812 4160  
Fax : +1 (415) 812 4105

**Jürgen SCHNEIDER**  
Fraunhofer-Institut für Angewandte Festkörperphysik  
Tullastrasse 72  
D-7800 Freiburg, Germany  
Tel : +49 (761) 5159 500  
Fax : +49 (761) 5159 400

**John M. ZAVADA**  
Electronics Division  
U.S. Army Research Office  
P.O. Box 12211  
Research Triangle Park, N.C. 27709, U.S.A.  
Tel : +1 (919) 549 4314  
Fax : +1 (919) 549 4310

**Supporting organizations :**

- European Research Office of the U.S. Army (London)
- Fraunhofer-Institut für Angewandte Festkörperphysik (Freiburg)
- Siemens (München)
- Université Pierre et Marie Curie (Paris)
- Xerox Corporation (USA)

## CONTENTS

Hydrogen passivation of carbon acceptors in GaAs grown from metalorganic sources M. Stavola, D.M. Kozuch, S.J. Pearton, C.R. Abernathy and W.S. Hobson	1
Raman spectroscopy of localized vibrational modes from carbon-hydrogen pairs in heavily carbon doped GaAs layers grown by metal organic vapor phase epitaxy J. Wagner, M. Maier, Th. Lauterbach and K.H. Bachem	5
H-enhanced oxygen diffusion in silicon R. Jones, S. Oberg and A. Umerski	9
Carbon-hydrogen complexes in gallium arsenide R. Jones and S. Oberg	10
The hydrogen-carbon complex in silicon : tunneling effect of electrons A. L. Endrös and M. Bernauer	13
Hydrogen ion-implanted into crystalline silicon B. Bech Nielsen, K. Bonde Nielsen and B. Holm	16
Hydrogen related complexes in neutron transmutation doped FZ silicon grown under hydrogen atmosphere Meng Xiang-ti	20
Vibrations of hydrogen complexes in silicon P. Deák, M. Heinrich, L. C. Snyder and J.W. Corbett	24
Hydrogen neutralization of double acceptor centers in silicon G. Pensl, M. Lang and P. Stolz	26
Stability of hydrogen complexes in semi-insulating indium phosphide grown by the liquid encapsulated Czochralski method B. Pajot, R. Darwich and C. Song	30
O-H and N-H complexes in semi-insulating gallium arsenide B. Pajot, R. Darwich and C. Song	31
What did we learn from PAC experiments about hydrogen in semiconductors ? M. Deicher, R. Keller, R. Magerle, W. Pfeiffer, P. Pross, H. Skudlik and Th. Wichert	33
Structure, stability and internal dynamics of Cd-H complexes in semiconductors A. Baurichter, N. Achtziger, D. Forkel, M. Gebhard, B. Vogt and W. Witthuhn	37
Structure and energy of interstitial hydrogen and hydrogen-related complexes in crystalline semiconductors C. G. Van de Walle	41
Hydrogen in silicon : aspects of solubility, diffusion and catalyzed enhanced oxygen diffusion R.C. Newman, M.J. Binns, S.A. McQuaid and J.H. Tucker	42
The stability of hydrogen complexes in Si and GaAs J. Weber, A.W.R. Leitch, Th. Prescha and T. Zundel	46

Recent studies of hydrogen in silicon and III-V semiconductors N.M. Johnson	50
Multitrapping of atomic hydrogen in doped crystalline silicon A. Amore Bonapasta	53
Modeling of hydrogen diffusion in semiconductors D. Mathiot	54
Diffusion and electronic states of hydrogen in n-GaAs : Si and n-Al <sub>x</sub> Ga <sub>1-x</sub> As : Si J. Chevallier, B. Machayekhi, C.M. Grattapain and B. Theys	58
The experimental evidence for various charge states of hydrogen in silicon C. H. Seager	61
Nitrogen-hydrogen complex and hydrogen charge states in GaP B. Clerjaud, D. Côte, W.-S. Hahn, C. Porte, D. Wasik and W. Ulrici	63
Hydrogen stability and passivation of shallow and deep centers in GaSb and InSb A.Y. Polyakov, S.J. Pearton, R.G. Wilson, P. Rai-Choudhury, R.J. Hillard, X. J. Bao, M. Stam, A.G. Milnes, T.E. Schlesinger and J.M. Zavada	67
Incorporation of hydrogen in II-VI epitaxial layers grown by MOCVD Y. Marfaing, L. Svob, H. Dumont, E. Rzepka, D. Ballutaud, R. Druilhe and C. M. Grattapain	71
Comments on hydrogen in natural diamond B. Dischler	75
<sup>2</sup> D interaction with ion implanted and annealed gallium arsenide D.K. Sadana, J.P. de Souza, E.D. Marshall, F. Cardone, K. M. Jones and M.M. Aljassim	79
Optical waveguides in GaAs crystals formed by hydrogen interactions J.M. Zavada, B.L. Weiss, I.V. Bradley, B. Theys, J. Chevallier, R. Rahbi, R. Addinall, R.C. Newman and H.A. Jenkinson	81
Hydrogen plasma devices fabrication and performance N. Ng Ching Hing, E. Constant and P. Godts	85
Thermal effusion as an analytical tool for hydrogen bonding in crystalline silicon and germanium M. Stutzmann, E. Bustarret, J.-B. Chevrier and P. de Mierry	86
Hydrogenation of SiGe/Si layered structures K.L. Wang, V. Arbet-Engels, J.S. Park and M.A. Kallel	90
Effects of hydrogen on the photoluminescence of Si-doped GaAs/AlGaAs multiple quantum wells F. Voillot, N. Lauret, R.G. Wilson, J.M. Zavada and B. Theys	94
<b>Author index</b>	98

## Hydrogen Passivation of Carbon Acceptors in GaAs Grown from Metalorganic Sources

Michael Stavola and D.M. Kozuch, Physics Bldg. 16, Lehigh University, Bethlehem, PA 18015

S.J. Pearton, C.R. Abernathy, and W.S. Hobson, AT&T Bell Laboratories, Murray Hill, NJ 07974

### ABSTRACT

For GaAs:C epitaxial layers, we have found that H<sub>2</sub> gas in growth and annealing ambients leads to the formation of C<sub>x</sub>-H complexes. Up to 40% of the C acceptors are estimated to be passivated in some cases. The C<sub>x</sub>-H centers have been shown to be stable or marginally stable at temperatures near 500°C. Hence, the unintentional passivation of C is especially likely because typical epitaxial growth and processing-related annealing steps are performed near 500°C and often in H<sub>2</sub> containing ambients.

Most recent work on H in semiconductors [1-3] has focussed on defect passivation in a plasma that contains atomic hydrogen. In III-V and II-VI materials, there are a few examples of H incorporation from H<sub>2</sub> gas of which we are aware. Svob and coworkers diffused D into GaAs [4] and II-VI materials [5] from D<sub>2</sub> gas and detected the indiffusion with SIMS. In more recent work, Svob et al. [6] showed with SIMS measurements that H was incorporated into II-VI materials grown by MOCVD from H<sub>2</sub> in the growth ambient. Defect passivation was not demonstrated in these experiments.

In our experiments on the passivation of GaAs:C, we have examined several epitaxial layers grown by MOMBE [7] and MOCVD [8] with various growth conditions and post-growth annealing treatments. Annealing experiments were performed either in an RTA oven with an ambient of forming gas or He or in a muffle furnace in sealed quartz ampules filled with H<sub>2</sub> (or D<sub>2</sub>). Characterization methods include Hall effect, SIMS, and IR absorption.

IR spectra for the H-stretching region are shown in Fig. 1 for samples from a MOMBE-grown layer with  $N_A = 2 \times 10^{20} \text{ cm}^{-3}$  that had been annealed in various ambients. In Fig. 1(a) a feature at  $2635 \text{ cm}^{-1}$  that was previously assigned to the C<sub>As</sub>-H center by Clerjoud et al. [9] and additional features at 2643, 2651, and  $2688 \text{ cm}^{-1}$  that also involve C and H [10] are seen in an as-grown layer. We use denotation C<sub>x</sub>-H for these centers.

In previous work it was found that H could be introduced into the GaAs:C layers grown by MOMBE from the TMG or the AsH<sub>3</sub> sources. [10, 11] Fig. 1 shows that H<sub>2</sub> in the annealing ambient is also an important source of H in the layers. The spectrum in Fig. 1(b) shows that annealing in H<sub>2</sub> enhances the strength of the C-H stretching feature at  $2635 \text{ cm}^{-1}$ . This anneal was performed in a sealed ampule; spurious sources of atomic H that might result

from the dissociation of H<sub>2</sub> on hot furnace components are unlikely. We presume that the H<sub>2</sub> dissociates at the sample surface and then diffuses into the epilayer where C<sub>x</sub>-H centers are readily formed. In Figs. 1(c) and (d), samples are compared following annealing in an RTA oven in forming gas (90% N<sub>2</sub> and 10% H<sub>2</sub>) and He gas. An anneal in the inert He ambient at 600°C eliminates the C-H stretching features whereas C<sub>x</sub>-H centers remain following an anneal at 600°C in forming gas.

The presence of C<sub>x</sub>-H centers in as-grown samples indicates that these defects are stable near the epi-growth temperature. Isochronal (5 min) annealing data are shown in Fig. 2. These anneals were performed in an RTA furnace in a He ambient. The 2635 and 2688 cm<sup>-1</sup> features are annealed away at temperatures of 800 K (527°C) and 900 K (627°C), respectively. Both centers are stable or marginally stable at the epi-growth temperatures of 500 to 545°C for the MOMBE and MOCVD growths, respectively, and persist to higher temperatures when samples are annealed in H<sub>2</sub>-containing ambients. [See Fig. 1(c)]. The stability of the C<sub>AS</sub>-H center (2635 cm<sup>-1</sup>) is consistent with previous results due to Clerjaud et al. [12] Recent results by Pearton et al. [13] show that in a reverse biased p-n junction, C<sub>AS</sub>-H complexes dissociate at 145°C in a 20 min anneal. Hence the stability we measure is greatly affected by retrapping of the H<sup>+</sup> at C<sub>AS</sub> sites.

We have made an approximate calibration of the concentration of centers that include C and H by making a direct measurement of the H concentration with SIMS. Typical profiles of GaAs:C into which H and D had been diffused are shown in Fig. 3. If it is assumed that all of the hydrogen in the layers is involved in stable C<sub>x</sub>-H complexes then the relationship between the infrared absorption strength and concentration of centers is,

$$[C_x-H]/A = 1.8 \times 10^{16} \text{ cm}^{-1}$$

Here A is the integrated absorption coefficient,  $A = \int a(\sigma) d\sigma$ , in units cm<sup>-2</sup> for the total H-stretching absorption due to the C<sub>x</sub>-H centers.

With the calibration factor given above we can estimate [C<sub>x</sub>-H] for the various epilayers from the strength of the IR absorption. The as-grown MOMBE layer in Fig. 1(a) has [C<sub>x</sub>-H] = 7x10<sup>18</sup> cm<sup>-3</sup>. Annealing in H<sub>2</sub> [Fig. 1(b)] increases the concentration of passivated carbon to [C<sub>x</sub>-H] = 1.2x10<sup>19</sup> cm<sup>-3</sup> or to roughly 11% of the total [C]. The highest concentrations of C<sub>x</sub>-H centers were observed in layers with H<sub>2</sub> in the growth ambient. The fraction of passivated C acceptors varies from 6% to 40% depending upon the growth method and growth conditions.

1. Hydrogen in Semiconductors, ed. J.I. Pankove, and N.M. Johnson, (Academic, San Diego, 1991).
2. Hydrogen in Semiconductors, ed. M. Stutzmann and J. Chevallier, (North Holland, Amsterdam, 1991).
3. S.J. Pearton, J.W. Corbett, and M. Stavola, Hydrogen in Crystalline

Semiconductors, (Springer-Verlag, Heidelberg, 1992), in press.

4. L. Svob, C. Grattepain, and Y. Marfaing, *Appl. Phys. A* **47**, 309 (1988).

5. L. Svob and Y. Marfaing, Shallow Impurities in Semiconductors, ed. G. Davies, (Trans Tech, Switzerland, 1991), p. 181.

6. L. Svob, Y. Marfaing, F. Desjonqueres and R. Druilhe, in ref. 2, p. 550.

7. C.R. Abernathy, S.J. Pearton, R. Caruso, F. Ren, and J. Kovalchik, *Appl. Phys. Lett.* **55**, 1750 (1989); C.R. Abernathy et al., *J. Crystal Growth* **105**, 375 (1990).

8. MOCVD samples were grown following the method of T. Kobayashi and N. Inoue, *J. Crystal Growth* **102**, 183 (1990).

9. B. Clerjaud, F. Gendron, M. Krause, and W. Ulrici, *Phys. Rev. Lett.* **65**, 1800 (1990).

10. D.M. Kozuch, M. Stavola, S.J. Pearton, C.R. Abernathy, and J. Lopata, *Appl. Phys. Lett.* **57**, 2561 (1990).

11. K. Woodhouse, R.C. Newman, T.J. de Lyon, J.M. Woodall, G.J. Scilla, and F. Cordone, *Semicond. Sci. Technol.* **6**, 330 (1991); K. Woodhouse, R.C. Newman, R. Nicklin and R.R. Bradley, preprint.

12. B. Clerjaud, F. Gendron, M. Krause, C. Naud, and W. Ulrici, in ref. 2, p. 417.

13. S.J. Pearton, C.R. Abernathy, J. Lopata, submitted *Appl. Phys. Lett.*

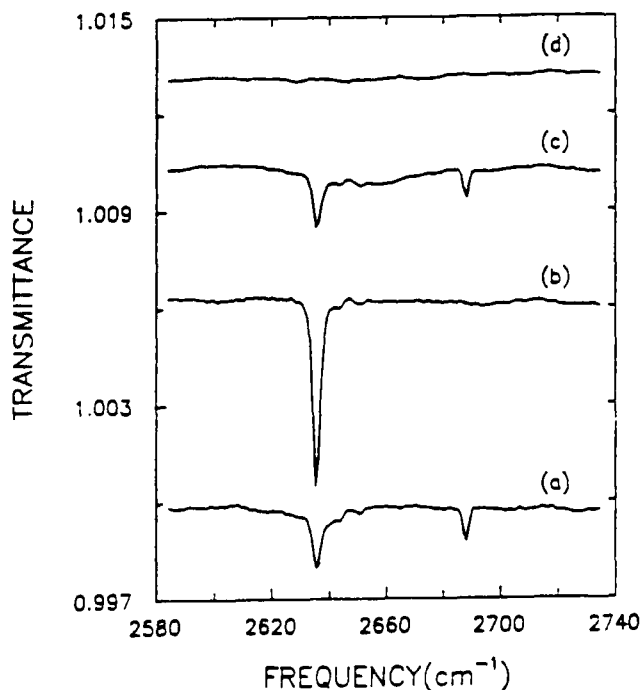


Fig. 1. IR spectra that demonstrate the effect of annealing ambient on C-H centers in GaAs:C grown by MOMBE. Samples were selected from the same wafer with  $N_A = 9.4 \times 10^{19} \text{ cm}^{-3}$ . (a) As-grown. (b) Anneal at 450°C in 0.6 atm  $\text{H}_2$  in a sealed ampoule. (c) Anneal for 5 min in forming gas at 600°C in an RTA oven. (d) Anneal for 5 min in He at 600°C in an RTA oven.

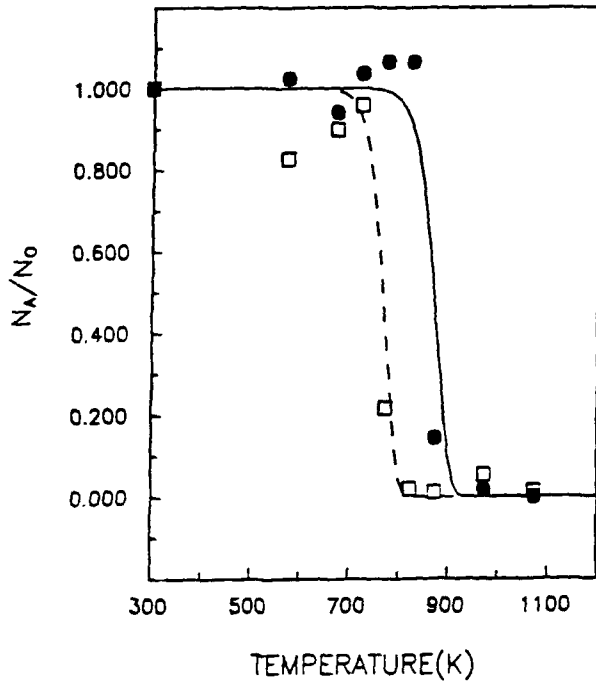


Fig. 2. Isochronal annealing data for the  $2636\text{ cm}^{-1}$  (open squares) and  $2688\text{ cm}^{-1}$  (closed circles) absorption signals in epitaxial GaAs:C grown by MOMBE. Anneals were performed for 5 min in a He ambient. Here,  $N_A = 2 \times 10^{20}\text{ cm}^{-3}$ .

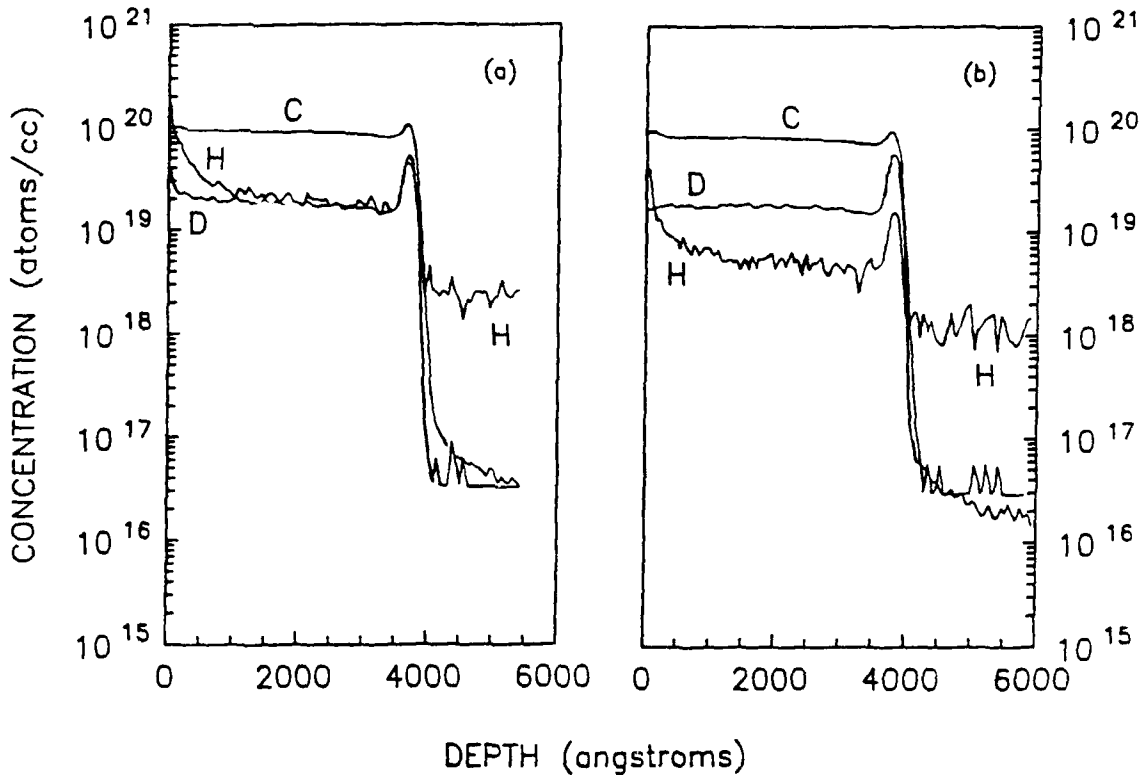


Fig. 3. SIMS profiles of H, D, and C in epitaxial GaAs grown by MOMBE (a) annealed in  $\text{H}_2/\text{D}_2$  and (b) annealed in  $\text{D}_2$ . Anneals were performed in sealed ampules at  $500^\circ\text{C}$  for 20 min with a gas pressure of  $2/3\text{ atm}$ . In (b) the hydrogen was present in the as grown sample.

Raman spectroscopy of localized vibrational modes from carbon-hydrogen pairs in heavily carbon doped GaAs layers grown by metal organic vapor phase epitaxy

*J. Wagner, M. Maier, Th. Lauterbach, and K.H. Bachem  
Fraunhofer-Institut für Angewandte Festkörperphysik,  
Tullastrasse 72, D-7800 Freiburg, Federal Republic of Germany*

There is considerable current interest in doping GaAs with carbon during epitaxial growth (see, e.g., Refs. 1-3). As an impurity significantly lighter than the host lattice atoms carbon produces a localized vibrational mode (LVM) which is at  $582 \text{ cm}^{-1}$  for  $^{12}\text{C}$  incorporated on an arsenic lattice site ( $^{12}\text{C}_{\text{As}}$ )<sup>4</sup>. LVM absorption spectroscopy has been successfully used to study the incorporation of carbon in epitaxial layers<sup>5-7</sup>. One of the results of this work is that carbon-hydrogen (C-H) pairs can be formed in such layers not only after intentional hydrogen treatment but also during the layer growth by metalorganic molecular beam epitaxy (MOMBE)<sup>5</sup> and by metal organic vapor phase epitaxy (MOVPE)<sup>7</sup>.

Here we report on a Raman spectroscopic study of the LVM produced by carbon and C-H pairs in as-grown heavily carbon doped GaAs layers grown by MOVPE using trimethylarsine and trimethylgallium<sup>8</sup>. The Raman spectroscopic work was complemented by secondary ion mass spectroscopy (SIMS), to assess the total carbon concentration [C], and by Hall effect measurements.

Fig. 1 shows a sequence of Raman spectra from samples doped with carbon to concentrations  $[C]$  of  $1.2 \times 10^{19} \text{cm}^{-3}$  and  $6 \times 10^{19} \text{cm}^{-3}$ , respectively. For reference purposes the spectrum of undoped GaAs is also displayed. All spectra were excited at 2.71 eV, which is below the  $E_1$ -band gap resonance. Besides second order phonon scattering with a broad band centered at  $540 \text{ cm}^{-1}$ , the  $^{12}\text{C}_{\text{As}}$  LVM is resolved at  $582 \text{ cm}^{-1}$ . For excitation at 3.00 eV in resonance with the  $E_1$ -band gap of GaAs the  $^{12}\text{C}_{\text{As}}$  LVM is masked by intrinsic scattering from two longitudinal optical phonons (2LO) occurring at the same frequency (Fig. 2). For carbon concentrations  $\geq 6 \times 10^{19} \text{cm}^{-3}$  an additional peak appears at  $454 \text{ cm}^{-1}$  (labelled X) which becomes the most intense feature for concentrations  $[C]$  exceeding  $10^{20} \text{cm}^{-3}$ . This peak is strongest in intensity for the polarization of the incident and scattered light parallel to each other, indicating that the vibrational mode causing this peak has  $A_1$  symmetry. Along with line X a high frequency mode can be resolved at  $2642 \text{ cm}^{-1}$  (Fig. 3). This mode is superimposed on a photoluminescence background arising from the recombination of non-thermalized electrons<sup>9</sup> which is by an order of magnitude more intense than the Raman signal. From a comparison with recent LVM absorption data on hydrogen treated carbon doped GaAs layers<sup>6,7</sup> the  $2642 \text{ cm}^{-1}$  Raman line can be assigned to the stretch mode of the  $^{12}\text{C}_{\text{As}}\text{-H}$  pair and the line X to a carbon mode of that pair.

For the two less heavily doped samples the concentration of free holes equals, within the experimental accuracy, the total carbon concentration  $[C]$ . In the most heavily doped sample, however, the hole concentration amounts to  $1.2 \times 10^{20} \text{cm}^{-3}$  which is less than the carbon concentration of  $1.8 \times 10^{20} \text{cm}^{-3}$ . It is not clear at present whether the formation of C-H pairs, which is evident from the above Raman spectroscopic data, can account for this discrepancy quantitatively. Thus the question remains open, whether the incorporation of hydrogen does limit the maximum achievable hole concentration in the present MOVPE process.

We would like to thank K. Winkler and T. Fuchs for valuable technical assistance as well as R.C. Newman for helpful discussions and for communicating results prior to publication.

**References:**

1. T.F. Kuech, M.A. Tischler, P.J. Wang, G. Scilla, R. Potemski, and F. Cardone, *Appl. Phys. Lett.* 53, 1317 (1988).
2. K. Saito, E. Tokumitsu, T. Akatsuka, M. Miyauchi, T. Yamada, M. Komagai, and K. Takahashi, *J. Appl. Phys.* 64, 3975 (1988).
3. C.R. Abernathy, S.J. Pearton, R. Caruso, F. Ren, and J. Kovalchik, *Appl. Phys. Lett.* 55, 1750 (1989).
4. See, e.g.: R.C. Newman, *Mat. Res. Soc. Proc.* Vol. 46, 459 (1985) and references therein.
5. D.M. Kozuch, M. Stavola, S.J. Pearton, C.R. Abernathy, and J. Lopata, *Appl. Phys. Lett.* 57, 2561 (1990).
6. K. Woodhouse, R.C. Newman, T.J. de Lyon, J.M. Woodall, G.J. Scilla, and F. Cardone, *Semicond. Sci. Technol.* 6, 330 (1991).
7. K. Woodhouse, R.C. Newman, R. Nicklin, and R.R. Bradley, to be published.
8. G. Neumann, Th. Lauterbach, M. Maier, and K.H. Bachem, *Inst. Phys. Conf. Ser.* 112, 167 (1990).
9. B.J. Aitchison, N.M. Haegel, C.R. Abernathy, and S.J. Pearton, *Appl. Phys. Lett.* 56, 1154 (1990).

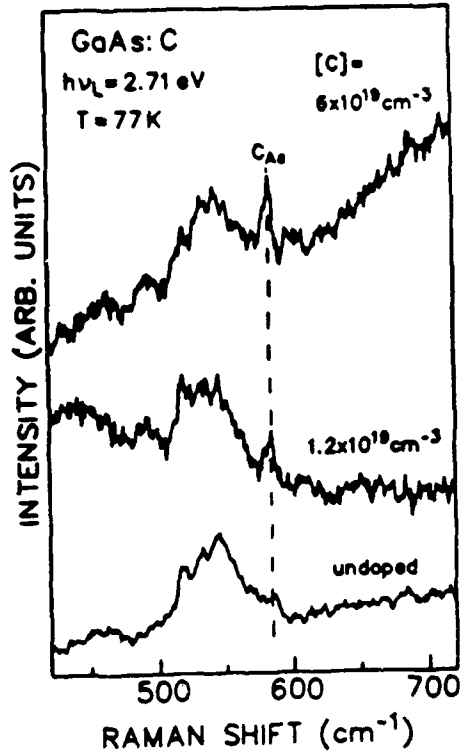


Fig. 1 Low-temperature Raman spectra of MOVPE grown GaAs:C showing the  $^{12}C_{As}$  LVM and of undoped GaAs. The total carbon concentrations [C] are given in the figure.

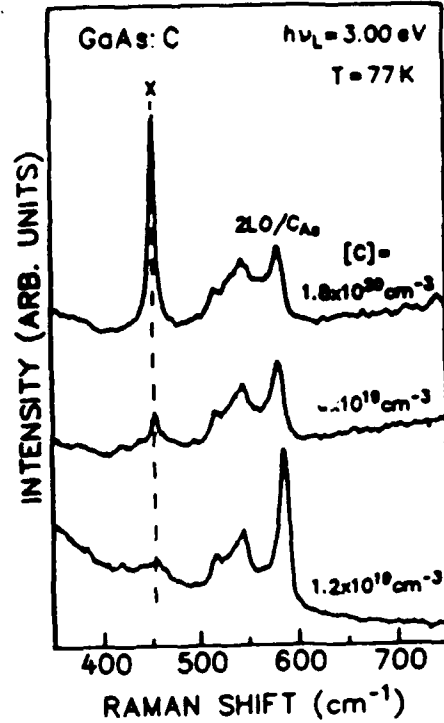


Fig. 2 Low-temperature Raman spectra of MOVPE grown GaAs:C for different total carbon concentrations [C] given in the figure. X denotes a carbon mode of the  $^{12}C_{As}$ -H pair.

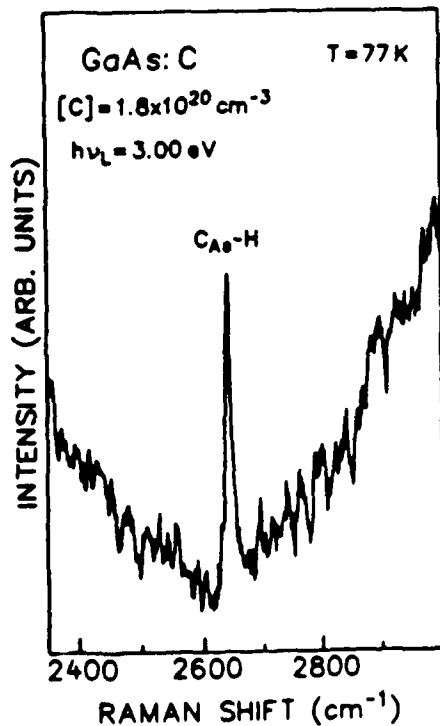


Fig. 3 Low-temperature Raman spectrum of MOVPE grown GaAs:C showing the C-H stretch mode of the  $^{12}C_{As}$ -H pair.

## H-ENHANCED OXYGEN DIFFUSION IN SILICON

R. JONES<sup>1</sup>, S. ÖBERG<sup>2</sup> AND A. UMERSKI<sup>1</sup>

<sup>1</sup>Department of Physics , University of Exeter, Exeter, EX44QL, UK

<sup>2</sup>Department of Mathematics, University of Luleå, Luleå, S95187, Sweden

Hydrogen is known to enhance the diffusion of O through silicon, reducing its activation energy from 2.5 eV to 1.6 eV [1, 2]. An understanding of this effect can come from carrying out calculations of the most stable site for H close to an O interstitial, and investigating how the energy required to displace the oxygen atom from its interstitial site to an adjacent one is affected by this hydrogen

We have carried out this programme [3] using a first-principles local density functional pseudopotential method applied to a cluster of 72 atoms. The method allows us to move atoms until an equilibrium structure is found and then to compute the energy necessary to distort the structure and determine saddle point energies.

We found that the isolated O atom has Si-O bonds of about 1.6 Å and Si-O-Si angle around 160°. The energy necessary to pull the cluster into a *ylid* saddle point configuration where the O atom changes from being bonded to atoms 1 and 3 (fig. 1) to 1 and 4 is 2.8 eV and is in reasonable agreement with observation.

In this *ylid* configuration the Si atom 1 is only 3-fold coordinated and has bonds 1.54 Å with the O atom 2 and 2.26 Å with the other two Si atoms (not 3 and 4). The bonds with 3 and 4 are 2.86 Å.

An extra H atom placed successively at an anti-bonding site ( along the continuation of the line starting at 2 and passing through 1 ) , a bond centred site (between 1 and 4) and one of the three equivalent tetrahedral sites all led to stable configurations when the cluster was relaxed. The energies of the latter two relative to the first ( H at the anti-bonding site ) are 1.5 and .75 eV respectively. Thus we believe the most stable site for H near O is at a anti-bonding configuration. If O traps H in this manner, then the solubility of H in Si should be dependent on the O concentration.

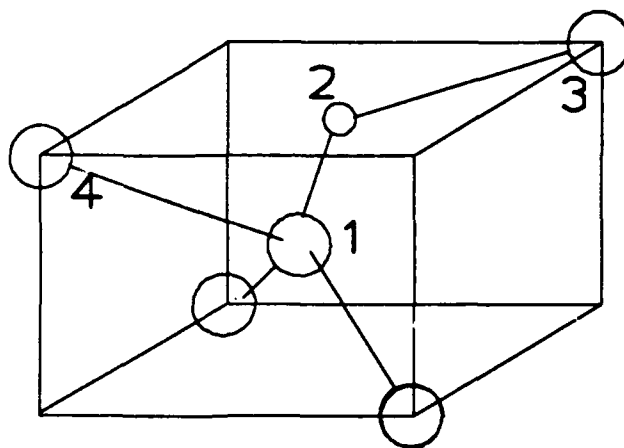
If O is now displaced into the *ylid* configuration, and the rest of the cluster including H, allowed to relax, the energy difference is now only .2 eV. This is because as the Si bond 1-4 weakens, the Si-H bond strengthens. Thus the Si atom always has 4-fold coordination and this leads to a reduction in the distortion energy.

When O moves from the *ylid* configuration towards the centre of the bond 1-4, the energy continues to increase reaching a maximum of 1.4 eV. The H atom being progressively pushed towards the tetrahedral site opposite O in fig.1 .

The final configuration then has an energy .75 eV above the original. The activation barrier along this path is then 1.4 eV. H must then hop to another anti-bonding site to O for a further motion of O to occur with a low barrier. This is likely to be an easy process and we conclude that the activation energy for O reorientation in the presence of H is 1.4 eV.

## References

- [1] R. C. Newman, *20th International Conference on The Physics of Semiconductors*, 1. ed. E. M. Anastassakis and J. D. Joannopoulos, World Scientific, Singapore , p 332. (1991).
- [2] R. Murray, *Physica. B* **170**, 115 (1991).
- [3] R. Jones, S. Öberg and A. Umerski, Proc. of 16 'th ICDS, Lehigh. (1991).



## CARBON-HYDROGEN COMPLEXES IN GALLIUM ARSENIDE

R. JONES<sup>1</sup> AND S. ÖBERG<sup>2</sup>

<sup>1</sup>Department of Physics, University of Exeter, Exeter, EX44QL, UK

<sup>2</sup>Department of Mathematics, University of Luleå, Luleå, S95187, Sweden

Infra-red absorption studies show that H-passivated C-rich GaAs has absorption lines due to C-H stretch at  $2635\text{ cm}^{-1}$  [1, 2, 3, 4],  $X^H$  at  $452\text{ cm}^{-1}$ , and  $Y$  at  $563\text{ cm}^{-1}$  [3, 4] as well as  $C_{As}$  at  $582\text{ cm}^{-1}$ .

We have carried out [5, 6] local density functional cluster calculations on models of defects giving rise to these lines. The calculations give the structures of the defects as well as their vibrational modes and effective charges. The latter control the intensity of the infra-red absorption.

We find:

- 1) The charged acceptor,  $C_{As}^-$ , has four C-Ga lengths of  $2.03\text{ \AA}$  and a triplet mode at  $544\text{ cm}^{-1}$  to be compared to the observed mode at  $582\text{ cm}^{-1}$ .
- 2) The charged donor,  $C_{Ga}^+$ , has C-As lengths of  $2.08\text{ \AA}$  and a triplet mode at  $538\text{ cm}^{-1}$ . The donor has not been positively identified but the closeness of this frequency to that of the  $Y$  line is not inconsistent with the view that donors are present in the material [4]. It is not clear, however, whether the line  $Y$  is independent of H [8].
- 3) The bond centred H- $C_{As}$  complex has three rather longer C-Ga bonds of  $2.18\text{ \AA}$ , a very short C-H bond of  $1.12\text{ \AA}$  and a weak H-Ga bond of  $2.05\text{ \AA}$ .

The longer C-Ga bonds probably arise in response to the very short C-H bond. The C-H entity behaves as an 'atom' isoelectronic with As and makes long bonds with Ga which drive the C-related local modes downwards, below those of the isolated substitutional impurity.

Table 1 gives the local modes and their effective charges. The small effective charge renders the H-bend modes infra-red invisible.

The highest  $A$  mode related to C is close to line  $X^H$  and has similar isotope shifts.

Table 1: Frequencies,  $\text{cm}^{-1}$ , and Effective Charges,  $\epsilon$ , of Local Modes of the Bond Centred C-H-Ga Complex and the  $\text{C}_{\text{As}}\text{-C}_{\text{Ga}}$  Pair

Mode	$\eta$	$^{12}\text{C } ^1\text{H}$	$^{13}\text{C } ^1\text{H}$	$^{12}\text{C } ^2\text{H}$
<b>C-H-Ga Complex</b>				
H. stretch	.96	2605	2598	1905
H. bend	.04	730	729	540
		707	704	528
C. A	1.66	413	399	402
C. E	1.15	392	379	376
		367	355	355
<b>Observed [1, 2, 3, 4]</b>				
H. stretch		2635	2628	1969
$X^{\text{H}}$		452		440
<b><math>\text{C}_{\text{As}}\text{-C}_{\text{Ga}}</math> pair</b>				
E	.55	556	534	
		551	530	
A	.48	425	410	
E		383	370	
		381	367	

The C related E modes fall below that of the A mode and have about 50% of the absorption intensity of the A mode.

- 4) The reorientation energy of the H is calculated to be .67 eV and observed  $\eta$  to be .5 eV.
- 5) H at an anti-bonding site has an energy .5 eV greater than the bond centred configuration above and the bond centred complex is then the most stable one. This is consistent with the assignment [1] of the  $2635 \text{ cm}^{-1}$  line to the bond centred defect.
- 6) The pair defect  $\text{C}_{\text{As}}\text{-C}_{\text{Ga}}$  has C-Ga, C-C, C-As bonds of lengths 2.12, 2.27 and 1.83 Å, and the local modes (table 1) are below those of the isolated defects. It also has a mid-gap empty level whose wave-function is made up of anti-bonding combination of  $sp^3$  orbitals on the C atoms.

## References

- [1] B. Clerjaud, F. Gendron, M. Krause and W. Ulrici, Phys. Rev., Lett., **65** (1991).
- [2] D. M. Kozuch, M. Stavola, S. J. Pearton, C. R. Abernathy and J. Lopata, Appl. Phys. Lett. **57** 2561 (1990).
- [3] K. Woodhouse, R. C. Newman, T. J. de Lyon, J. M. Woodall, G. J. Scilla and F. Cardone, Semiconductor Sci. and Technology, to be published (1991)
- [4] K. Woodhouse, R. C. Newman, R. Nicklin and R. R. Bradley, submitted for publication.
- [5] R. Jones and S. Öberg, Phys. Rev. B, **44**, 3673, (1991).
- [6] R. Jones, S. Öberg and A. Umerski, Proc. of 16<sup>th</sup> ICDS, Lehigh, (1991).

- [7] B. Clerjaud, D. Cote, F. Gendron, W-S. Hahn, M. Krause and C. Porte ,Proc. of 16'th ICDS (Lehigh), 1991.
- [8] K. Woodhouse. R. C Newman, R. Nicklin, R. R. Bradley and M. J. L. Sangster, to be published. J. Crystal Growth.

# The Hydrogen-Carbon Complex in Silicon: Tunneling Effect of Electrons

A. L. Endrös, M. Bernauer

Research Laboratories of Siemens AG, D-8000 München 83, Germany

Tel.: (+89) 63644834      FAX: (+89) 63649164

The properties of hydrogen (H) in crystalline silicon (Si) have been studied extensively [1]. It is now well established that H can passivate shallow acceptor and shallow donor impurities and forms H-acceptor [2,3,4] and H-donor complexes [5,6] which have been studied in detail. However, hydrogen can also be bound to isoelectronic group IV impurities in Ge [7] and Si [8] where it forms *electrically active* centers. H bound to substitutional carbon (C) in Si is known to form a hydrogen-carbon (H-C) related deep donor level [8]. Due to the isoelectronic behaviour of C in Si, this H-C complex is well suited for studying the possible charge states of H in silicon, i.e., it reflects the principal electronic properties of hydrogen. Ab initio calculations [9] even lead to the result that such an H-C complex has an energy level that is virtually identical to the level of an H atom at the same atomic site but *without* the C impurity. The most important electronic and kinetic properties of the H-C complex are already available [8,10]. The defect is a deep donor because it is visible in the *C-V*-profile [11] and a Poole-Frenkel effect should therefore exist.

In order to measure the Poole-Frenkel effect quantitatively the emission time constants of the H-C complexes are determined as a function of the electric field strength. This information is obtained from "double correlation deep level transient spectroscopy" (D-DLTS) transients which are measured at a fixed temperature. A systematic variation of the electric field strength  $E$  at the trap position finally permits a quantitative analysis of the Poole-Frenkel effect. In Fig. 1 the emission time constant of the H-C complex is plotted as a function of  $\sqrt{E}$  for two different temperatures.

The measurement in Fig. 1 shows that for electric fields  $\leq 2 \times 10^4$  V/cm the electric field dependence of the H-C emission time constant is much weaker than predicted by a three-dimensional Coulomb potential model [12] showing clearly that the potential of the H-C complex is not exactly coulombic. For electric fields  $E \geq 4 \times 10^4$  V/cm, however, the data appear to have a stronger electric field dependence than predicted. This effect could possibly be due to an emission process that is superimposed to the Poole-Frenkel effect like a (phonon-assisted) tunneling process of electrons through the barrier. With increasing field strength the height as well as the width of the barrier would decrease and the rate of tunneling would therefore increase — quite independently of temperature [13].

In order to test the possibility of electron tunneling out of the H-C complex, DLTS transients are recorded in the temperature range from 45 K to 90 K with a fixed electric field strength of  $\approx 1 \times 10^4$  V/cm at the trap position. The time constant  $\tau$  of the

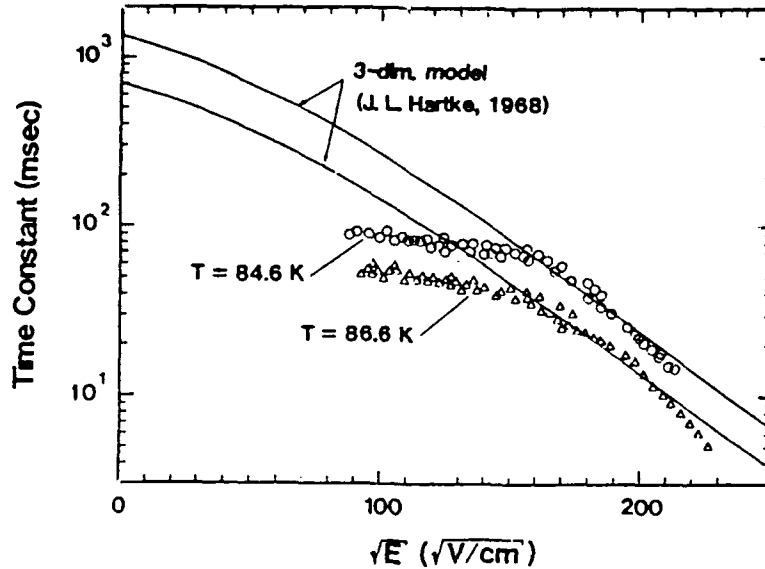


Figure 1: Emission time constant  $\tau$  of the H-C complex as a function of electric field strength  $E$  at two different temperatures. The dependence that is predicted from a 3-dimensional Coulomb potential model is plotted as a solid line.

transients is evaluated and is shown in Fig. 2 as a function of the inverse temperature in an Arrhenius plot. Fig. 2 clearly reveals that the measured emission time constants (triangles in Fig. 2) follow the usual Shockley-Read-Hall (SRH) behaviour  $\tau_{SRH} \sim \exp(E_A/kT)$  only for temperatures  $T$  higher than 70 K. For lower temperatures the emission time constant becomes completely independent of temperature with a constant value of 38 sec. The amount of this effect cannot be explained with the Poole-Frenkel effect (dashed line in Fig. 2) alone. Only if an additional tunneling effect is taken into account (solid line in Fig. 2) via a temperature independent time constant  $\tau_T = 38$  sec the rates add according to

$$\frac{1}{\tau} = \frac{1}{\tau_{SRH}} + \frac{1}{\tau_T}$$

and the experimental data can be explained. Phonon-assisted tunneling should not contribute significantly since the phenomenon is observed at low temperatures and is practically temperature independent. The effect is therefore contributed to pure tunneling.

## References

- [1] S.J. Pearton, J.W. Corbett and T.S. Shi, Appl. Phys. A 43 (1987) 153.
- [2] M. Stavola, K. Bergman, S. J. Pearton and J. Lopata, Phys. Rev. Lett. 61 (1988) 2786.
- [3] M. Stavola, S. J. Pearton, J. Lopata and W. C. Dautremont-Smith, Appl. Phys. Lett. 50 (1987) 1086.
- [4] M. Stutzmann, J. Harsanyi, A. Breitschwerdt and C. P. Herrero, Appl. Phys. Lett. 52 (1987) 1667.
- [5] N. M. Johnson, C. Herring and D. J. Chadi, Phys. Rev. Lett. 56 (1986) 769.
- [6] K. Bergman, M. Stavola, S. J. Pearton and J. Lopata, Phys. Rev. B 37 (1988) 2770.

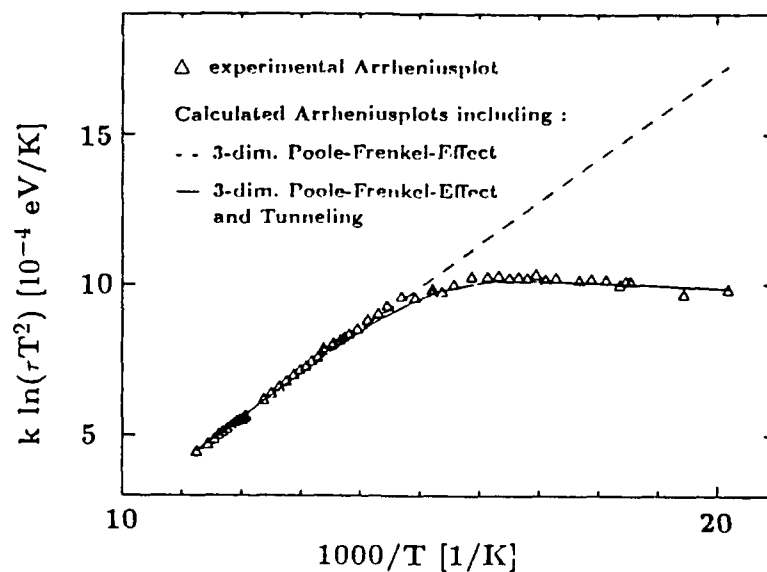


Figure 2: Emission time constant  $\tau$  of the H-C complex as a function of temperature  $T$  in an Arrhenius form.

- [7] L. M. Falicov and E. E. Haller, Solid State Comm. 53 (1985) 1121.
- [8] A. L. Endrös, Phys. Rev. Lett. 63, 70 (1989).
- [9] P. J. H. Denteneer, C. de Walle, and S. T. Pantelides, Phys. Rev. Lett. 62 (1989) 1884.
- [10] A. L. Endrös, W. Krühler and J. Grabmaier, Material Science and Engineering B4 (1989) 35.
- [11] A. L. Endrös, W. Krühler and J. Grabmaier, Physica B 170 (1991) 365.
- [12] J. L. Hartke, J. Appl. Phys. 39, 4871 (1968).
- [13] D. Vuillaume, J. C. Bourgoin, and M. Lannoo, Phys. Rev. B. 34 (1986), 1171.

## Hydrogen ion-implanted into crystalline silicon.

B. Bech Nielsen, K. Bonde Nielsen, and B. Holm  
Institute of Physics and Astronomy, University of Aarhus,  
DK-8000 Aarhus C, Denmark.

Hydrogen in crystalline silicon has been studied intensively during the last decade by a large number of experimental techniques[1]. In addition remarkable progresses in the theoretical description have been achieved by large-scale total-energy calculations[2]. Consequently, our knowledge about the properties of hydrogen in silicon has grown significantly.

Hydrogen may be introduced into silicon crystals in various ways, the one most widely used is to expose the surface at moderate temperatures to a hydrogen plasma. Ion-implantation is an alternative technique, which will be in focus in this talk. The major advantages offered by ion-implantation is the possibility to introduce well-controlled amounts of hydrogen at a given temperature. Moreover ion-implantation often leaves the impurities in a non-equilibrium state, a fact which makes the technique interesting for studies of defect-metastability[3]. The major disadvantage is that the creation of defects accompanies the implantation process. At a first glance this seems to represent a serious limitation for applications in studies of isolated hydrogen-defects. However, for typical implantation energies 50-500 KeV and at low temperatures a large fraction of the implanted hydrogen atoms may still end up in "semi-isolated" configurations, even for local concentrations up to  $\sim 10^{19}$  H/cm<sup>3</sup>, corresponding to doses in the range  $10^{14}$ - $10^{15}$  H/cm<sup>2</sup>. This point will be discussed further in the following.

Theoretical calculations[2] showed that hydrogen in silicon may exist in three charge states  $H^+$ ,  $H^0$  and  $H^-$ , where  $H^+$  and  $H^0$  occupy the bond-center site BC while  $H^-$  has minimum in energy at the tetrahedral site T (see fig. 1). The existence of neutral hydrogen at the BC site finds strong support in the EPR experiments by Gorelkinskii et al.[4]. They observed a hydrogen-related EPR-center, denoted AA9, after proton implantation at 80 K ( $\sim 5 \times 10^{17}$  H/cm<sup>3</sup>). The AA9-center is trigonal, involves two equivalent silicon atoms, and the hyperfine parameters are consistent with those found for anomalous muonium, for which the BC configuration has been confirmed[5].

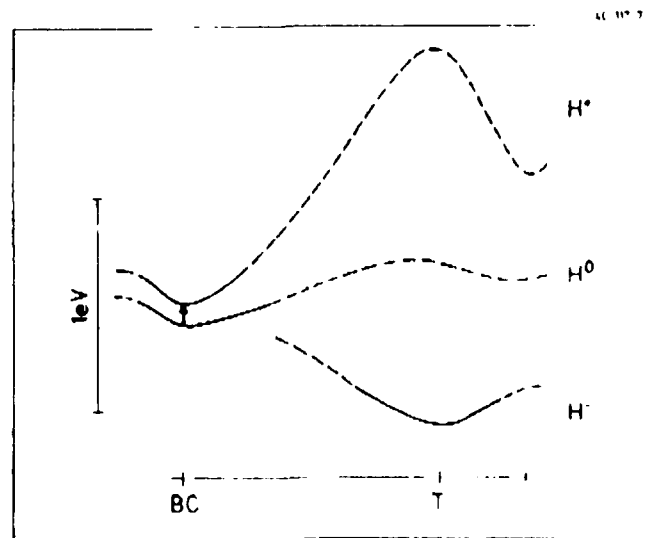


Fig. 1: Sketch of total-energy curves for  $H^+$ ,  $H^0$ , and  $H^-$  in n-type silicon based on the calculations in ref. [2]

As pointed out by Watkins[6] isolated hydrogen is expected to be a bistable defect. Recently, we have carried out DLTS experiments[3] in p-n diodes after implantation of about  $10^{10}$  H/cm<sup>2</sup> ( $\sim 3 \times 10^{14}$  H/cm<sup>3</sup>) at low temperatures (40 K). A hydrogen-related deep donor E3' with the ground state located at  $E_c - E_i = 0.16$  eV was observed. The E3'-defect transforms into a DLTS-invisible component at about 100 K (or 210 K) during zero-bias (or reverse-bias) annealing, and the decays of the E3'-signal are consistent with first-order processes,  $\nu = 3.0 \times 10^{12} \text{ s}^{-1} \exp[-0.29 \text{ eV}/k_b T]$  (or  $\nu = 1.3 \times 10^8 \text{ s}^{-1} \exp[-0.44 \text{ eV}/k_b T]$ ). The E3'-center is metastable, since the DLTS-signal can be regenerated by forward-bias injection at low temperatures. Very recent measurements of capacitance versus temperature indicate that the reverse-bias annealing of the ionized E3'-center occurs without any change in the charge state. However, as soon the bias is removed two electrons are captured. Thus in n-type silicon the DLTS-invisible component contains one additional electron compared with the non-ionized E3'-donor. On this basis it is suggested that the E3'-signal originates from the H<sup>0</sup> at the BC site. The zero-bias annealing stage at 100 K is ascribed to the transformation from H<sup>0</sup>(BC) to H(T), and the reverse-bias annealing stage is believed to reflect a jump from H<sup>0</sup>(BC) to H<sup>0</sup>(near-T), from which it relaxes into H(T) when electrons become available. In this context it is important to note that although H(T) represents the global minimum in energy (see fig 1), hydrogen may very well be trapped in the metastable configuration H<sup>0</sup>(BC) when it comes to rest in the crystal.

The assignment of E3' made above is consistent also with the EPR data of Gorelkinskii et al.[4]. In their case high-resistivity silicon was applied, and the local hydrogen concentration was about  $5 \times 10^{17}$  H/cm<sup>3</sup>. Thus the Fermi-level may be expected to have been close to mid-gap, and consequently the E3'-donor would have been ionized. This explains why the AA9-center was observed only during illumination[4]. In fig. 2 the lifetime  $\tau$  for annealing of the AA9-center (in the dark[4]) is shown as a function of inverse temperature together with the  $\tau$ -values from reverse-bias annealing of the E3'-defect. As can be seen from the figure the two sets of data are consistent, supporting that E3' originates from H<sup>0</sup>(BC).

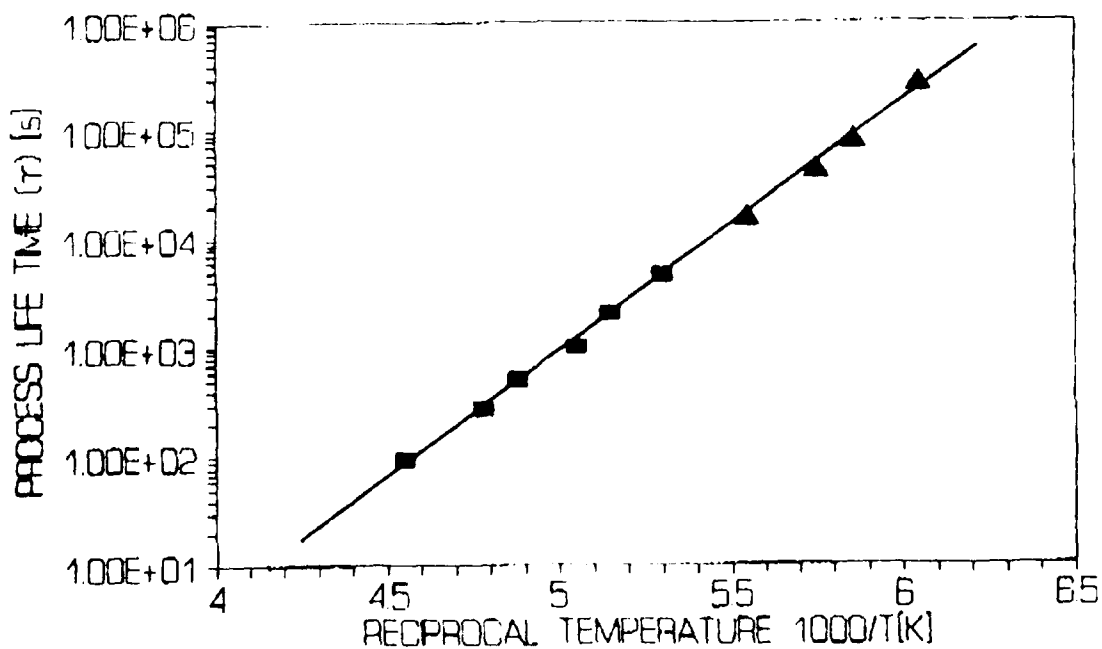


Fig. 2: The lifetimes  $\tau$  for the annealing of the AA9-center (■) (from ref.[4]) and the E3'-center (▲) (from ref. [3], reverse-bias annealing) shown as a function of inverse temperature.

Channeling measurements[7] was carried out after implantation of deuterium at 30 K ( $\sim 7 \times 10^{19}$  H/cm<sup>3</sup>) into intrinsic silicon (see fig. 3). The results showed that 80 % of the deuterium atoms occupies near-BC sites while the remaining 20% is located at near-T sites (see fig. 3). After annealing at 140 K the population of near-BC sites decreased and there was a corresponding growth of the near-tetrahedral component. Stein found a major Si-H stretching mode[8] at 1990 cm<sup>-1</sup> after implantation at 80 K ( $\sim 4 \times 10^{20}$  H/cm<sup>3</sup>) which annealed out at about 140 K with an activation energy of 0.36 eV. Since the implantation conditions in these experiments were rather similar the 1990 cm<sup>-1</sup> line was assigned to a local vibrational mode of hydrogen located at a near-BC site[7]. Stavola and Pearton suggested[9] that the 1990 cm<sup>-1</sup> may be associated with either H<sup>o</sup>(BC) or H<sup>+</sup>(BC). The frequency agrees with the theoretical estimates for H<sup>o</sup>(BC) which is  $1945 \pm 100$  cm<sup>-1</sup>, whereas the value  $2210 \pm 100$  cm<sup>-1</sup> calculated for H<sup>+</sup>(BC) seems a little high. Since the implanted doses were rather large the Fermi-level was close to mid-gap and the E3'-donor was therefore ionized, i.e. hydrogen at the BC site should have been positively charged. The activation energy for annealing of the 1990 cm<sup>-1</sup> line is apparently too low compared with that for the annealing of the AA9- or the ionized E3'-center. However, with a local concentration at about  $10^{20}$  H/cm<sup>3</sup> the average separation distance between hydrogen and the nearest defect will be less than 13 Å, and the BC configuration has to be distorted. Under such circumstances deviations should be expected. Never the less, the observations indicate that the dominant hydrogen-related complex formed during low temperature implantation may be described as "semi-isolated" BC site hydrogen.

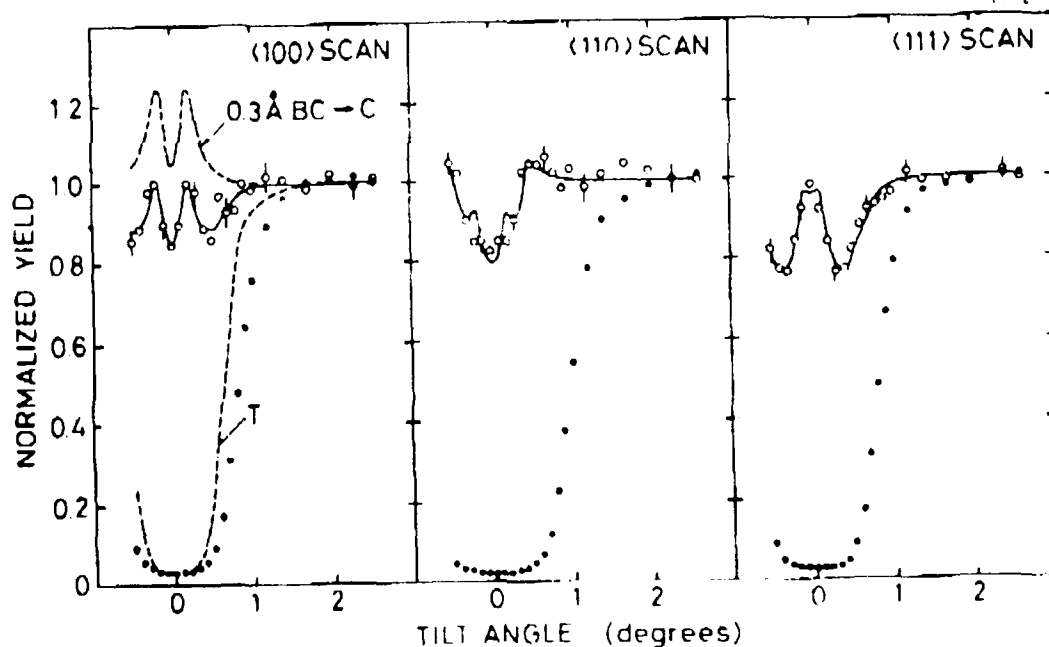


Fig. 3: Channeling scans for deuterium around the major axes in silicon. The solid line represents the best fit to the data, obtained with 80% of the atoms at near-BC sites and 20% at near-T sites.

As mentioned in the introductory remarks damage may represent a problem in application of ion-implantation. Hydrogen implanted at energies in the range 50-500 KeV creates 10-19 vacancy-interstitial pairs according to a TRIM calculation. However, due to recombination with migrating defects the actual number will be smaller. CV measurements on low-temperature hydrogen-implanted samples[3] (480 KeV) showed that about 1-2 electrically active defects were created per ion. In addition with a displacement energy of 20.4 eV a

hydrogen atom will have an average energy of about 150 eV just after its last collision. With this energy the hydrogen atom will be able to move about 200 Å away from the last vacancy-interstitial pair it created. This implies that for damage concentrations below  $\sim 10^{16}/\text{cm}^3$  (about  $10^{11} \text{ H}/\text{cm}^2$ ) the hydrogen atom will come to rest 200 Å away from the nearest defect. When the damage level is above  $\sim 10^{16}/\text{cm}^3$  we may assume that the hydrogen atoms come to rest in a region with a Gaussian distribution of defect traps. When the local hydrogen concentration is below  $10^{16} \text{ H}/\text{cm}^3$  ( $\leq 2 \times 10^{19}$  defects,  $\text{cm}^3$ ) the fraction of hydrogen atoms which end up being trapped to defects is  $\leq 5\%$ , if the defect-hydrogen trapping radius is 10 Å. This estimate is of course based on the assumption that hydrogen is immobile and does not recombine with migrating intrinsic defects. At low temperatures, below 60 K, only self-interstitials are believed to be mobile and most of these will recombine with vacancies. Thus a substantial part of the implanted hydrogen atoms may end up in a "semi-isolated" configuration, even for doses comparable to those applied in FTIR and channeling measurements.

Stein[8] found that the annealing of the  $1990 \text{ cm}^{-1}$  line at about 140 K is correlated with the growth in intensity of two other Si-H modes at  $1839 \text{ cm}^{-1}$  and  $2062 \text{ cm}^{-1}$ . These two lines are observed also after implantation at room temperature[10], and they disappear together after annealing at about  $200^\circ\text{C}$ . The annealing behavior of the lines are consistent with that of the near-T component observed with channeling[7], indicating that at least one of them is associated with hydrogen at a near-T site. However, in the same temperature range a strong near-BC component is also present[7]. In our view it is unlikely that hydrogen at a near-BC site should not give rise to a Si-H mode. On that basis it was suggested that the line at  $1839 \text{ cm}^{-1}$  (or  $2062 \text{ cm}^{-1}$ ) is associated with hydrogen at a near-BC site while the other at  $2062 \text{ cm}^{-1}$  (or  $1839 \text{ cm}^{-1}$ ) originates from hydrogen at a near-T site. Uniaxial stress measurements[10] demonstrated that both lines are associated with trigonal centers, and the stress-splitting could be analyzed with just one free parameter  $f_{\parallel}$  which describes the change in the effective Si-H force constant per unit stress applied parallel to the bond. The values obtained was  $f_{\parallel} = 0.58 \text{ N m}^{-1} \text{ GPa}^{-1}$  for the  $1839 \text{ cm}^{-1}$  line and  $f_{\parallel} = 3.30 \text{ N m}^{-1} \text{ GPa}^{-1}$  for the  $2062 \text{ cm}^{-1}$  line. Thus the stress dependence of the two centers are opposite and quantitatively very different, supporting the view that these lines reflect Si-H bonds in two different environments. Deák et al. suggested[11] that the two lines may originate from (the theoretical)  $\text{H}_2^+$ [11,12] so that the  $1839 \text{ cm}^{-1}$  and  $2062 \text{ cm}^{-1}$  lines correspond to vibrations of hydrogen at a near-BC site and at a near-T site, respectively. This assignment is seemingly consistent with the experimental findings mentioned above. However, one crucial check would be to see whether the lines split into two, in samples implanted both with hydrogen and deuterium. Such splitting was not observed in our previous work[10], but recently this result was disputed (see ref. [11]).

- [1] see e.g., S.J. Pearton, J.W. Corbett, and T.S. Shi, *Appl. Phys.* **A43**, 153 (1987)
- [2] C.G. Van de Walle, P.J.H. Denteneer, Y. Bar-Yam, and S.T. Pantelides, *Phys. Rev.* **B39**, 10791 (1989); R. Jones in "Proceedings of the 6th. Trieste Semiconductor Symposium, August 1990" (Eds. M. Stutzmann and J. Chevallier, North-Holland, 1991) p. 181
- [3] B. Holm, K. Bonde Nielsen, and B. Bech Nielsen, *Phys. Rev. Lett.* **66**, 2360 (1991)
- [4] Yu.V. Gurelinskii and N.N. Nevinnyi in "Proceedings of the 6th. Trieste Semiconductor Symposium, August 1990" (Eds. M. Stutzmann and J. Chevallier, North-Holland, 1991) p. 155; Yu V. Gurelinskii, private communication
- [5] R.F. Kiefl, M. Celio, T.L. Estle, S.R. Kretzman, G.M. Luke, T.M. Ruseman, and E.J. Ansaldo, *Phys. Rev. Lett.* **60**, 224 (1988)
- [6] G.D. Watkins in "Defects in Semiconductors 15, Budapest, Hungary, 1988" (Ed. G. Ferenczi, Materials Science Forum Vols 38-41, Trans Tech, 1989) p. 39
- [7] B. Bech Nielsen, *Phys. Rev.* **B37**, 6353 (1988)
- [8] H.J. Stein, *Phys. Rev. Lett.* **43**, 1030 (1979)
- [9] M. Stavola in "Hydrogen in Semiconductors, Semiconductors and Semimetals, Vol. 34, Eds. J.I. Pankove, and N.M. Johnson (Academic, NY, 1991)
- [10] B. Bech Nielsen and H.G. Grimmeiss, *Phys. Rev.* **B40**, 12403 (1989)
- [11] See P. Deák, L.C. Snyder, M. Heinrich, C.R. Ortiz, and J.W. Corbett in "Proceedings of the 6th. Trieste Semiconductor Symposium, August 1990" (Eds. M. Stutzmann and J. Chevallier, North-Holland, 1991) p. 253 and references therein.
- [12] K.J. Chang and D.J. Chadi, *Phys. Rev.* **B40**, 11644 (1989)

Hydrogen related complexes in neutron transmutation doped FZ silicon grown at a hydrogen atmosphere

Meng Xiang-ti

Institute of Nuclear Energy Technology  
Tsinghua University, Beijing 100084, CHINA

Hydrogen is one of the most important impurities in semiconductor materials. The study of the state and behavior of hydrogen and hydrogen-related defects in silicon is an interesting and noticeable area [1-4]. But still a great deal of confusion exists. In this paper, many obvious characters and new phenomena due to existence of hydrogen, the effect of hydrogen on electrical and optical properties of neutron irradiated and transmutation doped FZ silicon grown at a hydrogen atmosphere - NTD FZ(H<sub>2</sub>) Si, the hydrogen passivation of radiation defects, the behavior of hydrogen impurity, the interaction of hydrogen with radiation defects and other impurities, and the action of hydrogen as an indicator of some radiation defects and secondary defects were studied by Hall-coefficient-resistivity and minority carrier lifetime measurements, infrared (IR) absorption and deep level transient spectroscopy (DLTS) as well as positron annihilation technique (PAT).

Our main conclusion is as follows:

1. Hydrogen passivation effect

Hydrogen influences strongly the electrical properties of NTD FZ(H<sub>2</sub>) Si during annealing. A high concentration hydrogen-defect shallow donor (up to about  $2 \times 10^{15} \text{ cm}^{-3}$ ) produces in NTD FZ(H<sub>2</sub>) Si annealed at 300 - 600 °C [4]. Its maximum concentration, appearing and disappearing temperature depend on the starting silicon, thermal neutron doses and annealing parameters.

There is another big lifetime peak from 350 to 600 °C except a peak at about 850 °C on the minority carrier lifetime isochronal annealing curve.

Because of hydrogen the production rate of some radiation defects such as (V-V) and (V-O) decreases, the recovery temperature of the electrical properties such as free carrier concentration and mobility, and the annealing temperature of radiation defects lower [4, 5]. And hydrogen can prevent from the formation of the secondary defects related to vacancies (e.g., V<sub>4</sub> cluster: about 435 ps from positron annihilation lifetime measurements).

Hydrogen atoms begin to participate actively in the interaction with radiation defects above 200 °C. They diffuse into defects and saturate silicon dangling bonds to passivate the defects.

2. Hydrogen-related deep centers

We first measured many deep centers in as-grown, neutron and  $\gamma$ -ray irradiated FZ(H<sub>2</sub>) Si and studied their annealing behavior by DLTS, found several hydrogen-related deep centers although hydrogen in silicon has no energy level in energy gap, and suggested their possible structure models [4, 6]:

- 1).  $E_c - 0.20 \text{ eV}$ , Z center, (V+2H), observed in low dose neutron irradiated n- and p-type FZ(H<sub>2</sub>) Si,  $\gamma$ -ray irradiated n-type FZ(H<sub>2</sub>) Si and annealed NTD FZ(H<sub>2</sub>) Si irradiated with  $3 \times 10^{17} \text{ neutrons/cm}^2$ .
- 2).  $E_c - 0.35 \text{ eV}$ , E<sub>4</sub> center, (V-O+H), observed in low dose neutron irradiated n-type FZ(H<sub>2</sub>) Si and annealed NTD FZ(H<sub>2</sub>) Si.

- 3).  $E_v + 0.23$  eV,  $H_7$  center, ( $V_4 + nH$ ), observed in low dose neutron irradiated p-type FZ( $H_2$ ) Si.
- 4).  $E_c - 0.22$  eV, HD center, related to formation of the hydrogen-induced defects, observed in FZ( $H_2$ ) Si and NTD FZ( $H_2$ ) Si annealed in 500-650 °C.
- 5).  $E_c - 0.54$  eV wide DLTS peak, WB center, corresponding to the 4000  $cm^{-1}$  wide IR band (WB band) in NTD FZ( $H_2$ ) Si [7] due to electron transition from neutron radiation disordered region to hydrogen-defect shallow donor complexes or conduction band.

### 3. Si-H IR absorption bands

We have found about 20 new IR bands caused from the stretching vibration of Si-H bonds [7, 8], shown in Fig. 1.

In NTD FZ( $H_2$ ) Si cooled for 6 years at RT, the 1832 and 2054  $cm^{-1}$  strong neutron-induced Si-H IR peaks disappear, but the 1980 and 2065  $cm^{-1}$  IR peaks become still stronger, e.g., the strength of 1980  $cm^{-1}$  peak increases by 11 times. The change indicates that at RT the simple point defects can diffuse and interact, and hydrogen atoms may trap the vacancy and vacancy cluster [7].

We measured the formation and annealing activation energy, estimated the optical absorption cross sections and concentration for some important IR peaks. Comparing with the IR results of  $\gamma$ -ray irradiated and  $H^+$  implanted silicon as well as the DLTS and PAT results, based on their annealing behavior and activation energy as well as their dependence on neutron fluence and starting silicon, we identify them [7]:

- 1832 and 2054  $cm^{-1}$  ( $V+H$ )
- 1980  $cm^{-1}$  ( $V+2H$ ) ( $Z$  center:  $E_c - 0.20$  eV)
- 1970 and 1984  $cm^{-1}$  ( $V_2+nH$ ) ( $SiH_1$ )
- 2016  $cm^{-1}$  (split  $V_2+nH$ ) ( $SiH_2$ )
- 2162[9] and 1836  $cm^{-1}$  ( $V_3+mH$ ) ( $SiH_3$ )
- 1894  $cm^{-1}$  ( $V_4+nH$ ) ( $H_7$  center:  $E_v + 0.23$  eV)
- 2066  $cm^{-1}$  ( $V-O+2H$ )
- 2050-2150  $cm^{-1}$  wide IR band (disordered region +nH)

Among them, the identification of the 1832 and 2162  $cm^{-1}$  IR bands is basically in agreement with that in [10].

### 4. Hydrogen-defect shallow donor

The hydrogen-defect shallow donor in NTD FZ( $H_2$ ) Si is very different from the oxygen donor in CZ Si. It is the hydrogen and point defect complexes because there is no this shallow donor in as-grown, only fast neutron irradiated FZ( $H_2$ ) Si, or NTD FZ( $H_2$ ) Si kept for a longer time at RT.

It has been proposed that the 2162  $cm^{-1}$  IR absorption peak is due to the stretching vibration of the Si-H bond of hydrogen-defect shallow donor complex in the proton implanted silicon [9]. Indeed, we have observed the 2162  $cm^{-1}$  IR peak in NTD FZ ( $H_2$ ) Si irradiated by  $2.9 \times 10^{17}$  neutrons/cm<sup>2</sup>. This work has found that within the temperature range of the hydrogen-defect shallow defect, a new IR peak at 1836  $cm^{-1}$  appears and its annealing behavior is similar to that of the 2162  $cm^{-1}$  peak. In NTD FZ ( $H_2$ ) Si irradiated with  $1.13 \times 10^{18}$  neutrons/cm<sup>2</sup>, the concentration of the above donors

increases, but the  $2162\text{ cm}^{-1}$  peak does not appear, and another new peak at  $2016\text{ cm}^{-1}$  appears. In addition, a new peak at  $1954\text{ cm}^{-1}$  appears in both kinds of NTD FZ( $\text{H}_2$ ) Si. These show that hydrogen-defect shallow donors do not correspond to only one Si-H peak ( $2162\text{ cm}^{-1}$ ) and only one kind of Si-H vibrational center and defect structure.

The formation of hydrogen-defect shallow donor is because some weaker Si-H bonds break, and released hydrogen atoms diffuse and bind with the point defects. After the silicon dangling bonds are completely saturated by hydrogen atoms, or the Si-H bonds break and these vacancy-type defects anneal out, the donor property disappears.

#### 5. Disordered region-related wide IR band

A  $2050\text{--}2150\text{ cm}^{-1}$  wide IR band in NTD FZ( $\text{H}_2$ ) Si annealed at  $650\text{ }^\circ\text{C}$  has first been found[7]. Its appearance is due to hydrogen and neutron radiation defects, and is an evidence and hydrogen indication for the disordered region. It is the stretching vibrational mode of Si-H bonds formed because some weaker Si-H bonds break, hydrogen atoms diffuse into neutron radiation-induced disordered region defect clusters to saturate the silicon dangling bonds, and is similar to the wide IR band in a-Si:H[11]. The vibration frequency shift has been explained[12]. The hydrogen concentration in FZ( $\text{H}_2$ ) Si used in this study is estimated to be  $1\text{--}2 \times 10^{17}\text{ cm}^{-3}$  on the basis of the strength of this wide IR band. It is in a good agreement with the value  $1\text{--}1.5 \times 10^{17}\text{ cm}^{-3}$  measured with the melt-gas chromatography method. This supports the amorphous silicon-like model of the disordered region.

#### 6. Hydrogen-induced defect

The Si-H bond break and hydrogen aggregate in disordered region can cause the hydrogen-induced defects. We propose that the disordered region could be the nucleating centers of hydrogen and oxygen precipitation[7]. We also point out that a  $E_c\text{--}0.21\text{ eV}$  deep center ( $500\text{--}650\text{ }^\circ\text{C}$ ),  $250\text{ ps}$  positron lifetime component ( $650\text{ }^\circ\text{C}$ ) and minority carrier lifetime valley are all related to formation of the hydrogen-induced defect.

#### References

- [1] H.J. Stein, *Phys. Rev. Lett.* 43(1979)1030.
- [2] N.N. Gerasimenko, M. Rolle, L. J. Cheng, Y. H. Lee, J.C. Corelli, and J.W. Corbett, *Phys. Stat. Sol.(b)* 90 (1978) 689.
- [3] B.N. Mukashev, K.N. Nussupov, and M.F. Tamendarov, *Phys. Lett. A* 72 (1979) 381.
- [4] X. T. Meng, G. T. Du, and K. M. Liu, *Nucl. Sci. Engineering* 2 (1982) 172 (in Chinese).
- [5] X. T. Meng, B. Z. Zhang, Y. C. Du, and Y. F. Zhang, *Semicond. Tech.* 3 (1984) 31.
- [6] Y. C. Du, Y. F. Zhang, G. G. Qin, and X. T. Meng, *Acta Physica Sinica* 33 (1984) 477 (in Chinese); *Chin. Phys.* 5 (1985) 23 (in English).
- [7] X. T. Meng, Doctoral dissertation, Tsinghua University (1987).
- [8] X. T. Meng, Y. C. Du, and Y. D. Fan, *Phys. Stat. Sol.(a)* 101 (1987) 619.
- [9] L. C. Kimerling and J. M. Poate, *Lattice Def. in Semicond.* (1974), *Inst. Phys. Conf. Ser.* 23 (London and Bristol, 1975), p. 126.
- [10] B. B. Nielsen and H. G. Grimmeiss, *Phys. Rev. B* 40 (1989) 12403.
- [11] M. H. Brodsky, M. Cardona, and J. J. Cuomo, *Phys. Rev. B* 16 (1977) 3556.
- [12] X. T. Meng, Y. C. Du, Y. F. Zhang, and G. G. Qin, *J. Appl. Phys.* 63 (1988) 5606.

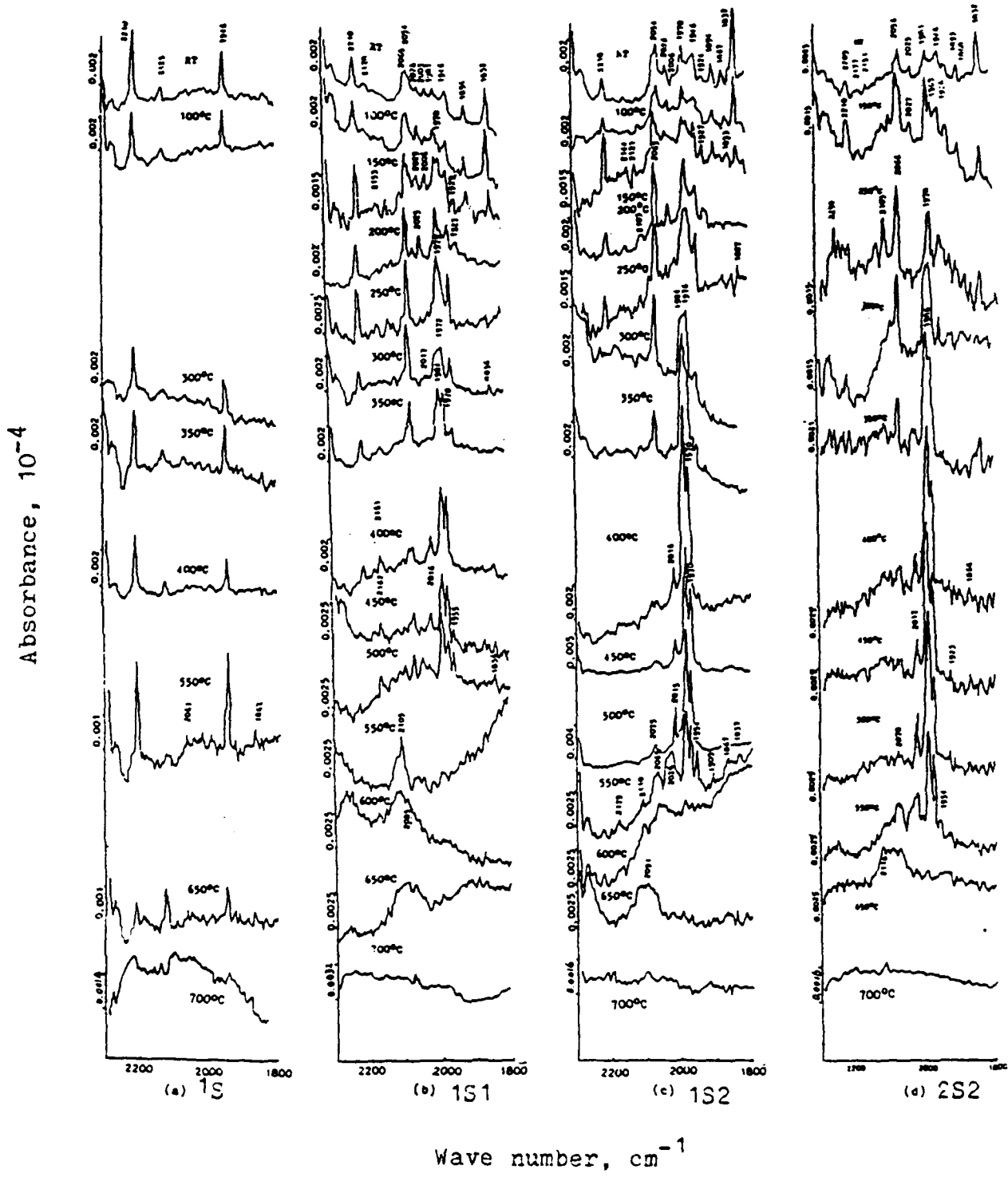


Fig. 1 Si-H stretching vibration IR absorption spectra of FZ(H<sub>2</sub>) Si and NTD FZ(H<sub>2</sub>) Si

- 1) 1S: FZ(H<sub>2</sub>) Si- 1
- 2) 1S1: NTD FZ(H<sub>2</sub>) Si- 1,  $2.9 \times 10^{17}$  neutrons /  $\text{cm}^2$
- 3) 1S2: NTD FZ(H<sub>2</sub>) Si- 1,  $1.13 \times 10^{18}$  neutrons /  $\text{cm}^2$
- 4) 2S2: NTD FZ(H<sub>2</sub>) Si- 2,  $1.13 \times 10^{18}$  neutrons /  $\text{cm}^2$

## VIBRATIONS OF HYDROGEN COMPLEXES IN SILICON

Peter Deák

Max-Planck-Institut für Festkörperforschung  
D-7000 Stuttgart 80, Heisenbergstr. 1, Germany

Michael Heinrich

Technische Universität Wien, Austria

Lawrence C. Snyder and James W. Corbett

State University of New York at Albany, USA

Infrared spectra of crystalline silicon grown in hydrogen or irradiated with protons exhibit a rich variety of hydrogen related bands.<sup>1,2</sup> Various centers have been proposed as the origin of these bands based on their behavior under heat treatment, uniaxial stress, isotope substitution, irradiation, or on their correlation with channeling results.<sup>3,4</sup> Using this information alone, a unique assignment has not yet been possible.

Si-H vibrations observe well defined trends in substituted silanes depending on the the nature and the environment of the bond. This can be well reproduced in a semi-empirical molecular orbital theory. Since the alternative structures proposed to explain the origin of a given band are very different (as far as the local environment of the Si-H bond is concerned), decision between them can be facilitated by properly scaled frequencies obtained from such calculations. As in our earlier calculations on hydrogen in silicon,<sup>5,6</sup> the MINDO/3 (modified intermediate neglect of differential overlap)<sup>7</sup> approximation has been employed to calculate the normal mode vibrations of defects involving a vacancy (V)

or self-interstitial (I) and/or hydrogen atoms. Details has been described earlier.<sup>8</sup>

We have found four basically different types of bonding with characteristic frequency regimes. The calculated (scaled) frequencies allow us to comment on the assignments proposed earlier.  $V(nH)$  and  $V_2(nH)$  complexes with  $n>1$  should give rise to vibration frequencies higher than  $2055\text{ cm}^{-1}$ , which is the frequency assigned to  $VH$  (or  $V_2H$ ). Our scaled frequencies for the hydrogen decorated split self-interstitial,  $I_{sp}HH$ , complex agree very well with the electron-irradiation sensitive double band at  $1980\text{ cm}^{-1}$ . Other self-interstitial related hydrogen complexes are also in this region. The calculated frequency of the negatively charged isolated hydrogen (in antibonding position) is close to the one observed at  $1835\text{ cm}^{-1}$  (such an assignment has been suggested as an alternative for this band).<sup>4</sup> Other possible assignments are also discussed.

1. S.J. Pearton, J. W. Corbett, and T. S. Shi, *Appl.Phys.A* **43**, 153 (1987).
2. H. J. Stein, *J.Electron.Mater.* **4** (1975) 159, and *Phys.Rev.Lett.* **43** (1979) 1030.
3. B.N. Mukashev, M. F. Tamendarov, and S. Z. Tokmoldin, in: "Defects in Semiconductors 15", G. Ferenczi ed., *Mater.Sci.Forum* 38-41, (Trans Tech Publications Switzerland-Germany-UK-USA, 1989) p. 1038.
4. B. Bech Nielsen and H. G. Grimmeiss, *Phys.Rev.B* **40** (1989) 12403.
5. P. Deák, L. C. Snyder, and J. W. Corbett, *Phys.Rev.B* **37** (1988) 6887.
6. P. Deák and L. C. Snyder, *Radiation Effects and Defects in Solids*, 111-112 (1989) 77.
7. R. C. Bingham, M. J. S. Dewar, and D. C. Lo, *J.Am.Chem.Soc.***97**, 1285 (1975).
8. P. Deák, L. C. Snyder, M. Heinrich, C. R. Ortiz, and J. W. Corbett, *Physica B* **170**, 253 (1991).

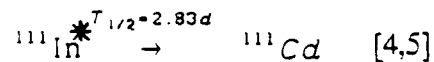
## HYDROGEN NEUTRALIZATION OF DOUBLE ACCEPTOR CENTERS IN SILICON

G.Pensl, M.Lang, and P.Stolz<sup>1)</sup>  
Institute of Applied Physics, University Erlangen-Nürnberg  
Staudtstr. 7, D-8520 Erlangen

### Energy levels in Zn-, Be- or Cd-doped Si samples

Zinc, beryllium, and cadmium form isolated substitutional centers in silicon and a variety of complexes containing further extrinsic atoms or intrinsic defects. The chemical nature of such complexes is usually not identified. The isolated substitutional centers act as double acceptors [1,2,3,4,5].

The investigated elements are incorporated in Si by diffusion (Zn, Cd) [2,4], by standard implantation (Be) [2], or by implantation of radioactive probe atoms which are transmuted into stable daughter nuclei, e.g. stable Cd according to



The generated defect levels are analyzed by deep level transient spectroscopy (DLTS), Hall effect and IR absorption measurements. The implantation damage is annealed in a Rapid Isothermal Annealing (RIA) system [6]. Be- and Cd-related centers are thermally unstable at relatively low temperatures as demonstrated in Figs. 1 and 4a,b; the investigated centers can be generated or annihilated depending on the annealing temperature, annealing period or ramp down velocity of the diffusion temperature. This thermal instability is responsible for the complicated experimental situation with respect to the hydrogen neutralization of Zn-, Be and Cd-related defects. The following levels are determined:

a) **Si(Al) : Zn** [2] (see Fig. 2)

$$\begin{aligned} \text{Zn}^{0/-} &= E_v + 319 \text{ meV}, \quad \text{Zn}^{-/2-} = E_v + 698 \text{ meV} \text{ (double acceptor)} \\ \text{Zn}(x1) &= E_v + 277 \text{ meV} \\ \text{Zn}(x2) &= E_v + 345 \text{ meV} \end{aligned}$$

b) **Si(B) : Be** [2] (see Fig. 3)

$$\text{Be}^{0/-} = E_v + 190 \text{ meV}, \quad \text{Be}^{-/2-} = E_v + 440 \text{ meV} \text{ (double acceptor)}$$

c) **Si(B) : Cd** [4,5] (see Fig. 4b)

$$\begin{aligned} \text{Cd}^{0/-} &= E_v + 485 \text{ meV}, \quad \text{Cd}^{-/2-} = E_c - 450 \text{ meV} \text{ (double acceptor)} \\ (\text{Cd}^{-/2-} &\text{ is observed in P-doped Si samples, not shown in Fig. 4, see [4]}) \end{aligned}$$

$$\begin{aligned} \text{Cd}(B1) &= E_v + 200 \text{ meV} \\ \text{Cd}(B2) &= E_v + 400 \text{ meV} \end{aligned}$$

---

1) present address: Eberle GmbH, Oedenberger Str. 55, 8500 Nürnberg

### Hydrogen neutralization of double acceptors

The hydrogen passivation of Zn-, Be- or Cd-doped Si samples was performed by a remote microwave plasma and exposed to monatomic hydrogen at sample temperatures of 200°C for 1h. All the observed levels were completely neutralized by the hydrogenation process (see Figs. 2 (dotted line), 3 (dashed line), and 4 (solid line)). The following additional levels appear after the hydrogenation process:

a) Si(B) : Be [2]

$$\text{Be(H)} = E_v + 101 \text{ meV}$$

b) Si(B) : Cd

$$\text{Cd(H1)} = E_v + 135 \text{ meV}$$

$$\text{Cd(H2)} = E_v + 260 \text{ meV}$$

These new levels could not be identified yet. We suggest that these complexes are H-related and contain at least one hydrogen atom [7,8].

Subsequent heat treatments of the neutralized defects result in DLTS spectra as given in Figs. 2,3, and 4c. The spectra demonstrate that the double acceptors recover simultaneously during the thermal anneal. The evaluation of the reactivation energy of the Zn double acceptor results in  $E_a = 2.2 \pm 0.3 \text{ eV}$  (see Fig.5)

It appears that a single hydrogen atom bonded at the defect site is sufficient to remove both energy levels of the double acceptor center. However, it is still an open question whether levels Be(H), Cd(H1), and Cd(H2) represent such an H-related complex. In order to obtain additional information on their chemical compositions, we plan to investigate the hydrogenated defects by IR absorption. This optical method becomes now applicable because of a new hydrogenation technique [9] that achieves the hydrogenation of defect centers throughout the bulk of a Si wafer. In a first run, we have tested this new technique and succeeded in passivating the total concentration of Zn-related levels in a Si sample of 400  $\mu\text{m}$  thickness.

### References

1. Landolt-Börnstein, Bd.22, Teilbandb, Störstellen und Defekte in Elementen der IV-Gruppe und III-V-Verbindung, Ed. M.Schulz, p.270 ff (1989) (see references herein)
2. P.Stolz, Ph.D.Thesis, Erlangen, 1990
3. B.Kaufmann, A.Dörmen, M.Lang, G.Pensl, D.Grünebaum, N.Stolwijk: Proceedings ICDS 16th, Bethlehem, 1991
4. M.Lang, G.Pensl, M.Gebhard, N.Achtziger, M.Uhrmacher: Appl.Phys.A53, 95(1991)
5. M.Lang, G.Pensl, M.Gebhard, N.Achtziger, M.Uhrmacher: Proceedings ICDS 16th, Bethlehem, 1991
6. P.Stolz, G.Pensl, D.Grünebaum, N.Stolwijk: Mat.Science and Eng. B4, 31 (1989)
7. K.Muro, A.J.Sievers: Phys. Rev. Lett. 57, 897 (1986)
8. E.Merk, J.Heyman, E.E.Haller: Mat.Res.Soc.Symp. Proc. 163, 15 (1990)
9. I.A.Veloarisoa, D.M.Kozuch, M.Stavola, R.E.Peale, G.D.Watkins: Proceedings ICDS 16th, Bethlehem, 1991

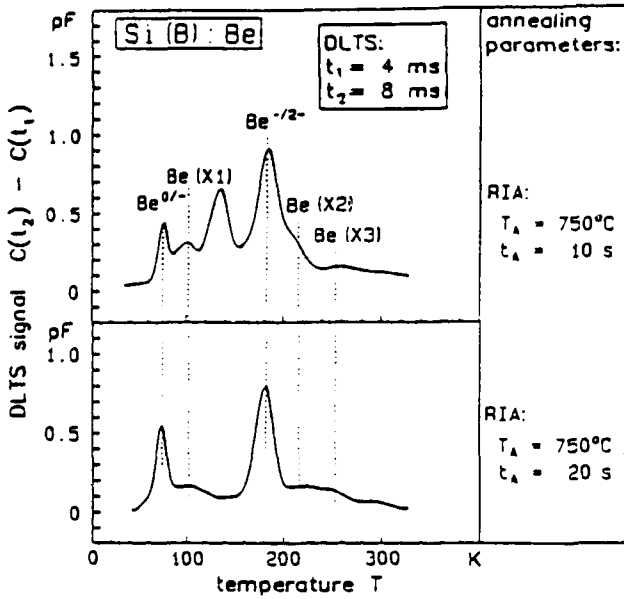


Fig.1. DLTS spectra of a Be-implanted Si sample recorded after various heat treatments in a RIA system.

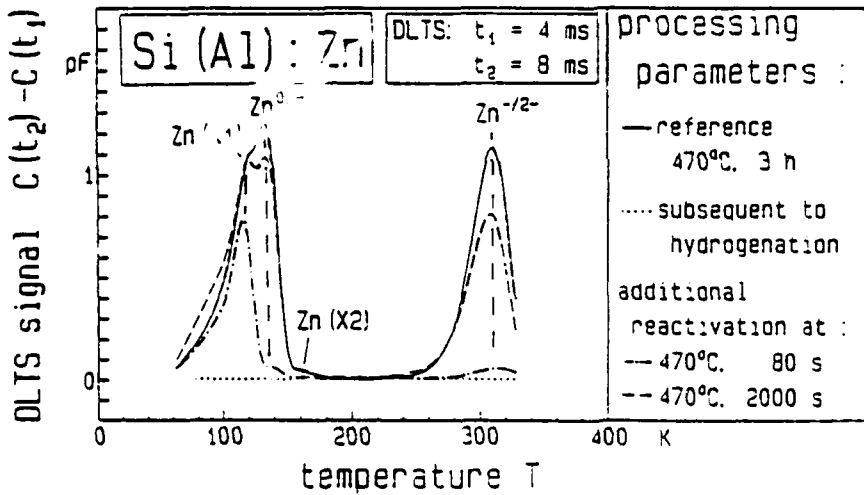


Fig.2. DLTS spectra of a Zn-diffused Si sample taken after different processing steps.

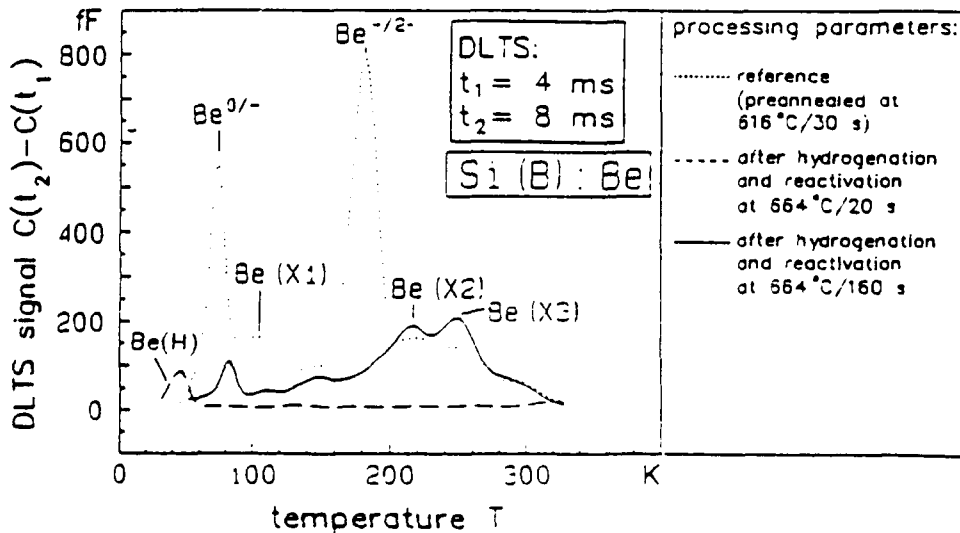


Fig.3. DLTS spectra of a Be-implanted Si sample taken after different processing steps.

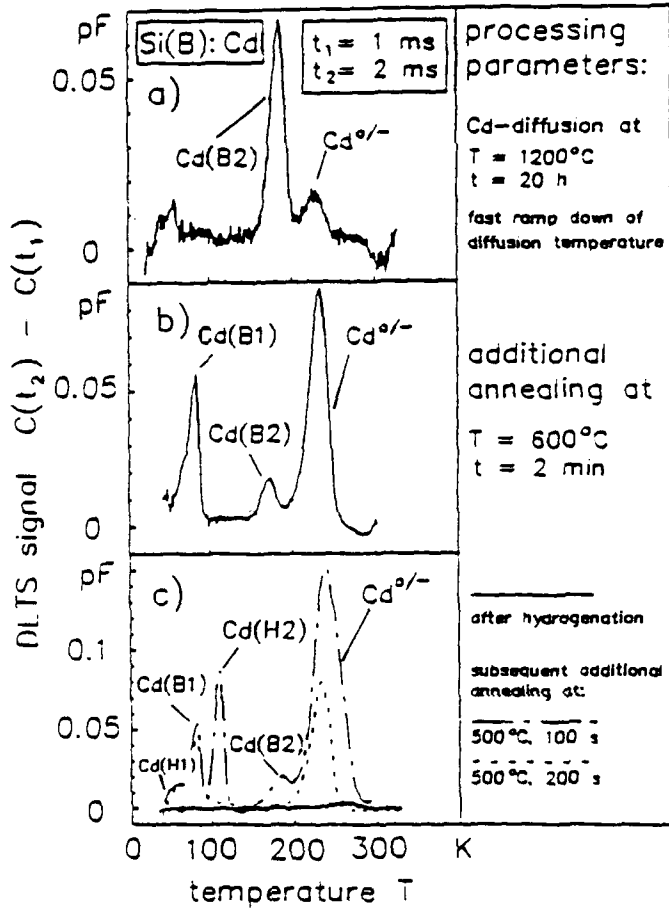


Fig.4. DLTS spectra of a Cd-diffused Si sample taken after different processing steps.

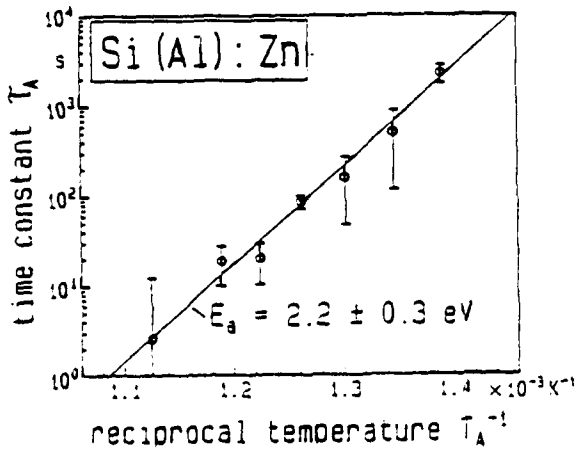


Fig.5. Time constant  $\tau_A$  vs. reciprocal anneal temperature  $T_A^{-1}$ ; the reactivation energy  $E_a$  of H-passivated Zn double acceptors is determined from the slope of the straight line.

**B. PAJOT, R. DARWICH AND C. SONG**

*Groupe de Physique des Solides, Tour 23, Université Paris 7, 2 place Jussieu, 75251, Paris  
Cedex 05, France*

**1. STABILITY OF HYDROGEN COMPLEXES IN SEMI-INSULATING (SI) INDIUM PHOSPHIDE GROWN BY THE LIQUID ENCAPSULATED CZOCHRALSKI (LEC) METHOD.**

In order to obtain highly doped InP samples which can be used for piezo-spectroscopic measurements after hydrogenation, relatively thick (1.5 mm) transparent SI InP substrates are required on which thin ( $\approx 3 \mu\text{m}$ ) epilayers are deposited. Now, SI LEC InP is known to contain hydrogen-related complexes<sup>1</sup> and their absorption have to be determined to differentiate it from the absorption of the active layer. Moreover, the growth of the epilayers by MOVPE is performed near  $650^\circ\text{C}$  so that the effect of such an annealing has to be studied on the substrate.

Oriented substrate slices and reference samples were cut from an as-grown SI InP:Fe cone kindly provided by J.P. Farges from L.E.P. The lines observed at 6 K in the reference samples are listed in Table 1. It shows in the as-grown sample the PH,Zn line<sup>3</sup> at  $2288 \text{ cm}^{-1}$ , the strong  $2316 \text{ cm}^{-1}$  line, related to an intrinsic H defect<sup>4</sup> and three new weak lines at  $2306.8$ ,  $2307.2$  and  $2311 \text{ cm}^{-1}$ . After annealing for 3 hours at  $600^\circ\text{C}$  in a sealed ampoule

Table 1

Lines observed at 6 K in LEC-grown SI InP:Fe #184 for characteristic heat treatments

Line position ( $\text{cm}^{-1}$ )	As-grown	Annealed 3 hours at $600^\circ\text{C}$	Annealed 3 hours at $650^\circ\text{C}$
2202.39*	NO	YES	YES
2250.74*	"	"	"
2254.7*	"	"	"
2273.42*	"	NO	"
2282.8	"	YES	NO
2287.71*	YES	"	YES
2306.82	"	"	"
2307.17	"	"	"
2311.28	"	"	"
2315.62*	"	"	"

\* Reported in Ref. 2

with a phosphorus overpressure, the lines at 2202, 2251 and 2255  $\text{cm}^{-1}$  emerge from the background at the expense of the intensity of the 2316  $\text{cm}^{-1}$  line. This can be interpreted as a partial dissociation of the complexes responsible for that line followed by the trapping of hydrogen by more stable defects or by the partial transformation of the 2316  $\text{cm}^{-1}$  defect into other defects. For non cumulative annealing for 3 hours at 650  $^{\circ}\text{C}$ , the intrinsic 2202  $\text{cm}^{-1}$  line still grows at the expense of the 2316  $\text{cm}^{-1}$  line and a very weak and sharp line is also observed at 2273  $\text{cm}^{-1}$ . After this annealing, the Zn,H line is only reduced by a factor of 2, indicating a relatively high stability of this complex at low concentration ( $\approx 2 \times 10^{14}$   $\text{at}/\text{cm}^3$ ).

The structure of the defects related to the lines at 2202 and 2316  $\text{cm}^{-1}$  have been discussed in ref. 4. It is clear from the spectroscopic measurements under a uniaxial stress that the centres associated with these lines and with the new lines at 2306.8, 2311  $\text{cm}^{-1}$  have a trigonal symmetry. A comparison with the spectra of the InP:Zn/InP:Fe structures shows the presence of the 2202  $\text{cm}^{-1}$  line indicating that the corresponding center has also been formed during the growth of the epilayer.

## 2. OH AND NH COMPLEXES IN SEMI-INSULATING GALLIUM ARSENIDE

OH- and NH-related lines have been observed at 6 K in as-grown LEC SI GaAs in the 2945-3500  $\text{cm}^{-1}$  range. Oxygen has been identified to be involved in the strongest line at 3300  $\text{cm}^{-1}$  because of the  $^{18}\text{O}$  isotope effect. The intensity of some of these lines is photo-sensitive in the samples where EL2<sup>+</sup> is present at thermal equilibrium (Fig. 1).

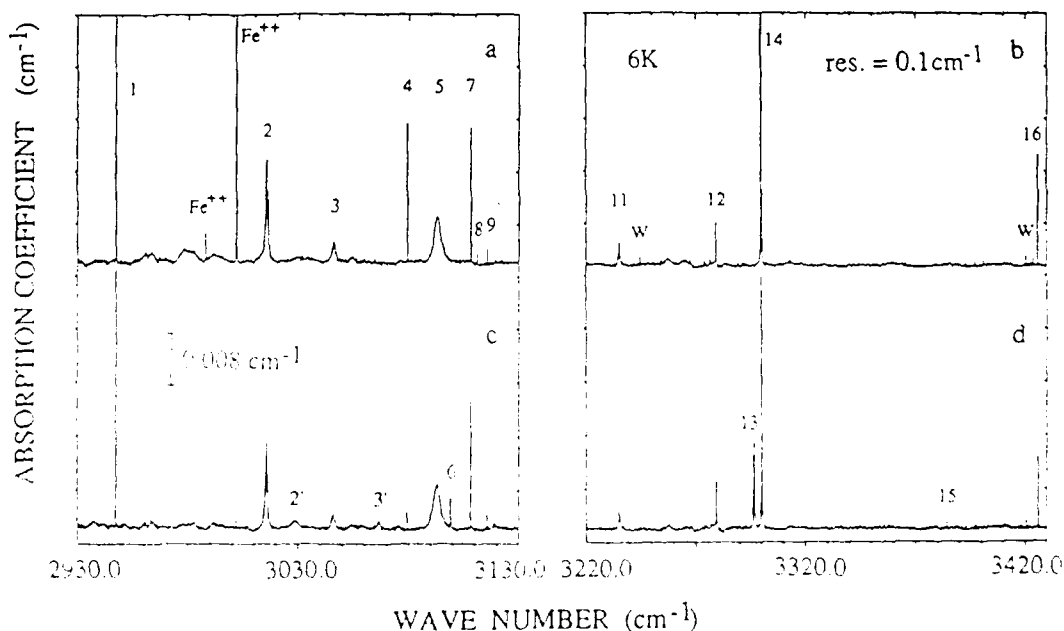


Figure 1. a and b: Absorption of GaAs sample #1 under thermal equilibrium. The labelling is that of Table 1. Line 10 is not observed in this sample and line 17 (not shown) is about 2 times larger than line 15. Line 14 is truncated at 16% of its peak absorption. c and d: Same as a and b after 150 minutes illumination with 1.25 eV photons. Line 14 is truncated at 20% of its peak absorption. Residual water vapor lines are noted W.

There is proof that it is due to the trapping of free holes by these H complexes which can exist under at least two charge states<sup>5,6</sup>.

The properties of the OH bond related to the 3300 cm<sup>-1</sup> line has been specially investigated. It seems to be weakly bonded to the lattice and the splitting behaviour of the line under uniaxial stress indicates that the OH bond can reorient at low-temperature.

These XH centres seems to be relatively stable under electron irradiation, but after such an irradiation, a new XH line is however observed which must come from the dissociation of existing complexes. The stability of these complexes after annealing under different atmospheres is presently investigated.

1. B. Clerjaud, D. Côte and C. Naud, Phys. Rev. Lett. 58, 1755 (1987).
2. J. Chevallier, B. Clerjaud and B. Pajot in Semiconductors and Semimetals, Vol 34 (Academic Press, Inc., Orlando, 1991), p. 447.
3. B. Pajot, J. Chevallier, A. Jalil and B. Rose, Semicond. Sci. and Technol. 4, 91 (1989).
4. B. Clerjaud, Physica B 170, 383 (1991).
5. B. Pajot and C. Song and C. Porte, to be published in the Proc. of ICDS16, Lehigh 21-26 July 1991, edited by G. Davies (Trans Tech Public., Singapore).
6. B. Pajot and C. Song, to be published in Phys. Rev. B.

## What did we learn from PAC Experiments about Hydrogen in Semiconductors ?

M. Deicher<sup>1</sup>, R. Keller<sup>1</sup>, R. Magerle<sup>1</sup>, W. Pfeiffer<sup>1</sup>, P. Pross<sup>1</sup>, H. Skudlik<sup>1</sup>,  
Th. Wichert<sup>2</sup>  
and ISOLDE Collaboration<sup>3</sup>

<sup>1</sup>*Fakultät für Physik, Universität Konstanz, D-7750 Konstanz, FRG*

<sup>2</sup>*Technische Physik, Universität des Saarlandes, D-6600 Saarbrücken, FRG*

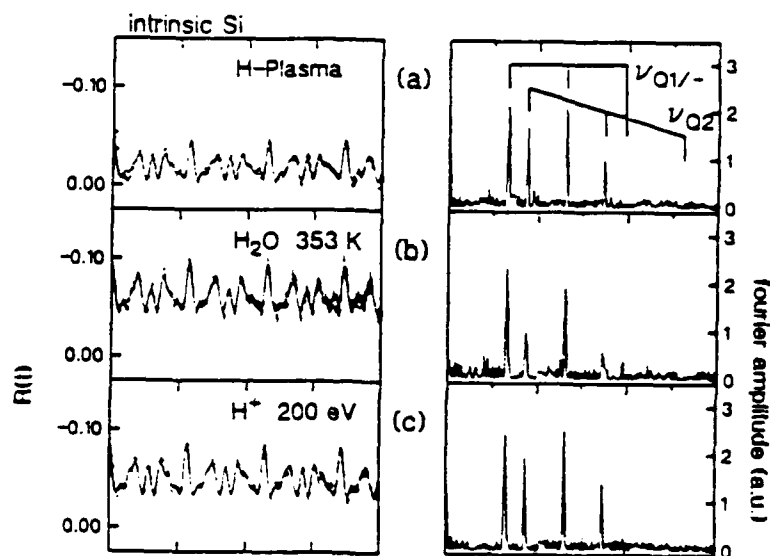
<sup>3</sup>*CERN, CH-1211 Geneva 23, Switzerland*

Using the radioactive probe atoms  $^{111}\text{In}$  or  $^{111m}\text{Cd}$  the Perturbed Angular Correlation technique (PAC) is able to investigate the formation of acceptor-H complexes in elemental semiconductors as well as in III-V compound semiconductors. PAC is sensitive to the direct vicinity of the probe atom, any impurity or point defect in next neighborhood creating an electrical field gradient (efg) at the probe nucleus site is deduced via the modulation of the spatial anisotropy of two subsequently emitted gamma quanta. More information on the technique and its application in semiconductors is given by Wichert et al. (1). The total number of probe atoms necessary to perform PAC experiments is in the order of  $10^{11}$ , allowing experiments with local concentrations well below  $10^{17} \text{ cm}^{-3}$  after implantation of the probe atoms and subsequent annealing of irradiation damage.

Unfortunately the chemical nature of the defect could not be extracted from the observed modulation. To use this technique to obtain general information on the passivation process, an unquestionable identification of the chemical nature of observed defects is necessary. This is achieved by combination of different passivation procedures, especially the use of low energy hydrogen implantation (about 150 eV implantation energy), and the application of electrical measurements. Knowing the chemical nature of the complex PAC reveals information on the amount of formed complexes, its symmetry and dynamic behavior.

To investigate a possible acceptor-hydrogen complex formation an intrinsic Si sample was doped with  $^{111}\text{In}$  and exposed to a hydrogen plasma (13.56 MHz, 320 V). In Fig. 1a the PAC spectra and its corresponding Fourier transform taken from this sample at 300K are shown. Pronounced oscillations indicating the formation of two well defined complex configurations around about 50 % of the probe atoms are seen. Each complex is characterized by a frequency triplet in the Fourier transform. The efg's are labeled  $\nu_{Q1/2} = 349 \text{ MHz}$  and  $\nu_{Q2} = 463 \text{ MHz}$ . The same efg's are observed after boiling an identical sample in water for 100 min in darkness (Fig. 1b) and after low

Figure 1



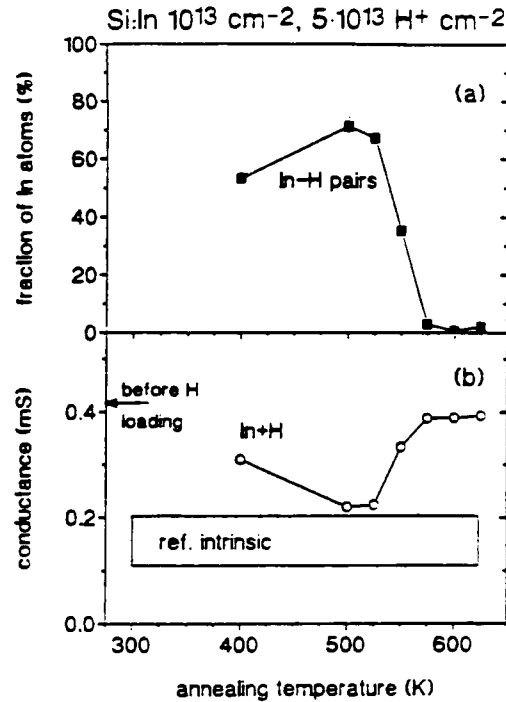
energy hydrogen implantation with 200 eV and a total dose of  $10^{14} \text{ cm}^{-2}$  (Fig. 1c) (2). An additional configuration labeled  $\nu_{Q1/0} = 270 \text{ MHz}$  is observed in highly B-doped Si. Because no or very few intrinsic defects are created in case of the  $H_2O$  treatment or during low energy implantation, complexes formed between In and intrinsic defects can be ruled out. Because of mass selected implantation nothing but hydrogen was introduced into the sample verifying that hydrogen has been trapped at the  $^{111}\text{In}$  probe atoms (3). Isochronal annealing experiments reveal the same stability for all three observed configurations, indicating, that only one In-H complex is formed.

The PAC result reveals the symmetry of the complex after the decay from  $^{111}\text{In}$  to  $^{111m}\text{Cd}$ . Therefore, from measurements with different sample orientations we can only determine the symmetry and dynamic behavior of the resulting Cd-H complex, which should now act as a single acceptor in Si. All efg's are oriented along  $\langle 111 \rangle$  lattice directions. The occurrence of different defect configurations as a function of electronic parameters was investigated in more detail (4, 5, 6) and is well understood for the transition between the two complex configurations labeled  $\nu_{Q1/-}$  and  $\nu_{Q1/0}$ . It is described in terms of different charge states of the Cd-H acceptor according to the position of the fermi level (4, 6).

Having undoubtedly identified the chemical nature of the observed complex PAC can be used to investigate more general aspects of hydrogen passivation. The correlation between electrical deactivation deduced from electrical measurements and acceptor-H pair concentration measured by PAC in the same sample, clarifies the question whether every deactivated acceptor atom is involved in an acceptor-H pair. In other words,

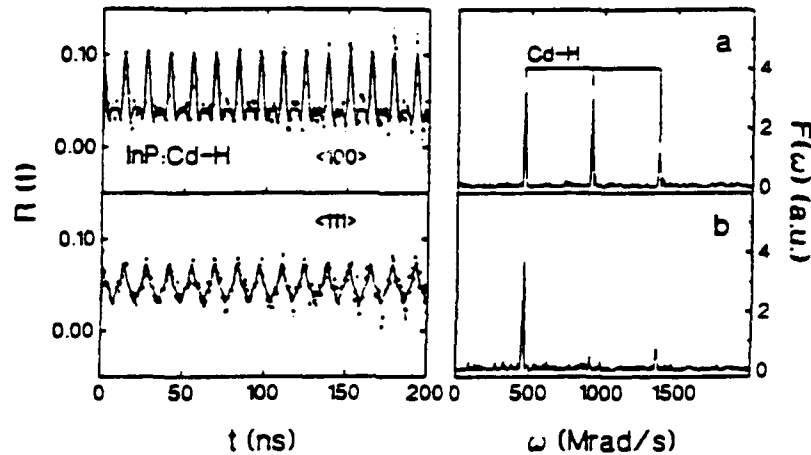
whether the passivation process and not compensation is the only relevant deactivation mechanism. For this purpose four point resistivity measurements were performed parallel to the PAC experiment. In order to achieve a detectable electrical conductivity intrinsic Si was implanted with stable  $^{115}\text{In}$  ( $10^{13} \text{ cm}^{-2}$ , 350 keV) in addition to the implanted radioactive  $^{111}\text{In}$  ( $10^{11} \text{ cm}^{-2}$ ). After annealing of implantation damage (1173 K, 10 min, furnace) an electrical conductivity of about 0.4 mS was observed (Fig. 2b), indicating that about 80% of the implanted In was electrically active after this procedure. Subsequently the sample was loaded by low energy hydrogen implantation (200 eV,  $5 \cdot 10^{13} \text{ cm}^{-2}$ , implantation temperature 400 K). A drop of electrical conductivity to 0.2 mS (Fig 2b) and the formation of In-H pairs at 60 % of the In atoms was detected by PAC (Fig 2a). Annealing of this sample above 500 K is leading to a reduction of the amount of In-H pairs accompanied by an increase of electrical conductivity (Fig. 2a,b). A quantitative analysis of this experiment proved that the amount of In-H pairs seen by PAC follows directly the fraction of deactivated In in the sample. This direct correlation proves that passivation is the only deactivation mechanism (3).

Figure 2



In III-V compound semiconductors we have used the probe atom  $^{111m}\text{Cd}$ , an excited state of  $^{111}\text{Cd}$ , which could be produced and implanted (60 keV) at the ISOLDE facility in Geneva. Since no elemental transmutation takes place in this case, the PAC results reveal directly the properties of the formed complexes. The implantation damage after implantation in InP and GaAs was removed by rapid thermal annealing. In Fig. 3 a,b the PAC signal after hydrogenation with low energy ion implantation ( $150 \text{ eV}, 3 \cdot 10^{14} \text{ cm}^{-2}$ , implantation temperature 370 K) proves the formation of Cd-H. The efg is symmetric along  $\langle 111 \rangle$  lattice directions and the corresponding hyperfine coupling constant is  $\nu_Q = 484 \text{ MHz}$ . The same signal was observed after hydrogen plasma treatment (7,9). Additional to the investigation of the thermal stability of this complex.

Figure 3



which is reported by Baurichter et al. (7,9) we have also investigated the formation efficiency of Cd-H pairs as function of the achieved electrical activation of the acceptor Cd controlled by the annealing temperature and with variation of the hydrogen implantation temperature. The efficiency of pair formation reflects directly the activation of Cd, indicating that the Cd atom must be in a negative charge state to attract the hydrogen atom. Therefore hydrogen should be most probably in a positive charge state during diffusion. The efficiency of pair formation is increased with higher implantation temperature reflecting the higher mobility of hydrogen.

### References

- (1) Th. Wichert, M. Deicher, G. Grübel, R. Keller, N. Schulz, and H. Skudlik, Appl. Phys. A 48, 59 (1989).
- (2) H. Skudlik, M. Deicher, R. Keller, R. Magerle, W. Pfeiffer, and P. Pross, presented on the E-MRS Spring Meeting (1991), Strasbourg, France, Nucl. Instr. and Meth. B, in press.
- (3) H. Skudlik, M. Deicher, R. Keller, R. Magerle, W. Pfeiffer, P. Pross, and E. Recknagel, submitted to Phys. Rev. B
- (4) H. Skudlik, M. Deicher, R. Keller, R. Magerle, W. Pfeiffer, D. Steiner, and E. Recknagel, submitted to Phys. Rev. B
- (5) M. Gebhard, B. Vogt, and W. Witthuhn, Phys. Rev. Lett., 67, 847 (1991).
- (6) N. Achtziger and W. Witthuhn, in "Submicroscopic Investigation of Defects in Semiconductors", ed. by G. Langouche, North Holland, in press
- (7) A. Baurichter, N. Achtziger, D. Forkel, M. Gebhard, B. Vogt, and W. Witthuhn, Contribution to this workshop.
- (8) W. Pfeiffer, M. Deicher, R. Keller, R. Magerle, E. Recknagel, H. Skudlik, Th. Wichert, H. Wolf, D. Forkel, N. Moriya, and R. Kalish, Appl. Phys. Lett. 58, 1751 (1991).
- (9) A. Baurichter, M. Deicher, S. Deubler, D. Forkel, H. Plank, H. Wolf, and W. Witthuhn, Appl. Phys. Lett. 55, 2301 (1989).

## Structure, Stability and Internal Dynamics of Cd-H Complexes in Semiconductors

A. Baurichter, N. Achtziger, D. Forkel\*, M. Gebhard, B. Vogt, and W. Witthuhn

*Physikalisches Institut der Universität Erlangen-Nürnberg, D-8520 Erlangen, Germany*

*\*present address: PPE Division, CERN, CH-1211 Geneva 23, Switzerland*

Information on hydrogen decorated acceptors in elemental and compound semiconductors is obtained from the interior of the complexes by analyzing the perturbed angular correlation (PAC) of gamma quanta emitted by radioactive acceptor atoms. Since the PAC spectroscopy detects the electrical field gradient at the site of a probe nucleus via hyperfine interaction, it enables the study of structure and stability of impurity-hydrogen pairs, as well as the investigation of dynamical processes like charge fluctuations inside and around these complexes in the time range from nanoseconds to microseconds. Examples for each of these observables will be given.

The structure and stability of Cd-defect complexes formed in H-plasma exposed GaAs, InAs, GaP, InP, and InSb samples have been studied through the PAC probe atom  $^{111}\text{mCd}$ , which decays into the ground state of  $^{111}\text{Cd}$  via a  $\gamma\text{-}\gamma$  cascade. Undoped III-V-compound samples were implanted by 60 KeV  $^{111}\text{mCd}^+$  ions to doses of  $10^{11}\dots 10^{12}\text{ cm}^{-2}$  at the on-line mass separator ISOLDE of CERN. After rapid thermal annealing (GaAs, InAs, GaP, InP) or furnace annealing in sealed quartz ampoules (InSb), most of the probe atoms (50-80%) were located on lattice sites with vanishing electrical field gradients, indicating substitutional lattice positions. Finally, the specimens were exposed to a parallel plate dc  $\text{H}_2$  glow discharge (30 min. at 400...500 K), with the implanted surface in direct contact with the plasma. This treatment yields in the formation of at least one Cd-defect complex per compound, as revealed by PAC analysis [1,2]. The formation of two complexes is observed in GaAs and InAs. All defect configurations are characterized by axially symmetric field gradients. The orientation of the electrical field gradients in  $\langle 111 \rangle$  lattice directions can be extracted from the spectra, except for one of the complexes in InAs, and the complex in InSb. The data are insufficient for the determination of the orientation in the latter cases. The quadrupole coupling constants vary between  $\nu_Q = 357\text{ MHz}$  (InSb) and  $\nu_Q = 581\text{ MHz}$  (InAs) and scale approximately with the inversed cube of the lattice constants. A simple point charge model approach indicates, that the same defect species is trapped at the Cd acceptors. Since experiments on low energy proton implantation ( $E = 150\text{-}$

400 eV) yield in the same PAC results [3], this species can be identified with hydrogen. The observed symmetry reflects the symmetry of the structural model proposed for acceptor hydrogen pairs in III-V-compounds, based on results from IR spectroscopy on GaAs and InP with various acceptors [4]. The assignment in terms of Cd-H pairs is supported by annealing experiments. Figure 1 and figure 2 display the results of isochronal (10 min.) annealing experiments on hydrogenated GaAs, InP and InAs samples. A first order dissociation reaction is fitted to the GaAs and InP data, assuming a value of  $\nu = 7 \cdot 10^{13} \text{ s}^{-1}$  for the attempt frequency, which was found for Zn-H pairs in GaAs [5], and which can also be related to the stretching mode of the As-H bond [4]. The fits yield a dissociation energy of  $E_D = 1.3(0.1) \text{ eV}$  for GaAs (for both complexes) [2,3]. This values agree quite well with those obtained recently from electrical measurements in GaAs:Zn ( $E_D = 1.33 \text{ eV}$ ) [5]. The Cd-H pairs in InP are more stable compared to the Cd-H pairs in GaAs. This observation has also its analogy to Zn-H pairs in these two compounds [6]. The fit to the annealing data obtained by PAC exhibits a dissociation energy of  $E_D = 1.6 \text{ eV}$ . The similarities in the dissociation energies for Zn and Cd acceptors can also be related to IR measurements. These experiments indicate, that hydrogen is bonded to the group V atom rather than to the adjacent acceptor in the bond center configuration. Hence the dissociation should be governed by the bond between hydrogen and the group V atom. A metastable annealing behaviour is observed for the complexes in InAs (fig. 2). Here, one complex dissociates between 300 K and 350 K, accompanied by an increase of the population of the other configuration. The more stable configuration then anneals at approximately the same temperature as the complexes in GaAs. This phenomenon indicates, that the same defect species is involved in both complexes, most likely hydrogen.

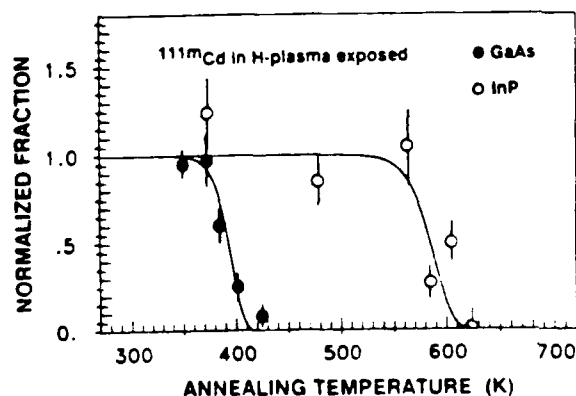


Figure 1 (see text)

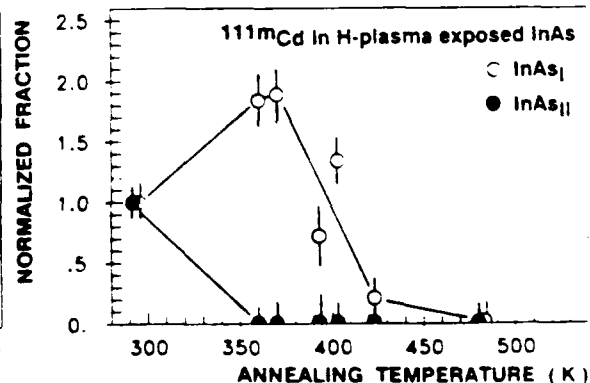


Figure 2 (see text)

Another example for thermal metastability of acceptor hydrogen complexes was observed in silicon on Cd-H pairs. Boron doped silicon crystals have been implanted by radioactive  $^{111}\text{In}^+$  ions with an energy of 400 KeV to a dose of  $10^{11} \dots 10^{12} \text{ cm}^{-2}$  at the IONAS implanter of the Göttingen University. The samples were subsequently sealed in quartz ampoules and the radiation damage was annealed in a furnace at 800...1200 K. After annealing the radiation damage, the specimens were hydrogenated in an atomic hydrogen atmosphere, originating from a remote H-plasma. PAC measurements performed after these treatments reveal the formation of two to three distinct defect complexes, depending on the boron concentration and the measuring temperature. The hyperfine interaction is again observed at  $^{111}\text{Cd}$ , the decay product of  $^{111}\text{In}$ . The configurations are all axially symmetric and oriented in  $\langle 111 \rangle$  lattice directions. All three configurations have been previously identified to be In/Cd-H pairs [7,8]. The discussion of the experimental situation will be focussed on the thermal metastability of the two complexes characterized by quadrupole coupling constants  $\nu_Q = 350 \text{ MHz}$  (at  $T=295\text{K}$ ), and  $\nu_Q = 270 \text{ MHz}$  (at  $T=100\text{K}$ ). They can be assigned to two different charge states of an electrically active Cd-H complex [8]. A set of PAC data has been recorded under variation of the Fermi energy with respect to the energy level of the Cd-H state in the band gap by varying the boron concentration (between  $10^{15}$  and  $10^{18} \text{ cm}^{-3}$ ) and the measuring temperature. These experiments permit the time resolved study of charge carrier recombination processes [9,10]. This charge carrier recombination results in fluctuating electrical field gradients, which is described by the dynamical PAC theory. The analysis reveals the hole emission time constant for the Cd-H center as a function of temperature (figure 3), and permits the determination of the Cd-H energy level to  $E = E_V + 80(20) \text{ meV}$  (fit in figure 3).

The pronounced fluctuation of electrical field gradients in Si material with high boron concentration ( $> 10^{18} \text{ cm}^{-3}$ ) cannot be due to the carrier recombination of the Cd-H center. This dynamic behaviour can be explained by the localized motion of hydrogen in the complexes

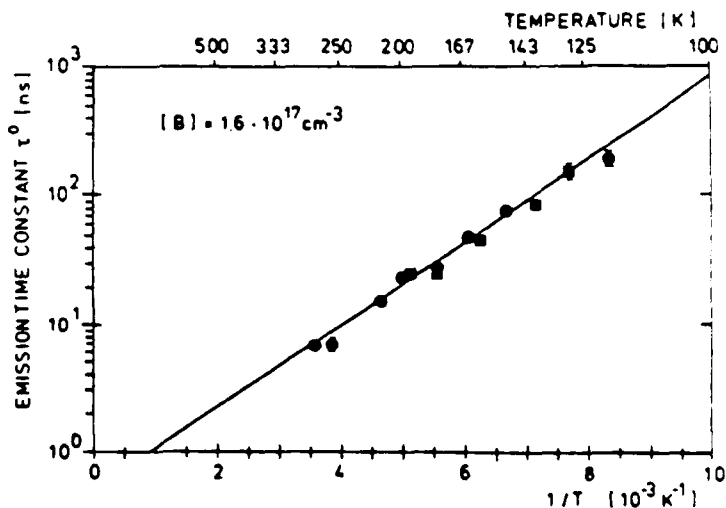


Figure 3 (see text)

as it is observed in other acceptor-hydrogen pairs [11,12]. The impact of the detailed understanding of the Cd-H system on previously published PAC data on the annealing of In-H pairs will be discussed [13].

- [1] A. Baurichter, M. Deicher, S. Deubler, D. Forkel, H. Plank, H. Wolf, and W. Witthuhn, *Appl. Phys. Lett.* **55** (22), 2301 (1989)
- [2] A. Baurichter, M. Deicher, S. Deubler, D. Forkel, J. Meier, and W. Witthuhn, presented on the ICDS 91, Bethlehem, Pennsylvania (to be published)
- [3] W. Pfeiffer, M. Deicher, R. Keller, R. Magerle, E. Recknagel, H. Skudlik, Th. Wichert, H. Wolf, D. Forkel, N. Moriya, and R. Kalish, *Appl. Phys. Lett.* **58**, 1751 (1991), and W. Pfeiffer, private communication
- [4] B. Pajot, B. Clerjaud, J. Chevallier, *Physica B* **170**, 371 (1991)
- [5] A.W.R. Leitch, Th. Prescha, M. Stutzmann, *Appl. Surface Science* **50**, 390 (1991)
- [6] J. Chevallier, B. Clerjaud, B. Pajot, "Hydrogen in Semiconductors", in *Semiconductors and Semimetals Vol.34*, Volume editors: J.I. Pankove, N.M. Johnson (1991)
- [7] Th. Wichert, H. Skudlik, M. Deicher, G. Grübel, R. Keller, E. Recknagel, and L. Song, *Phys. Rev. Lett.* **59**, 2087 (1987)
- [8] A. Baurichter, S. Deubler, D. Forkel, M. Gebhard, H. Wolf, and W. Witthuhn, *Mat. Science and Eng.*, **B4**, 281 (1991)
- [9] N. Achtziger and W. Witthuhn, in "Submicroscopic Investigation of Defects in Semiconductors", ed. by G. Langouche, North Holland, in press
- [10] M. Gebhard, N. Achtziger, A. Baurichter, D. Forkel, B. Vogt, and W. Witthuhn, *Physica B* **170**, 320 (1991)
- [11] M. Gebhard, B. Vogt, W. Witthuhn, *Phys. Rev. Lett.* **67**, 847 (1991)
- [12] M. Stavola, K. Bergmann, S.J. Pearton, and J. Lopata, *Phys. Rev. Lett.* **61**, 2786 (1988)
- [13] M. Gebhard, B. Vogt, and W. Witthuhn, presented on the ICDS 91, Bethlehem, Pennsylvania (to be published)

## Structure and energy of interstitial hydrogen and hydrogen-related complexes in crystalline semiconductors

Chris G. Van de Walle

*Xerox PARC, 3333 Coyote Hill Road, Palo Alto, CA 94304, USA*

I will present a number of recent results, interpreting them in the context of what we already know about the atomic and electronic structure of hydrogen in semiconductors, and highlighting directions for future work.

For hydrogen in silicon, I will discuss results for energies of hydrogen in various configurations, expressed with respect to hydrogen in free space. The configurations include hydrogen on the surface, isolated interstitial hydrogen, hydrogen at dangling bonds, and hydrogen in various complexes with shallow impurities. These results shed light on issues of solubility, stability, and reactivity.

For the compound semiconductors, I have carried out first-principles calculations of hyperfine parameters for isolated interstitial hydrogen in GaAs, in the configurations that were determined by Pavesi *et al.*<sup>1</sup> The values for the two types of tetrahedral interstitial sites are quite close, and close to the experimental value obtained from muon spin rotation.<sup>2</sup> The calculated values for the bond-center site also agree with experiments for "anomalous muonium".<sup>3</sup>

Finally, for hydrogen in ZnSe, I will discuss the relative stability of various sites, show results for hyperfine parameters, and comment on the stability of hydrogen-impurity complexes. The latter issue may be of great importance in light of the recent successes in p-type doping of ZnSe and fabrication of blue laser diodes.

<sup>1</sup>L. Pavesi, P. Giannozzi, and F. K. Reinhart, *Phys. Rev. B* **42**, 1864 (1990).

<sup>2</sup>R. F. Kiefl, J. W. Schneider, H. Keller, W. Kundig, W. Odermatt, B. D. Patterson, K. W. Blazey, T. L. Estle, and S. L. Rudaz, *Phys. Rev. B* **32**, 530 (1985)

<sup>3</sup>R. F. Kiefl, J. H. Brewer, S. R. Kreitzmann, G. M. Luke, T. M. Riseman, T. L. Estle, M. Celio, and E. J. Ansaldo, in *Proceedings of the 15th International Conference on Defects in Semiconductors*, Budapest, Hungary, 1988 (Trans Tech Publications, Switzerland), p. 967.

## HYDROGEN IN SILICON: ASPECTS OF SOLUBILITY DIFFUSION AND CATALYZED ENHANCED OXYGEN DIFFUSION

R C Newman, M J Binns \*, S A McQuaid and J H Tucker

Interdisciplinary Research Centre for Semiconductor Materials  
The Blackett Laboratory  
Imperial College  
London SW7 2BZ, UK

The earliest estimates of the solubility and diffusion of hydrogen in silicon were obtained by Van Wieringen and Warmoltz [1] from permeation measurements made in the limited temperature range 967°C to 1200°C. They obtained  $[H_s] = 4.96 \times 10^{21} \exp(-1.86\text{eV}/kT) \text{cm}^{-3}$  (Figure 1) so that at 1200°C  $[H_s] \sim 2 \times 10^{15} \text{cm}^{-3}$ . By extrapolating these results, a vanishingly small solubility of  $6 \times 10^3 \text{cm}^{-3}$  would be expected at 250°C. However, measurable effects believed to be due to the presence of mobile hydrogen have been found at these low temperatures [2-6], implying that the real concentration is significantly higher. Subsequent work by Ichimiya and Furiuchi [7], involving the use of tritium, yielded  $[H_s] = 6.61 \times 10^{19} \exp(-1.39\text{eV}/kT) \text{cm}^{-3}$ , and also gave  $[H_s] \sim 1 \times 10^{15} \text{cm}^{-3}$  at 1200°C but larger values compared with those of Van Wieringen and Warmoltz, at low temperatures because of the smaller heat of solution. More recently, Peale et al [8] showed that hydrogen diffused into Si at 1280°C from a gas source was retained in the solid during a quench to room temperature and led to the formation of H-S complexes.

We have quantified the heat and quench procedure by using silicon doped with boron in a concentration in the range  $6 \times 10^{16} \text{cm}^{-3}$  to  $4 \times 10^{17} \text{cm}^{-3}$  and measuring the concentration of [H-B] pairs, deduced from the strength of the localized vibrational (stretch) mode (LVM) of the paired hydrogen atoms [9,10]. We showed that pairing occurred in both Cz and FZ Si, that D-B pairs were produced if the diffusion was carried out in deuterium gas, the distribution of H-B pairs was uniform throughout samples up to 1mm in thickness and [H-B] saturated for the highest values of [B]. The IR absorption (Figure 2) was converted to concentrations of [H-B] pairs by establishing calibrations made on passivated boron doped layers prepared by MBE or ion implantation into CVD epitaxial layers [9]. The concentration [H-B] increased as the heating temperature was increased and we obtained values of  $[H_s] = 3.7 \times 10^{19} \exp(-1.2\text{eV}/kT) \text{cm}^{-3}$  for the range 900-1300°C, by assuming that all the dissolved hydrogen was trapped. We then found an extrapolated value of  $[H_s] \sim 10^8 \text{cm}^{-3}$  at 250°C, which appears to be reasonable in relation to other observations. Similar measurements have been obtained by other workers [11], and there is a common view that pairing of hydrogen with phosphorus does not occur in such heated and quenched samples.

---

\* Also with MEMC Hüls (UK) Ltd, Edinburgh House, 43-51 Windsor Road, Slough, Berks SL1 2HL

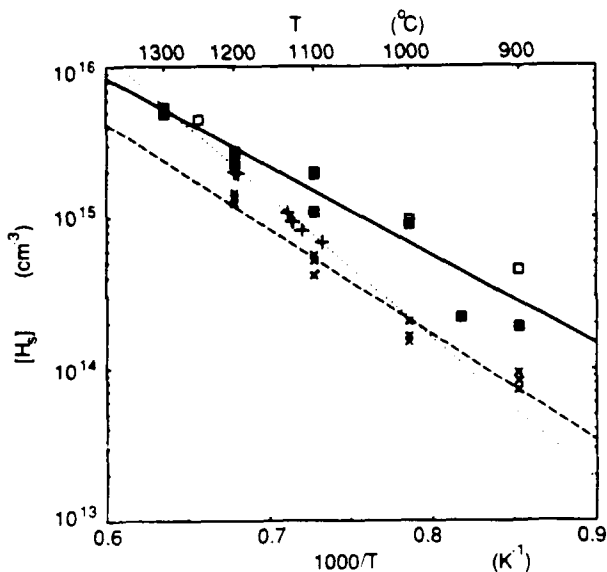


Fig. 1. The solubility of hydrogen in Si: ■ present results; □ our previous values; + and dotted line from [1]; x and dashed line from [6].

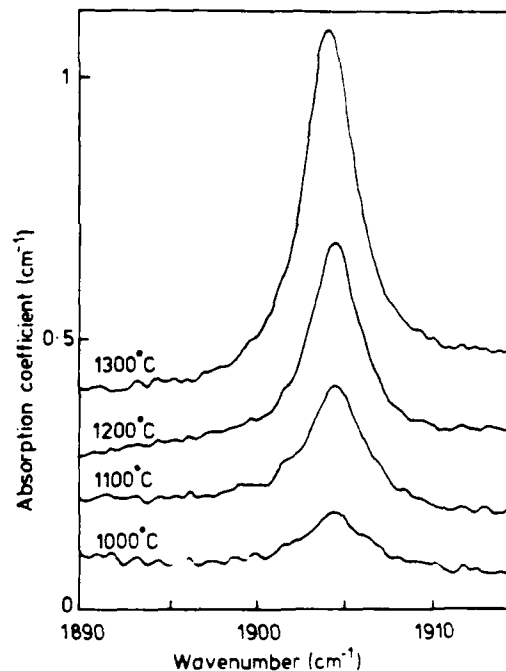


Fig. 2. Absorption (20K) from H-B stretch mode in CZ Si with  $[B] \sim 9 \times 10^{16} \text{cm}^{-3}$  after annealing in  $\text{H}_2$  and quenching to 300K.

We measured the diffusion coefficient of oxygen ( $D_{\text{oxy}}$ ) in our heated and quenched samples by the method of relaxation of stress-induced dichroism.  $D_{\text{oxy}}$  was enhanced at low temperatures (225°C to 350°C), compared with  $D_{\text{oxy}} (\text{Equil}) = 0.11 \exp(-2.51\text{eV}/kT)\text{cm}^2\text{s}^{-1}$ , and  $D_{\text{oxy}} (\text{Enh})$  has an activation energy close to 2.0 eV; however, the pre-exponential factor increased as  $[\text{H}_2]$  increased, for the higher quench temperatures in the range 600°C to 800°C (Figure 3). We proposed a model in which diffusing hydrogen atoms collided with oxygen atoms to form a transient complex which subsequently dissociated [3,4,5,10]. Such interactions have been modelled by two different first principles calculations [13,14].

The dichroism measurements related only to a limited number of diffusion jumps but it is implied that there would be enhanced long-range oxygen diffusion unless the hydrogen concentration was depleted by out-diffusion, by trapping of diffusing atoms at defects, or the formation of hydrogen molecules or larger clusters. In fact, we have now observed enhanced rates of thermal donor formation in heated and quenched n-type samples, confirming the enhancement of  $D_{\text{oxy}}$  for times up to 100h at 430°C. Our results confirm the early observation of Fuller & Logan [15] who found that the rate of TD-formation at 450°C in Cz Si grown in a hydrogen atmosphere was ten times greater than that measured for ingots grown in helium.

We now consider heat treatments of samples in the temperature range 225°C - 350°C in a hydrogen (or deuterium) plasma (13.56 MHz, 40W, 2 Torr). It is known that

hydrogen diffuses into a surface layer to a depth  $\sim 0.1\mu\text{m}$  in a concentration of  $\sim 10^{20}\text{cm}^{-3}$ . SIMS profiles indicate that  $[\text{H}]$  becomes smaller than  $10^{15}\text{-}10^{16}$  at depths greater than a few microns. Nevertheless, stress dichroism measurements of aligned oxygen impurities reveal enhancements in  $D_{\text{oxy}}$  that extend from the surfaces of the samples to depths in excess of  $0.5\text{mm}$ . By measuring the time dependence of the critical depth for the loss of the dichroism, we obtain a rate of diffusion for hydrogen of  $1.7 \times 10^2 \exp(-1.2\text{eV}/kT)\text{cm}^2\text{s}^{-1}$  (Figure 4). It is unclear whether this expression for  $D_{\text{H}}$  corresponds to a trap limited process of atomic hydrogen (our samples contained  $[\text{B}] \sim 10^{15}\text{cm}^{-3}$ ) or whether the molecular species is involved. Similar profiles with an abrupt interface have been found by spreading resistance measurements [6] for the formation of TD-centres. Thus, there is a greatly enhanced rate of TD-formation in a surface region which is n-type, whereas our samples were p-type.

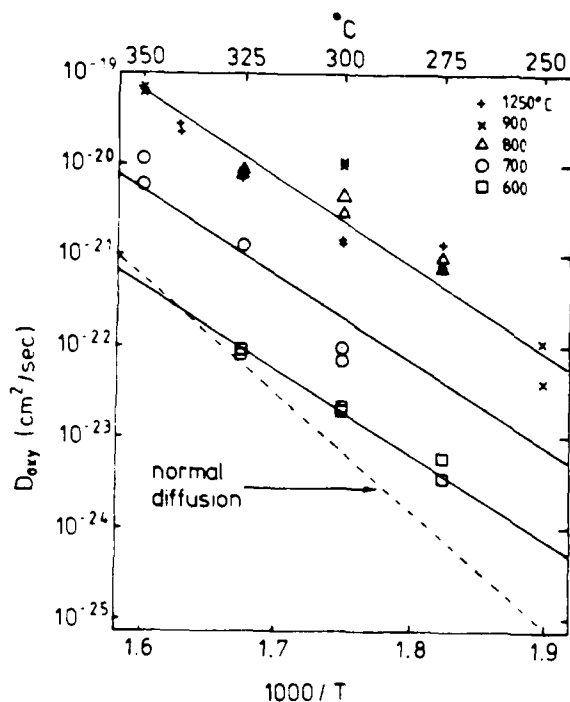


Fig. 3. Arrhenius plot of enhanced  $D_{\text{oxy}}$  (Enh.) as a function of pre-anneal temperature in  $\text{H}_2$  (g).

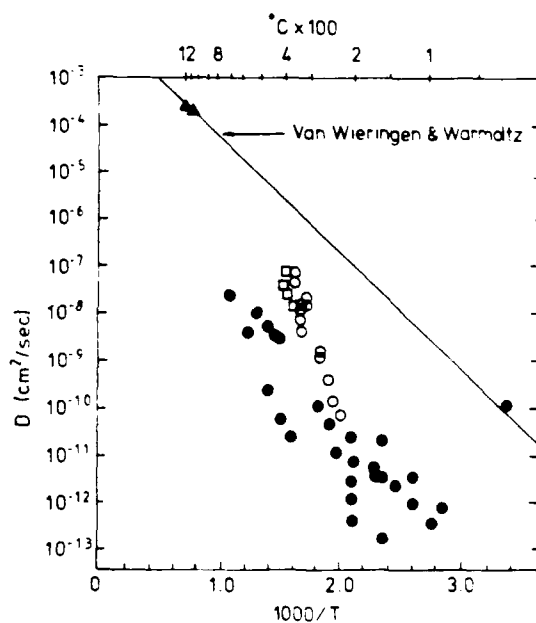


Fig. 4. Arrhenius plot of the hydrogen diffusion coefficient:  $\blacktriangle$  and solid line from [1];  $\bullet$  other previously published data;  $\square$  result from [6];  $\circ$  present results

We have also reported that the total TD-concentration may rise to a value as high as  $10^{17}\text{cm}^{-3}$  in samples heated in a plasma at a temperature of  $350^\circ\text{C}$  and that there are enhanced rates of formation of carbon-oxygen complexes in magnetic Czochralski Si [4]. A set of auxiliary experiments has demonstrated that self-interstitials, vacancies, fast diffusing metals etc are not involved in these various effects. The conclusion is that hydrogen is responsible for the enhancement of the oxygen diffusion. There may be technological applications in view of the extensive use of plasma processing and the passivation of samples in forming gas (hydrogen-nitrogen mixtures).

## References

1. A Van Wieringen and N Warmoltz, *Physica* 22 849 (1956)
2. A R Brown, M Claybourn, R Murray, P S Nandhra, R C Newman and J H Tucker, *Semicon Sci & Technol* 3 591 (1988)
3. A R Brown, R Murray, R C Newman and J H Tucker, *Proc Mat Res Soc Symp* 163 555 (1990)
4. R C Newman, A R Brown, R Murray, A Tipping and J H Tucker, 6th Int Symp on Silicon Mater Sci & Technol in Semiconductor Silicon edited by H R Huff, K G Barraclough and J Chikawa (The Electrochem Soc: Pennington NJ) 90-7 734 (1990)
5. R C Newman, J H Tucker, A R Brown and S A McQuaid, *J Appl Phys* (1991) in the press
6. H J Stein and S Hahn, in Symp on Defects in Silicon, Washington (Electrochem Soc: Pennington) 1991 in the press
7. T Ichimiya and A Furuichi, *Int J Appl Rad Isotopes* 19 2114 (1968)
8. R E Peale, K Muro and A J Sievers, in Shallow Impurities in Semiconductors edited by G Davies *Mat Sci Forum* 65-60 151 (1990)
9. S A McQuaid, R C Newman, J H Tucker, E C Lightowlers, R A A Kubiak and M Goulding, *Appl Phys Lett* 58 2933 (1991)
10. S A McQuaid, R C Newman and E C Lightowlers, 16th ICDS Lehigh University Bethlehem (1991) in press: R C Newman, J H Tucker and S A McQuaid *ibid* (1991) in the press
11. I A Veloarisco, D M Kozuck, M Stavola, R E Peale, G D Watkins, S J Pearton, C R Abernathy and W S Hobson, 16th ICDS Lehigh University Bethlehem (1991) in the press
12. R C Newman, *Proc 20th ICPS* edited by E M Anastassakis and J D Joannopoulos (World Scientific: Singapore) 1 525 (1990)
13. S K Estreicher, *Phys Rev* B41 9886 (1990)
14. R Jones, S Öberg and A Umerski, 16th ICDS Lehigh University Bethlehem (1991) in the press
15. C S Fuller and R A Logan, *J Appl Phys* 28 1427 (1957)

## The stability of hydrogen complexes in Si and GaAs

J. Weber, A.W.R. Leitch, Th. Prescha, and T. Zundel

Max-Planck-Institut für Festkörperforschung

D-7000 Stuttgart 80

A summary of our capacitance measurements on Si and GaAs samples containing various hydrogen complexes is presented. The stability of these complexes is studied under thermal annealing, optical excitation, or in an electric field.

In Si, the thermal dissociation of electrically neutral, shallow acceptor-hydrogen complexes (AH with A = B, Al, Ga, and In) is found to follow first-order kinetics over the entire annealing process, provided the isothermal anneal is performed with a reverse bias applied to the Schottky diode [1,2]. An example of the  $C(V)$ -profile is presented in Fig. 1. A boron-doped hydrogenated sample is annealed at a temperature  $T_a = 80^\circ\text{C}$  with a reverse bias  $V_R = 60\text{ V}$ . The active acceptor profiles are shown for different annealing times  $t_a$  (crosses). As  $t_a$  increases, the dopant is progressively reactivated in the region  $x \leq 7\ \mu\text{m}$ , while the neutralization becomes more pronounced in the region  $7\ \mu\text{m} < x < 12.5\ \mu\text{m}$ . The dopant passivation results from the formation of a neutral BH complex which can be thermally dissociated. The positively charged atomic hydrogen released, drifts under the electric field present in the space charge region and accumulates in the low field region, where new BH complexes are then able to form. The profiles  $N_I(x, t_a)$  are almost flat in the region  $x < 3\ \mu\text{m}$ . A quantitative analysis of the acceptor

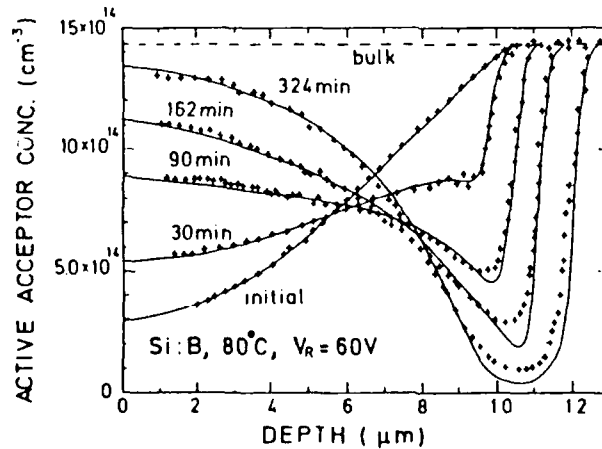


Figure 1: Evolution of the active boron concentration profile as a function of the reverse-bias annealing time ( $V_R = 60\text{ V}$ ,  $T_a = 80^\circ\text{C}$ ). Prior to the anneal, the sample is treated in a H plasma ( $120^\circ\text{C}$ , 2 h), and the 2- $\mu\text{m}$ -thick surface layer is removed. The solid lines represent the profiles calculated.

reactivation in the high-electric field region ( $x < 3 \mu\text{m}$ ) is established by plotting the electrically inactive acceptor concentration  $A(t_a) = N_{A0} - N_I(2 \mu\text{m}, t_a)$  vs  $t_a$  (Fig. 2).  $N_{A0}$  is the uniform acceptor concentration in the nonhydrogenated control sample. The reactivation of the acceptor follows the equation for first-order kinetics, characterized by  $A(t_a) = A(t_a = 0) \exp[-\nu(T_a)t_a]$ , and the dissociation frequencies  $\nu$  follow an Arrhenius law

$$\nu(T_a) = \nu_0 \exp(-E_d/kT), \quad (1)$$

where  $\nu_0$  and  $E_d$  are the attempt frequency and the dissociation energy, respectively.

A corresponding study of the behavior of the different impurity hydrogen complexes has been carried out for GaAs, using both n- and p-type material [3,4,5]. The drift of hydrogen in an applied electric field convincingly demonstrates the existence of negatively charged hydrogen in n-type GaAs and positively charged hydrogen in p-type GaAs as the mobile species. Table I summarizes the dissociation energies and attempt frequencies in Si and GaAs, determined by the  $C(V)$  method described above.

A dramatic enhancement of the reactivation of the inactive donors and acceptors occurs for above band gap illumination of the sample [5,6,7,8]. A careful analysis of the reactivation kinetics reveals a second order process, due to the formation of stable hydrogen centers which contain at least two hydrogen atoms [6].

The  $C(V)$  profiling technique allowed us to determine the diffusion constant for hydrogen. In p-type Si the hydrogen diffusion was studied in the temperature range 60°C-140°C for different boron concentrations. Reverse bias annealing of the samples for long periods generates a step-like profile of the inactive acceptor concentration. Annealing

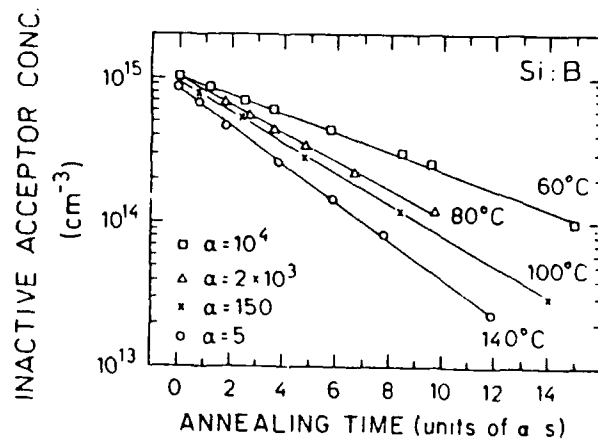


Figure 2: Inactive boron concentration vs annealing time, measured in the high-field region ( $x = 2 \mu\text{m}$ ) of a reverse-biased diode. A reduced time scale is used to clearly reveal the first-order kinetics in the entire annealing temperature range

	Silicon				GaAs	
	BH	AlH	GaH	InH	ZnH	SeH
$E_d$	$1.28 \pm 0.03$	$1.44 \pm 0.02$	$1.40 \pm 0.03$	$1.42 \pm 0.05$	$1.33 \pm 0.03$	$1.52 \pm 0.05$
$\nu_0$	$2.8 \times 10^{14}$	$3.1 \times 10^{13}$	$6.9 \times 10^{13}$	$8.4 \times 10^{13}$	$7 \times 10^{13}$	$2 \times 10^{13}$
Ref.	[1]	[1]	[1]	[1]	[3]	[4]

Table 1: Dissociation energies  $E_d$  (eV) of acceptor and donor-hydrogen pairs and attempt frequencies  $\nu_0$  in Si and GaAs.

without applied bias leads to a levelling out of the step due to the diffusion of hydrogen (Fig. 3). An analysis of the profiles after different annealing times and temperatures allows us to evaluate the hydrogen diffusion constant. Under our experimental conditions the diffusion of hydrogen appears to be entirely trap limited [9].

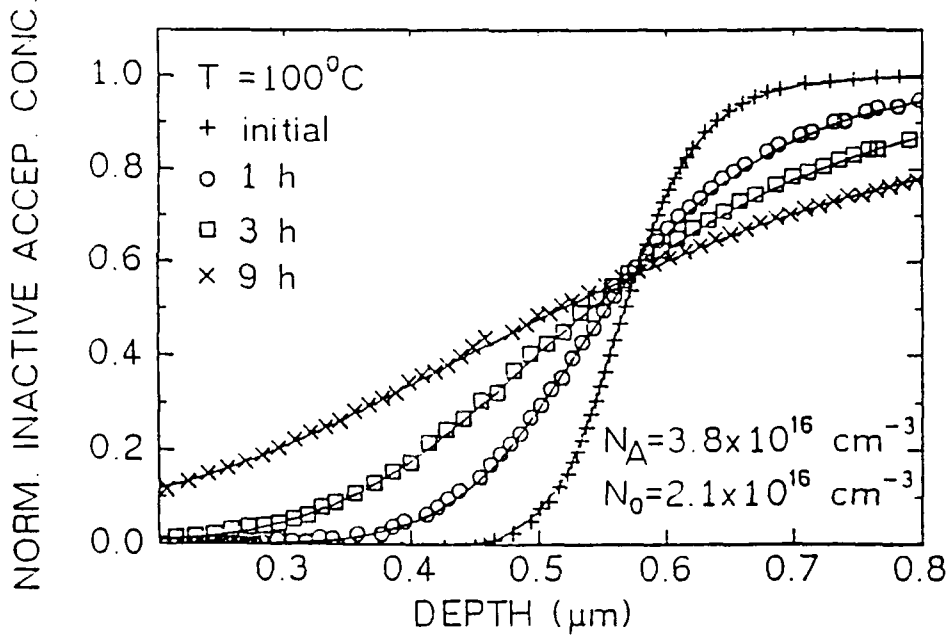


Figure 3: Normalized inactive boron profiles after zero bias annealing for increasing times  $t_D$  at  $100^\circ\text{C}$ . The symbols  $N_A$  and  $N_0$  denote the total boron concentration and the normalization factor.

We would like to acknowledge the interest and support of H.J. Queisser throughout this work. Thanks are also due to M. Stutzmann and M. Brandt for the passivation of samples and to W. Heinz and W. Krause for technical assistance.

## References

- [1] T. Zundel and J. Weber, *Phys. Rev. B* **39**, 13549 (1989)
- [2] T. Zundel and J. Weber, *Mat. Res. Soc. Symp. Proc. Vol. 163*, 443 (1990)
- [3] A.W.R. Leitch, Th. Prescha, and M. Stutzmann, *Appl. Surf. Science* **50**, 390 (1991)
- [4] A.W.R. Leitch, Th. Prescha, and J. Weber, *Phys. Rev. B* **44**, 1375 (1991)
- [5] A.W.R. Leitch, Th. Prescha, and J. Weber, *Phys. Rev. B* **44**, 5912 (1991)
- [6] T. Zundel and J. Weber, *Phys. Rev. B* **43**, 4361 (1991)
- [7] T. Zundel, J. Weber, and L. Tilly, *Physica B* **170**, 361 (1991)
- [8] A.W.R. Leitch, T. Zundel, Th. Prescha, and J. Weber, *Proc. ICDS 16*, 1991, to be published
- [9] T. Zundel and J. Weber, submitted to *Phys. Rev. B*

## RECENT STUDIES OF HYDROGEN IN SILICON AND III-V SEMICONDUCTORS

N. M. Johnson  
Xerox Palo Alto Research Center  
Palo Alto, California 94304, USA

### Summary

Given below are summaries with highlights of several recent studies performed at the Xerox Palo Alto Research Center on hydrogen in crystalline semiconductors. The references at the end of the summary identify the individual contributors and where the full-length papers have been or will be published.

#### **Migration of the $H_2^*$ Complex and its Relation to $H^-$ in $n$ -type Si:<sup>1</sup>**

Thermally-induced depth redistribution of the  $H_2^*$  complex was determined from SIMS. The activation energy for migration was found to be  $0.81 \pm 0.06$  eV. However, the data do not determine whether the migration involves dissociation. Both the migration kinetics and direct measurements on reverse-bias-annealed Schottky diodes show that for annealing times up to 25 h at temperatures near  $60^\circ\text{C}$  there is no detectable redistribution or dissociation of  $H_2^*$ , contradicting a currently-ambiguous claim that such annealing produces a large redistribution due to dissociations yielding  $H^-$ . The effect of the presence of  $H_2^*$  on the evolution of the neutralized-donor profiles at such temperatures is negligible.

#### **H-induced Platelets in Silicon--Separation of Nucleation and Growth:<sup>2</sup>**

It has been demonstrated that the growth of hydrogen-induced platelets in  $n$ -type single-crystal silicon can be controlled independently of the nucleation process. The results demonstrate that the suppression of platelet formation at high hydrogenation temperatures (e.g.,  $>250^\circ\text{C}$ ) is a consequence of the suppression of platelet nucleation and that platelets nucleated at lower temperatures (e.g.,  $150^\circ\text{C}$ ) grow markedly at the higher temperatures. The kinetics of platelet formation are qualitatively explicable by classical nucleation theory. The platelets, though somewhat reminiscent of the Guinier-Preston zones long familiar in certain metallic

alloys, have novel traits that suggest that short-range interatomic forces are sufficiently anisotropic to produce the two-dimensional silicon-hydride phase.

### **Thermal Dissociation Energy of the Si-H Complex in *n*-type GaAs:<sup>3</sup>**

The thermal dissociation kinetics of the Si-H complex in *n*-type GaAs:Si were determined from bias-temperature anneals on hydrogenated Schottky diodes. The anneal kinetics are approximately first order and yield a thermal dissociation energy of  $1.2 \pm 0.1$  eV. Depth redistribution of the Si-H complex both within the depletion layer of biased diodes and in the field-free region of unbiased diodes suggests that hydrogen in *n*-type GaAs can migrate as a negatively charged species.

### **Hydrogen Passivation and Reactivation of Se Dopants in AlGaAs:<sup>4</sup>**

The reactivation kinetics of Se-H complexes in *n*-type  $\text{Al}_x\text{Ga}_{1-x}\text{As}$  ( $x=0.25$ ) were determined in the space-charge layer of reverse-biased Schottky diodes. The thermal dissociation energy for recovery of Se shallow donors was found to be  $1.48 \pm 0.15$  eV. The observed redistribution of Se-H complexes in the depletion layer strongly suggests that hydrogen migrates in *n*-type AlGaAs as a negatively charge species.

### **Hydrogen Passivation of Si and Be Dopants in InAlAs:<sup>5</sup>**

Hydrogen passivation and thermal reactivation of Si donors and Be acceptors were investigated in InAlAs. The alloy was grown by MBE, lattice matched on InP, and passivated by exposure to monatomic hydrogen at 250°C (1h) from a remote hydrogen plasma. In both Si and Be doped samples, the dopants were passivated by over two orders of magnitude to a depth of  $\sim 2$   $\mu\text{m}$  (the epilayer thickness). Furthermore, DLTS revealed essentially complete passivation of three known deep donor levels, which are commonly designated EA1, EA3, and EA4. A subsequent anneal at 500°C (2 min) completely reactivated the passivated shallow donors. In addition, SIMS was performed on deuterated samples to determine the distribution of hydrogen. In both Si and Be doped material, the deuterium profiles were essentially identical to the dopant profiles throughout the epilayers. This behavior resembles the situation of H in B-doped Si and suggests that hydrogen migration in InAlAs is limited by dopant trapping.

## References

1. N. M. Johnson and C. Herring, Phys. Rev. B 43, 14297 (1991).
2. N. M. Johnson, C. Herring, C. Doland, J. Walker, G. Anderson, and F. Ponce, Proc. 16th International Conference on Defects in Semiconductors, Bethlehem, PA, 22-26 July 1991, in press.
3. G. Roos, N. M. Johnson, C. Herring, and J. S. Harris, Jr., Appl. Phys. Lett. 59, 461 (1991).
4. G. Roos, N. M. Johnson, C. Herring, H. F. Chung, R. L. Thornton, and J. S. Harris, Jr., to be published in the Proceedings of the Electrochemical Society Meeting, Phoenix, Arizona, 13-18 October 1991.
5. G. Roos, N. M. Johnson, Y. C. Pao, J. S. Harris, Jr., and C. Herring, to be published in the Symposium Proceedings Series for the 1991 Fall Meeting of the Materials Research Society, Boston, MA, 2-6 December 1991.

## **Multitrapping of atomic Hydrogen in doped crystalline silicon.**

A. Amore Bonapasta

*National Research Council (CNR), ITSE,*

*V. Salaria Km. 29,5 - CP 10, 00016 Monterotondo Scalo, Italy.*

The multitrapping of H atoms near boron or phosphorus sites in doped crystalline silicon has been investigated in the framework of pseudopotential-density-functional methods. Although both dopants give rise to metastable complexes containing several H atoms, only the P dopant has the capability to trap H ions by Coulombic attraction. This is due to the peculiar electronic structure of the metastable configurations of the Si-H-P complex. The different properties shown by the phosphorus- and boron-containing complexes may explain the different diffusion behaviour shown by the H diffusion in boron- and phosphorus-doped silicon.

## Modeling of Hydrogen Diffusion in Semiconductors

Daniel Mathiot

CNET-CNS, BP.98, 38243 Meylan Cedex (France)

We present a theoretical model for the diffusion of hydrogen in semiconductors. This model was initially developed to describe the diffusion of H in Si [1-4], but has been shown later convenient in the case of GaAs [5]. In fact, due to the generality of the equations used, it is believed that this model can likely be used for any semiconductor, with a suitable choice of the model parameters.

In this analysis, it is considered that hydrogen can have both an acceptor ( $E_a$ ) and a donor ( $E_d$ ) level in the band gap, and thus exists in the three charge states  $H^+$ ,  $H^0$ , and  $H^-$ , the relative concentrations of which depend on the local Fermi level position :

$$[H^-] = (n/n_a)[H^0] \quad (1a)$$

$$[H^+] = (n_d/n)[H^0] \quad (1b)$$

where  $n$  is the local concentration of free electrons, and  $n_a$  and  $n_d$  reflect the position of the  $E_a$  and  $E_d$  levels in the gap.

$$n_a = N_c \exp[-(E_c - E_a)/kT] \quad (2)$$

and the corresponding relation for  $n_d$ . The isolated hydrogen atoms can react with the ionized acceptors ( $A^-$ ) or donors ( $D^+$ ) to form neutral complexes :



In addition to these neutralization reactions (dopant passivation), the possible formation of  $H_2$  complexes is also taken into account, either by reaction between two  $H^0$  atoms, or by reaction between  $H^0$  and  $H^+$  :



Finally, the high H concentration in the damaged surface region is described by trapping on plasma-related unidentified traps  $T$  :



Assuming that the only mobile species are the free hydrogen species in their various charge states, the evolution of the various concentrations is given by the following set of differential equations :

$$\frac{\partial [H]^{tot}}{\partial t} = - \frac{\partial J_H}{\partial x} \quad (6a)$$

$$\frac{\partial [H_2]}{\partial t} = k_{H_2}[H^0]^2 + k_{H_2}^+[H^0][H^+] - k_{H_2}^-[H_2] \quad (6b)$$

$$\frac{\partial [AH]}{\partial t} = k_{AH}[A^-][H^+] - k_{AH}^-[AH] \quad (6c)$$

$$\frac{\partial [DH]}{\partial t} = k_{DH}[D^+][H^-] - k_{DH}^-[DH] \quad (6d)$$

$$\frac{\partial [TH]}{\partial t} = k_{TH}[T][H^0] \quad (6e)$$

where the total hydrogen flux is given by:

$$- J_H = \left( D_{H^0} + \frac{n}{n_a} D_H + \frac{n_d}{n} D_{H^+} \right) \frac{\partial [H^0]}{\partial x} \quad (7)$$

The local density of free carriers is obtained by the simultaneous resolution of Poisson's equation.

In Eqs.(6), the rate constants for the reactions (3) to (5) are calculated from the values of the diffusivities, assuming purely diffusion limited reactions. The corresponding capture radii are either 5 Å, or the Coulombic radius for reactions (3).

Fits on numerous experimental profiles, covering experimental results obtained on substrates with different starting doping levels, allow the determination of the unknown parameters. Examples of fitted profiles, and the corresponding extracted diffusivities, are given in the two pages of figures, in the case of n- and p-type Si, and for semi-insulating and p-type GaAs(Zn).

It is emphasized that the fits on the experimental profiles led us to rule out the possibility of H<sub>2</sub> formation at the diffusion temperature.

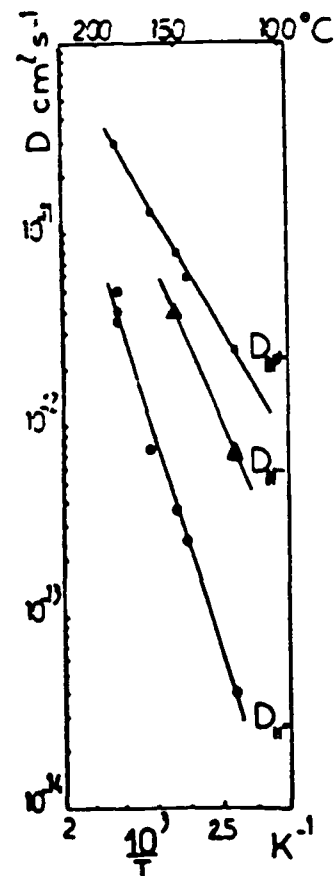
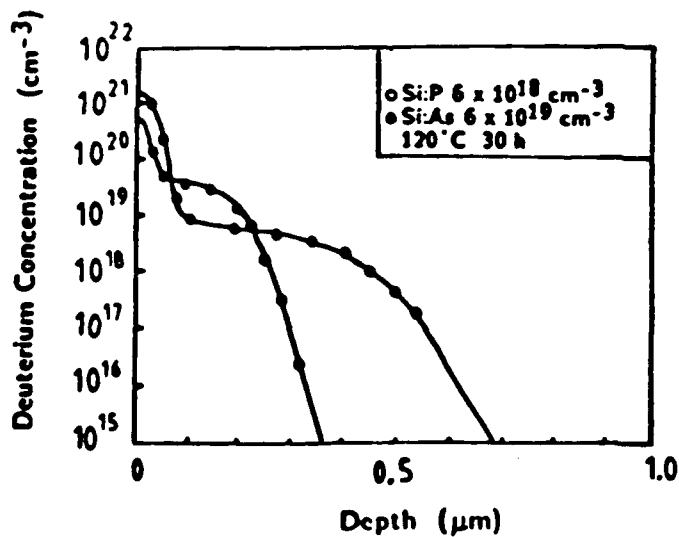
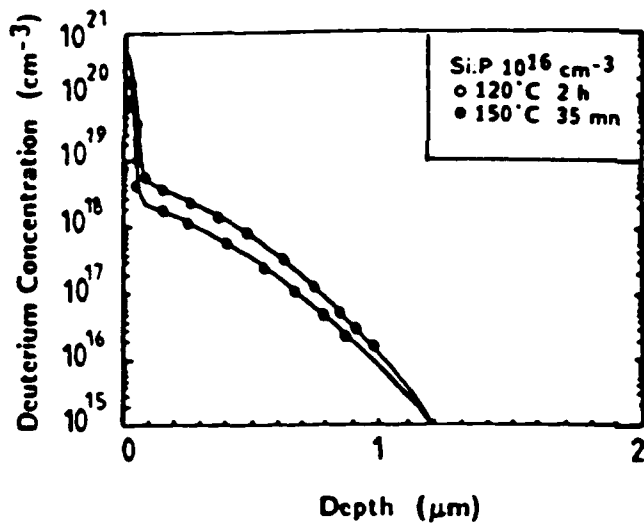
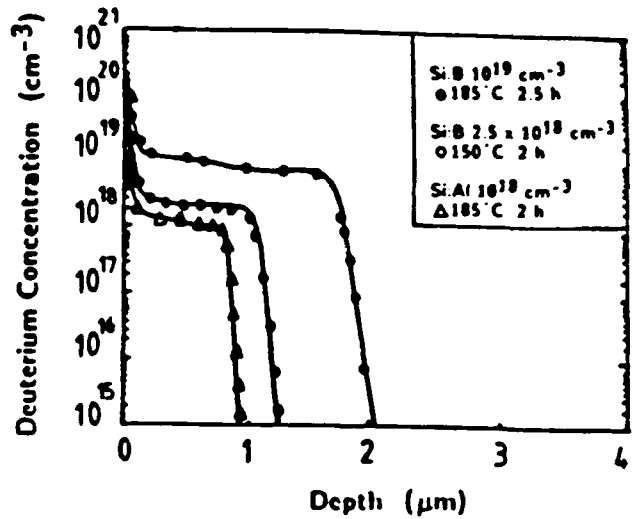
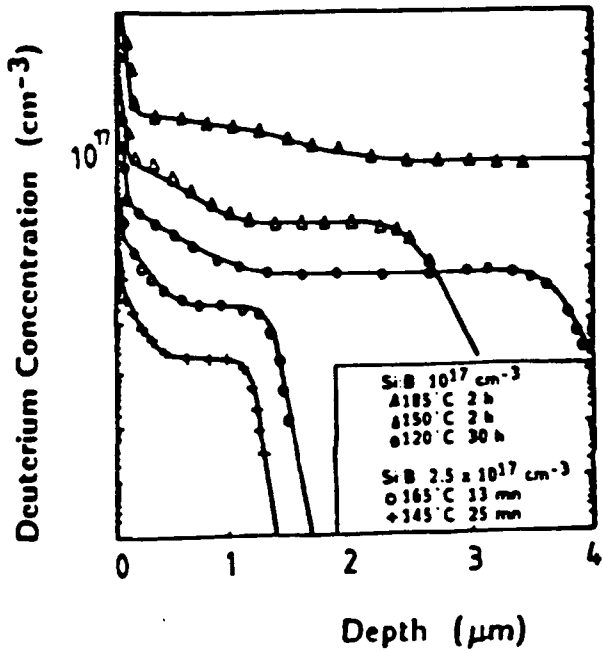
#### Acknowledgements

This work has been performed in close collaboration with the groups of the Laboratoire de Physique du Solide of CNRS Bellevue. The author is particularly grateful to M. Aucouturier, D. Ballutaud, P De Mierry, and R. Rizk for the Si results, and to J. Chevallier and R. Rahbi in the case of GaAs.

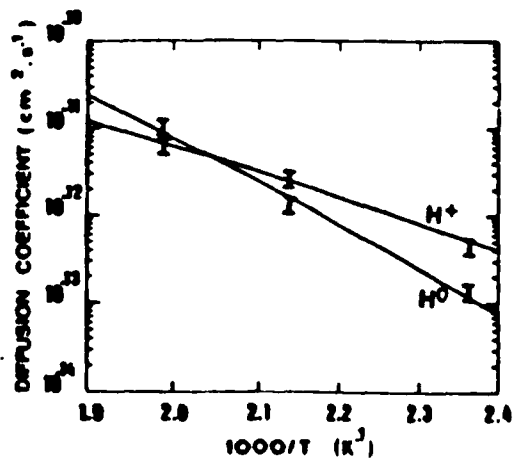
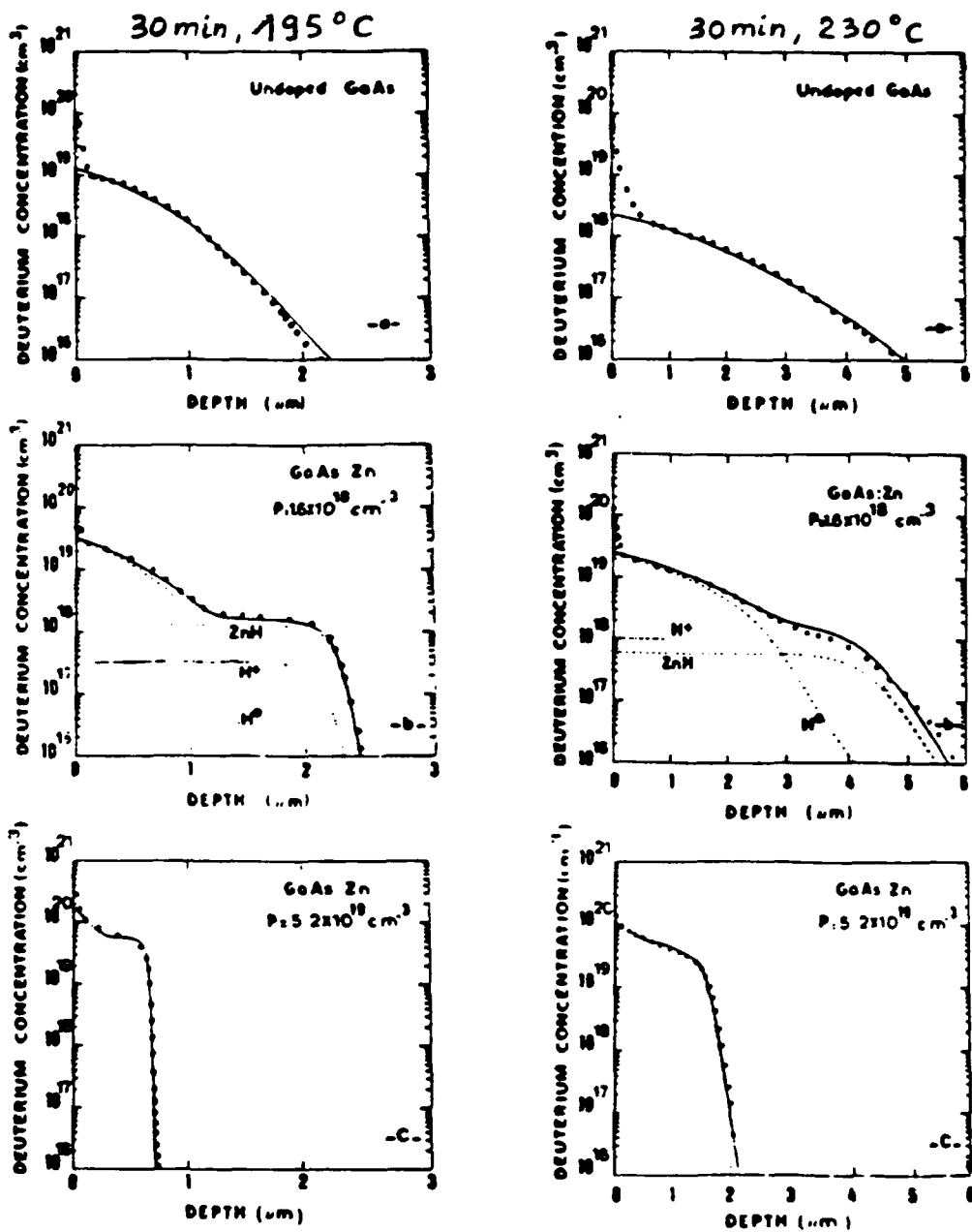
#### References

1. D.Mathiot : Phys. Rev. B **40**, 5867 (1989)
3. R.Rizk, P.DeMierry, D.Ballutaud, M.Aucouturier, and D.Mathiot : Physica B **170**, 129 (1991)
4. R.Rizk, P.DeMierry, D.Ballutaud, M.Aucouturier, and D.Mathiot : Phys Rev B, in press
5. R.Rahbi, D.Mathiot, J.Chevallier, C.Grattapain, and M.Razeghi : Physica B **170**, 135 (1991)

**H in Si : Simulated Profiles and Extracted Diffusivities.**



**H in GaAs : Simulated Profiles and Extracted Diffusivities.**



*(Extended Abstract for the Workshop on Hydrogen Migration and the Stability of Hydrogen Related Complexes in Crystalline Semiconductors, Horben bei Freiburg, Germany, 3-6 November 1991).*

## **"DIFFUSION AND ELECTRONIC STATES OF HYDROGEN IN n-GaAs: Si and n-Al<sub>x</sub>Ga<sub>1-x</sub>As: Si".**

J.CHEVALLIER, B.MACHAYEKHI, C.M.GRATTEPAIN and B.THEYS

Laboratoire de Physique des Solides de Bellevue

C.N.R.S.

1 place Aristide Briand

92195 MEUDON (France)

Among the different problems raised by the behaviour of monatomic hydrogen in crystalline semiconductors, one is related to its charge states and its interactions with impurities as it migrates in the lattice.

From drift experiments of hydrogen under electric field it has been recently established that H<sup>-</sup> is a migrating species in hydrogenated n-GaAs doped with tellurium [1] or selenium [2] and also in n-GaAs and n-AlGaAs doped with silicon [3]. Based on the evolution of the hydrogen diffusion profiles with the alloy composition and with the silicon donor concentration, we bring information on the dominant diffusing species in Si doped Al<sub>x</sub>Ga<sub>1-x</sub>As alloys. To explain the data we propose a model based on the alloy composition dependence of the hydrogen acceptor level position with respect to the conduction band of the materials.

Deuterium diffusion experiments have been performed on a series of MBE grown Al<sub>x</sub>Ga<sub>1-x</sub>As epilayers doped with silicon. The alloy composition ranges from x = 0 to x = 0.30. Two silicon doping levels have been used: 1.5x10<sup>18</sup>cm<sup>-3</sup> and 2x10<sup>17</sup>cm<sup>-3</sup>. All these samples have been exposed to a R.F. plasma at T = 190-240°C for t = 30 min.

Figures 1 and 2 present the deuterium diffusion profiles in the series of highly doped samples. In GaAs, we find a deuterium distribution very close to a complementary error function (erfc). As the aluminum content increases, the erfc function is progressively replaced by a diffusion profile characterized by a plateau followed by an abrupt decrease of the deuterium concentration. This shape is characteristic of a strong trapping mechanism. This situation occurs above x ≈ 0.06 for this doping level of 1.5x10<sup>18</sup>cm<sup>-3</sup>. For all studied compositions above this critical value, the diffusion profiles are very similar with the same diffusion depths.

The solubility of deuterium in the plateau region of alloys with  $0.035 < x < 0.15$  is markedly close to the active dopant concentration. For  $x > 0.22$ , DX centers governed the electrical properties of AlGaAs: Si alloys. For  $x = 0.30$ , a freeze-out of the free carriers occurs at 300K but, at 513K, which is the hydrogen diffusion temperature, most of the DX centers are ionized and the exhaustion regime occurs. Then, the solubility of deuterium in  $\text{Al}_{0.30}\text{Ga}_{0.70}\text{As}$  alloys is still equal to the active dopant concentration at the diffusion temperature and deuterium species interact with the positively charged  $\text{DX}^+$  centers. This interaction is at the origin of the neutralization of the silicon donors observed in deuterated  $\text{Al}_x\text{Ga}_{1-x}\text{As}$ : Si alloys with  $0 < x < 0.37$  [4, 5, 6].

For the series of alloys containing  $2 \times 10^{17} \text{cm}^{-3}$  silicon donors, we qualitatively have the same change of diffusion profiles as the aluminum content increases, but the appearance of profiles exhibiting trapping characteristics occurs above  $x \approx 0.25$  (instead of  $x \approx 0.06$  for the high doping level).

From vibrational absorption spectroscopy it is known that the neutralization of silicon donors by hydrogen in GaAs: Si and AlGaAs: Si proceeds through the formation of Si-H bonds. It has been established that the wagging modes of Si-H in GaAs and AlGaAs are very close to each other ( $896.8 \text{cm}^{-1}$  in GaAs: Si and  $896.4 \text{cm}^{-1}$  in  $\text{Al}_{0.2}\text{Ga}_{0.8}\text{As}$ : Si) [7, 8] and that the dissociation energy of Si-H bonds is basically independent on the aluminum composition [3]. For these reasons, we rule out the possibility that the above changes of deuterium profiles with alloy composition are associated with a change of the thermal dissociation probability of Si-H complexes.

Instead, we propose an explanation in terms of hydrogen diffusing with different charges states. In other words, we assume that hydrogen behaves as a deep acceptor level which is slightly resonant in the conduction band of GaAs and which merges as a localized state in the forbidden gap of  $\text{Al}_x\text{Ga}_{1-x}\text{As}$ . As a consequence, for samples where the Fermi level is well above the hydrogen acceptor level,  $\text{H}^-$  is the dominant diffusing species and the hydrogen diffusion profile will result in a trapping of  $\text{H}^-$  by the positively charged donors, by a long range interaction. For samples where the Fermi level is close to or somewhat below the hydrogen acceptor level, hydrogen diffuses in two different charge states  $\text{H}^0$  and  $\text{H}^-$ . However, in this case, the high effective diffusivity of neutral hydrogen governs the experimental hydrogen diffusion profile.

**ACKNOWLEDGMENTS.** We would like to thank B.CLERJAUD (LAOMC, Paris VI), B.PAJOT (GPS, Paris VII) and R.RAHBI (CNRS, Meudon) for stimulating discussions.

#### REFERENCES.

- [1] M.H.YUAN, L.P.WANG, S.X.JIN, J.J.CHEN and G.G.QIN, Appl. Phys. Lett., 58, 925 (1991).
- [2] A.W.R.LEITCH, Th. PRESCHA and J.WEBER, Phys. Rev., B, 44, 1375 (1991).
- [3] G.ROOS, N.M.JOHNSON, C.HERRING and J.S.HARRIS, Appl. Phys. Lett., 59, 461 (1991) and also 16th ICDS, Lehigh University, July 1991.
- [4] J.CHEVALLIER, W.C.DAUTREMONT-SMITH, C.W.TU and S.J.PEARTON, Appl. Phys. Lett., 47, 108 (1985).

- [5] J.C.NABITY, M.STAVOLA, J.LOPATA, W.C.DAUTREMONT-SMITH, C.W.TU and S.J.PEARTON, *Appl. Phys. Lett.*, **50**, 921 (1987).
- [6] R.MOSTEFAOUI, J.CHEVALLIER, A.JALIL, J.C.PESANT, C.W.TU and R.F.KOPF, *J. Appl. Phys.* **64**, 207 (1988).
- [7] B.PAJOT, R.C.NEWMAN, R.MURRAY, A.JALIL, J.CHEVALLIER, and R.AZOULAY, *Phys. Rev. B* **37**, 4188 (1988).
- [8] B.PAJOT, *Inst. Phys. Conf. Ser.* **95**, 437 (1989).

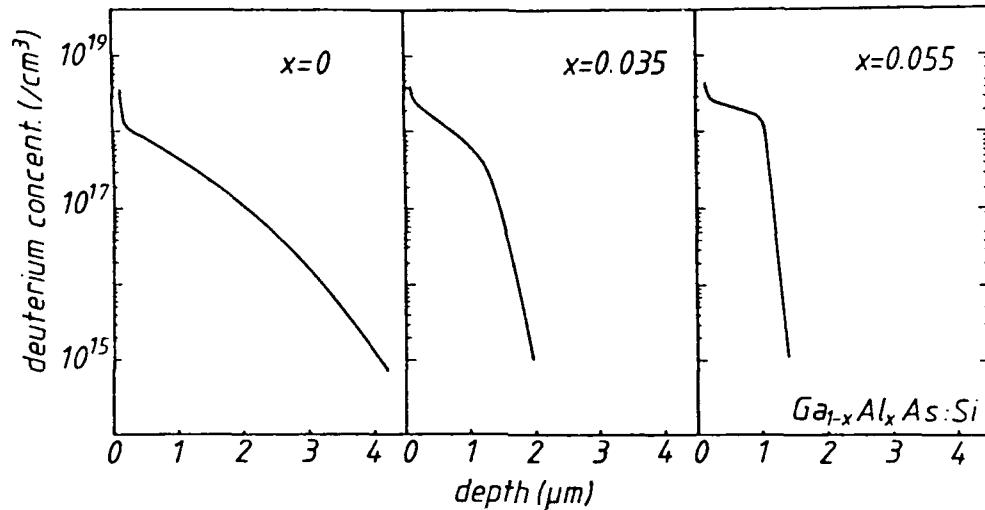


**Figure 1** : Deuterium diffusion profiles in n-type GaAs: Si and  $\text{Al}_x\text{Ga}_{1-x}\text{As: Si}$  alloys with low amounts of aluminum. The plasma conditions are  $T = 240^\circ\text{C}$ ,  $t = 30 \text{ min.}$  and  $P = 0.04\text{W/cm}^2$ .

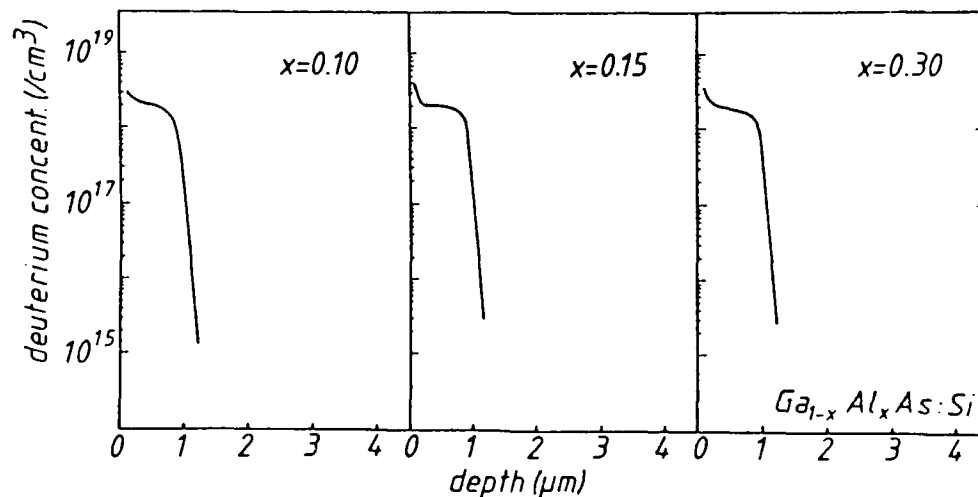


**Figure 2** : Deuterium diffusion profiles in a series of n-type  $\text{Al}_x\text{Ga}_{1-x}\text{As: Si}$  alloys with different values of  $x$ . Same plasma conditions as figure 1.

## THE EXPERIMENTAL EVIDENCE FOR VARIOUS CHARGE STATES OF HYDROGEN IN SILICON

C. H. Seager

Sandia National Laboratories  
Albuquerque, N. M. 87185

The question of the preferred charge states of interstitial hydrogen in the silicon lattice has generated increasing controversy in the past few years. Theoretical investigations<sup>1-3</sup> of the minimum free energy of  $H^0$ ,  $H^+$ , and  $H^-$  by Local Density Functional methods, Molecular Orbital techniques, and Hartree-Fock calculations have not generated the unanimity of results that experimentalists find comforting. In addition, while recent experimental results have been interpreted as supporting the existence of  $H^0$  and  $H^+$ , the evidence for  $H^-$  is controversial. In this talk I will attempt to review the available experimental data for various charge states of hydrogen; I will also point out some caveats that should be kept in mind when interpretation of these measurements is attempted.

Recently Herring<sup>4</sup> and others<sup>5</sup> have presented a Schockley, Read, Hall analysis of the fractional occupation of various H charge states as a function of the local electron and hole populations. I will review these briefly because they should guide us in anticipating the charge states expected in neutral and depleted regions. I say "should" because the complications of charge dependent lattice positions, Franck-Condon shifts, and negative U phenomena have not really been addressed and may well complicate the picture. In addition to the simple equilibrium case, where the position of the Fermi level with respect to the  $+0$  and  $0/-$  demarcation energies determines the H charge occupation, this analysis also predicts that the charge state ratios in depletion depend only on emission rates and thus should be independent of the dopant type.

Early work by Tavendale et al<sup>6</sup> and Johnson<sup>7</sup> established that electric fields applied during annealing of p-type Schottky diodes or during hydrogenation of n<sup>+</sup>/p junctions strongly affected the resultant evolution of H bonded to acceptors. The first group suggested that these data were strong evidence for field-induced drift of  $H^+$ , while Johnson cautioned that they might only prove that holes were necessary for the H-acceptor bonding process. A later, more complete study of the thermal dissociation of H from acceptors by Zundel and Weber<sup>8</sup> established that, under reverse diode bias, all debonded hydrogen (within the error limits of the measurement) was driven deeper into their diodes and rebonded to acceptors. This conservation of H proved that all of the released H moved under the influence of the applied field and is strong evidence for the existence of  $H^+$  in depletion. Studies of H penetration and debonding<sup>5,9</sup> by our own group at Sandia have also shown that: 1. room temperature motion of H is accelerated by increasing depletion layer electric fields, and 2. the debonding rate of H from acceptors is strongly dependent on the local population of majority and minority carriers. We find that it is difficult to explain the detailed functional dependence of our results without supposing that H is usually neutral but positive  $\sim 1/10$  of the time in depletion and almost always positive in equilibrium.

The evidence for  $H^-$  is more problematic. Work by Johnson and Herring<sup>10</sup> showed that SIMS-determined densities of H (D) in n-type Si deuterated at 300 C increased with donor density in the  $10^{17} - 10^{19} \text{ cm}^{-3}$  range. This was even true when a lightly n-doped epitaxial layer covered a more heavily doped substrate. They interpreted these results by suggesting that  $H^- > H^0$  at 300 C, and that the population of  $H^-$  became larger as the Fermi level approached the conduction band bottom. However, it seems unlikely that mobile  $H^-$  would remain in their samples between treatment and analysis; thus the form of H detected by these SIMS analyses is likely some other trapped species. This clouds the interpretation of

these results. More recently, work by Tavendale et al<sup>11</sup>, Zhu et al<sup>12</sup>, and our group<sup>13</sup> has shown that **some, but not all** of the H thermally released from donors rebonds deeper in the sample when n-type Schottky diodes are reverse-bias-annealed. By analogy with data seen in p-type diodes, the first two groups cited these data as evidence for the field-induced motion of H<sup>-</sup>. However, our group has offered the explanation that depletion enhances the thermal debonding rate, and this causes the transfer of some of the debonded H to donors located deeper in the diode. Other data<sup>13</sup> showing the influence of the electron and hole density on the debonding rate clearly shows that interpretation of these types of debonding measurements must be approached with caution. Perhaps the most serious objections to supposing that H<sup>-</sup> exists in depletion are: 1. From the SRH analyses we anticipate that the same admixture of charge states exists in a depletion region regardless of doping type, but no evidence of H<sup>-</sup> can be found in any data from reverse biased p-type samples<sup>8,9</sup>. 2. Penetration of H in reverse biased n-type diodes at temperatures where H-donor pairs are stable has been shown to be consistent with the same mixture of H<sup>0</sup> and H<sup>+</sup> seen in p-type diodes<sup>9</sup>. We conclude that, unless H<sup>-</sup> is a long lived, metastable byproduct of donor-H dissociation, its existence in silicon is doubtful.

Finally I shall review the evidence that the introduction of hydrogen gives rise to trapped positive charge in a form that appears to be quite distinct from mobile H<sup>+</sup>. Support for this assignment comes directly from H penetration studies on n-type diodes<sup>9</sup> and, indirectly, from p-type penetration and debonding measurements. This trapped charge decays slowly (hours to days) and appears to be the primary reason for the large impedance changes seen in hydrogenated Schottky diodes. One interesting consequence of this charge is that it eventually establishes fields which repel H<sup>+</sup> back toward H exposed surfaces; this may contribute to the very slow, non t<sup>1/2</sup>-like, dependence of H penetration that is almost always observed in capacitave and SIMS profiling work on H exposed samples.

1. C. G. Van de Walle, Y. Bar-yam, and S. T. Pantelides, Phys. Rev. Lett. 60, 2761 (1988).
2. S. K. Estreicher, Phys. Rev. B36, 9122 (1987).
3. P. Deak, L. C. Snyder, and J. W. Corbett, Phys. Rev. B37, 6887 (1988).
4. C. Herring, Chapter 10 in Hydrogen in Semiconductors, Edited by J. I. Pankove and N. M. Johnson (Academic Press, Boston, 1991).
5. C. H. Seager and R. A. Anderson, Appl. Phys. Lett. 59, 585 (1991).
6. A. J. Tavendale, D. Alexiev, and A. A. Williams, Appl. Phys. Lett. 47, 316 (1985).
7. N. M. Johnson, Appl. Phys. Lett. 47, 874 (1985).
8. T. Zundel and J. Weber, Phys. Rev. B39, 13549 (1989).
9. C. H. Seager, R. A. Anderson, and D. K. Brice, J. Appl. Phys. 68, 3268 (1990).
10. N. M. Johnson and C. Herring, Defects in Semiconductors 15, (Trans Tech Publ. Ltd, Switzerland, 1989), ed. by G. Ferenczi, Materials Science Forum 38-41, 961 (1989).
11. A. J. Tavendale, S. J. Pearton, and A. A. Williams, Appl. Phys. Lett. 56, 949 (1990).
12. J. Zhu, N. M. Johnson, and C. Herring, Phys. Rev. B41, 12354 (1990).
13. C. H. Seager and R. A. Anderson, Solid State Comm. 76, 285 (1990).

## NITROGEN-HYDROGEN COMPLEX AND HYDROGEN CHARGE STATES IN GaP

B. CLERJAUD, D. COTE, W.-S. HAHN\* , C. PORTE and D. WASIK†  
Acoustique et Optique de la matière condensée,  
Université Pierre et Marie Curie, Boîte 86, F-75252, Paris cedex 05, France

and

W. ULRICI  
Zentralinstitut für Elektronenphysik, O-1086 Berlin, F.R. Germany

In the case of GaAs, the donor level of hydrogen has been located within the bandgap by monitoring the type of complexes formed as function of the Fermi energy.<sup>1,2</sup> The complex used for probing  $H^+$  was the C-H complex which is formed according to the reaction :  $C^- + H^+ \rightarrow (C-H)^0$ . On the other hand, the complexes used for probing  $H^0$  were involving lattice defects and in particular a gallium vacancy having one of its dangling bonds saturated with hydrogen.<sup>3,4</sup> The formation of this type of complexes is not well understood and it is possible that in fact, the vacancy and neutral hydrogen do not exist independently, but that the presence of neutral hydrogen itself is at the origin of the hydrogenated defect. In order to avoid this ambiguity, a hydrogen related complex involving an impurity would have been a more suitable probe for  $H^0$ .

The few results available<sup>5,6</sup> concerning the passivation of impurities in GaP by hydrogen seem at first sight contradictory. Singh and Weber<sup>5</sup> report on the passivation of carbon and nitrogen impurities, whereas Mizuta et al.<sup>6</sup> claim that carbon is not neutralized in n-type GaP and isolated nitrogen not passivated in p-type material. Having in mind the concept developed in Ref. 1 and 2, these two types of results are not necessary in contradiction, but can be due to Fermi energy effects. The neutralization of carbon in p-type GaP having been recently demonstrated,<sup>7</sup> we have investigated the passivation of nitrogen in GaP using infrared spectroscopy.

In semi-insulating GaP grown by the liquid encapsulated Czochralski (LEC) technique containing nitrogen (in low concentration in order to avoid the formation of nitrogen pairs) and unintentional hydrogen as it is always the case in this type of material,<sup>8</sup> we have observed an intense absorption line at  $2885.5 \text{ cm}^{-1}$  (at 6 K). This line is always accompanied by an other one at  $2879.7 \text{ cm}^{-1}$  whose intensity is  $3.6 \pm 0.5 \%$  of the  $2885.5 \text{ cm}^{-1}$  one as shown in Fig. 1. This ratio matches exactly the ratio of the natural abundances of  $^{15}\text{N}$  and  $^{14}\text{N}$ ; moreover, the  $5.8 \text{ cm}^{-1}$  shift between the two lines is very close to the isotopic shift calculated for the stretching mode of an imaginary N-H diatomic molecule having an energy of vibration of  $2885 \text{ cm}^{-1}$  (for  $^{14}\text{N}$ ) :  $6.4 \text{ cm}^{-1}$ . This demonstrates that the two lines observed correspond to the vibration of  $^{14}\text{N-H}$  and  $^{15}\text{N-H}$  bonds. One can safely conclude that unpaired nitrogen is passivated by hydrogen in semi-insulating GaP.

In all the samples investigated, an other line at  $2054.0 \text{ cm}^{-1}$  is always present; the ratio of the integrated intensities  $I(2885) / I(2054) = 9.5 \pm 0.5$  is sample independent. We are therefore tempted to attribute the  $2054 \text{ cm}^{-1}$  line to one of the vibration modes of the N-H complex. In all of our samples, the intensity of the  $2054 \text{ cm}^{-1}$  line was unfortunately not strong enough for observing the corresponding mode involving  $^{15}\text{N}$ .

\* On leave from Korea Telecom, Seoul, Korea

† On leave from Institute of Experimental Physics, Warsaw, Poland

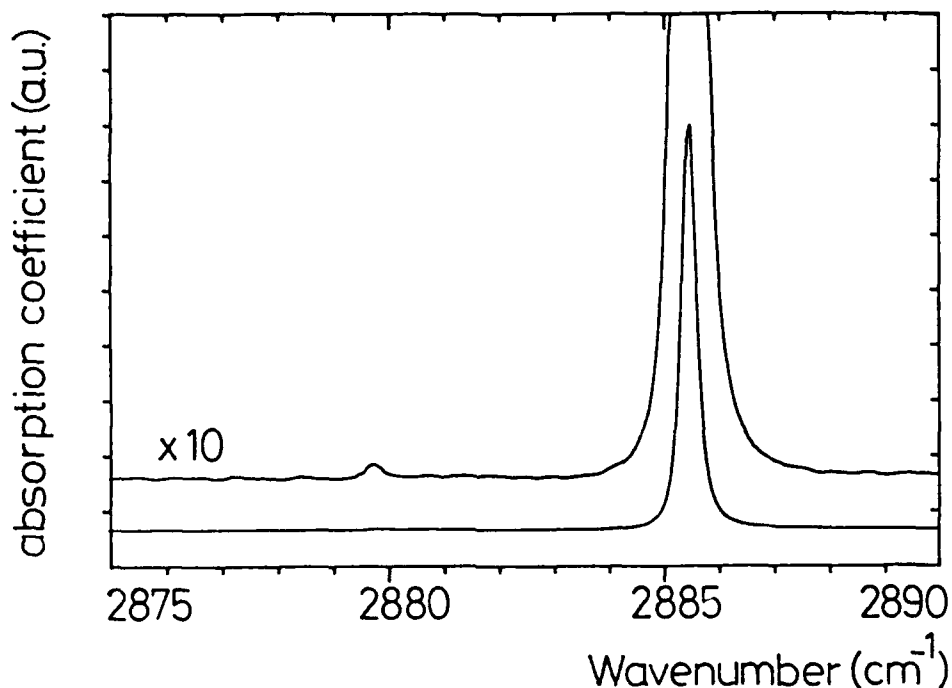


FIG. 1. Absorption of the N-H stretching modes of vibration. Both  $^{14}\text{N}$ - and  $^{15}\text{N}$ -related modes can be observed.

We have performed experiments under uniaxial stress on both modes of vibration at 2885 and 2054  $\text{cm}^{-1}$  in order to have a deeper insight into the microscopic structure of the N-H complex. The effects of stress on the 2885  $\text{cm}^{-1}$  line correspond to what is expected for a non degenerate mode of vibration of a center of trigonal symmetry<sup>9</sup> (with equal populations of the four equivalent configurations). Therefore this mode of vibration corresponds to a stretching mode of N-H bonds aligned along the four trigonal axes. In order to know whether the complex is able to reorient among its four equivalent configurations, we have undertaken stress-induced dichroism experiments.<sup>9</sup> In fact, applying uniaxial stress for one hour at room temperature, we have not been able to induce any dichroism. This means that the complex is not able to reorient among its four equivalent configurations at room temperature.

We have also performed uniaxial stress experiments on the 2054  $\text{cm}^{-1}$  local vibrational mode. Very surprisingly, this LVM does not split for any direction of the applied stress; it is just shifted independently of the stress direction. Such a behavior for this LVM is not understandable without assuming a motion of the complex which averages the stress effects.

In order to explain the stress measurements on both LVMs, we propose that the 2885  $\text{cm}^{-1}$  and 2054  $\text{cm}^{-1}$  LVMs are respectively the stretching and wagging modes of the N-H complex. The complex precesses around a trigonal axis in such a way that the precession averages out the stress effects on the wagging mode and gives a trigonal impression on the stretching one. The precession is supposed to occur around an antibonding position for the following reasons : i) this location leads to high energy wagging modes (in contrast with the bond center one) ii) reorientation among the four equivalent configurations is difficult in this location. The proposed microscopic structure is schematized in Fig.2.

In order to have an insight into the formation of the N-H complex, we have looked at its existence in various samples containing carbon and nitrogen (and of course hydrogen) with various Fermi energies. There is practically no coexistence of the C-H and N-H complexes. This means that different hydrogen charge states are involved in the

formation of the two complexes.  $H^+$  being involved in the formation of the C-H complex,  $H^0$  is responsible of the formation of the N-H one. Isoelectronic impurities are therefore the most suitable probes for  $H^0$ .

We have used the same procedure as the one used previously in GaAs<sup>1,2</sup> for locating the hydrogen donor level in GaP. We have observed that in the few very small samples in which both the C-H and N-H complexes were observed (most probably in different parts of the samples), two charge states of the vanadium impurity could also be observed :  $V^{(+)}$  and  $V^{(0)}$ . This means that the donor level of vanadium almost coincide with the hydrogen one. This would be strictly true if the complexes were formed at zero temperatures; in fact, they are formed during the cooling stage of the LEC growth at temperatures below 400 °C. At this temperature, the decrease of the Fermi function extends over about 0.2 eV and therefore, we can say that the vanadium and hydrogen donor levels coincide within 0.1 eV.

Several values of the vanadium donor level have been given :  $0.35 \pm 0.1$ ,<sup>10</sup>  $0.2 \pm 0.05$ ,<sup>11</sup>  $0.33 \pm 0.03$ ,<sup>12</sup> and  $0.25 \pm 0.02$ <sup>13</sup> above the top of the valence band. All these values seem to converge around 0.25-0.30 eV above the top of the valence band. Therefore the hydrogen donor level in GaP is located at  $0.3 \pm 0.1$  eV above the top of the valence band.

It had been assumed<sup>14</sup> that, among the III-V compounds, the hydrogen donor level is pinned to an absolute energy with respect to the vacuum level; the comparison between GaAs<sup>1,2</sup> and GaP shows that this assumption is not relevant.

We have shown that the nitrogen-hydrogen complex only forms if the Fermi level is higher than 0.3 eV above the valence band maximum. This explains why several attempts<sup>6</sup> of nitrogen passivation have been unsuccessful : at high nitrogen doping level, nitrogen pairs are formed; the pairs act as shallow acceptors and the samples become p-type with a Fermi level too low for the unpaired nitrogen to be passivated.

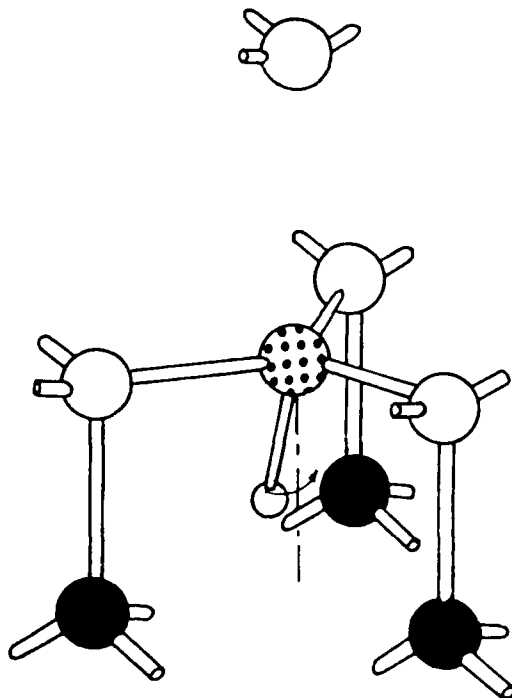


FIG. 2. Schematic representation of the N-H complex.

### **Acknowledgements**

The Laboratory "Acoustique et Optique de la Matière Condensée" is a "unité associée au Centre National de la Recherche Scientifique". Part of this work has been supported by the Direction des Recherches, Etudes et Techniques under contract 90.34.044.00.470.75.01. We thank M. Lernal for orienting and cutting the samples used for the stress experiments.

### **REFERENCES**

1. B. Clerjaud, F. Gendron, M. Krause and W. Ulrici, *Phys. Rev. Lett.* **65**, 1800 (1990).
2. B. Clerjaud, F. Gendron, M. Krause and W. Ulrici, *Mod. Phys. Lett. B* **5**, 877 (1991).
3. B. Clerjaud, M. Krause, C. Porte and W. Ulrici, in *Proceedings of the 19th Conference on the Physics of Semiconductors*, ed. W. Zawadzki (Institute of Physics, Polish Academy of Sciences, 1988) 1175.
4. J. Chevallier, B. Clerjaud and B. Pajot, in *Hydrogen in Semiconductors*, eds J.I. Pankove and N.M. Johnson, *Semiconductors and Semimetals Vol. 34* (Academic Press, 1991) 447.
5. M. Singh and J. Weber, *Appl. Phys. Lett.* **54**, 424 (1989).
6. M. Mizuta, Y. Mochizuki, N. Takadoh and K. Asakawa, *J. Appl. Phys.* **66**, 891 (1989).
7. B. Clerjaud, D. Côte, W.-S. Hahn and W. Ulrici, *Appl. Phys. Lett.* **58**, 1860 (1991).
8. B. Clerjaud, *Physica B* **170**, 383 (1991).
9. M. Stavola and S.J. Pearton, in *Hydrogen in Semiconductors*, eds J.I. Pankove and N.M. Johnson, *Semiconductors and Semimetals Vol. 34* (Academic Press, 1991) 139.
10. W. Ulrici, L. Eaves, K. Friedland and D.P. Halliday, *Phys. Stat. Sol. (b)* **141**, 191 (1987).
11. W. Ulrici, J. Kreissl, D.G. Hayes, L. Eaves and K. Friedland, *Materials Science Forum*, **38-41**, 875 (1989).
12. P. Omling and B.K. Meyer, *Materials Science Forum*, in press.
13. G. Bremond, P. Roura, G. Guillot and W. Ulrici, to be published.
14. E.M. Omeljanovsky, A.V. Pakhomov and A.Y. Polyakov, *Phys. Lett. A* **141**, 75 (1989).

## HYDROGEN STABILITY AND PASSIVATION OF SHALLOW AND DEEP CENTERS IN GaSb AND InSb

A.Y. Polyakov,<sup>1</sup> S.J. Pearton,<sup>2</sup> R.G. Wilson,<sup>3</sup> P. Rai-Choudhury,<sup>4</sup> R.J. Hillard,<sup>4</sup>  
X.J. Bao,<sup>1</sup> M. Stam,<sup>1</sup> A.G. Milnes,<sup>1</sup> T.E. Schlesinger,<sup>1</sup> and J.M. Zavada,<sup>5</sup>

<sup>1</sup>Dept. Electrical and Computer Engineering, Carnegie Mellon University,  
Pittsburgh, PA 15213-3890 USA

<sup>2</sup>AT&T Bell Laboratories, Murray Hill, NJ 07974-2070 USA

<sup>3</sup>Hughes Research Laboratories, Malibu, CA 90265 USA

<sup>4</sup>Solid State Measurements, Inc., Technology Drive, Pittsburgh, PA 15275 USA

<sup>5</sup>Army Research Office, Research Triangle Park, NC 27709-2211 USA

### Abstract

Spreading resistance and C-V measurements show that hydrogen can passivate shallow acceptors and to some extent, shallow donors in GaSb and InSb. Deep levels, as revealed using DLTS and photoluminescence, have also been passivated. The hydrogen-defect complexes are destroyed by heating at 250 to 300°C. SIMS has been used to determine the physical location of the hydrogen atoms and the doping densities of impurities.

**INTRODUCTION:** Hydrogen passivation of defects and impurities in some III-V materials (GaAs, InP, AlGaAs, InGaAs) is documented, and understood to some degree.<sup>1-3</sup> Recently, studies have begun on InSb,<sup>4</sup> InGaP,<sup>5</sup> and GaP.<sup>6</sup> A common concern is whether there are general trends in the behavior of H in these III-V materials, and whether this behavior can be utilized in the fabrication of devices in these materials, which have less mature processing technologies. In this paper, we report the effects of H treatment on GaSb, and to a lesser degree, on InSb. One application for GaSb is with quaternaries to produce lasers and photodetectors in the 2- $\mu$ m wavelength range.<sup>7,8</sup>

**EXPERIMENTAL APPROACH:** Hydrogen treatment studies were carried out on p<sup>+</sup>-GaSb samples doped with either Si or Zn ( $10^{16}$ - $10^{19}$  cm<sup>-3</sup>), on n-GaSb samples doped with Te ( $2 \times 10^{17}$ - $2 \times 10^{18}$  cm<sup>-3</sup>), on undoped GaSb samples with native acceptors of about  $10^{17}$  cm<sup>-3</sup>, on Be-doped GaSb layers ( $\sim 1 \mu$ m) grown on SI-GaAs using MBE, on InSb, and on AlGaSb. Hydrogenation or deuteration was performed in a parallel plate capacitor reactor at 30 kHz between 100 and 250°C for times between 0.5 and 1 h.<sup>9</sup> Deuterium profiles for hydrogen diffusion and defect-complexing location studies were measured using SIMS (14.5-keV Cs primary ions and negative secondary ions).<sup>10,11</sup> Resistivity and free carrier density profiles were measured using the two-probe spreading resistance profiling (SRP) method.<sup>12</sup> The measured SRPs are converted to densities using calibration curves from n- and p-type samples with known densities.<sup>12,13</sup> On the more lightly doped n-GaSb(Te) samples, electron density was also determined from C-V measurements on Au/n-GaSb Schottky diodes.<sup>14</sup> The influence of H on deep centers in GaSb was studied using DLTS on Au/GaSb(Te) Schottky diodes and room temperature PL. DLTS spectra were obtained in the range from 100 to 300K using a SULA-1 spectrometer and a cooled Ge photodetector with sensitivity between 0.8 and 1.8  $\mu$ m.

**RESULTS AND DISCUSSION:** We found that H diffusivity in GaSb depends on the conductivity type and doping density. In Fig. 1, four deuterium (<sup>2</sup>H) profiles that correspond to 100, 150, 200, and 250°C are shown for the p<sup>+</sup>-GaSb(Zn) sample with hole density  $2 \times 10^{18}$  cm<sup>-3</sup>. These profiles can be approximated by an erfc-type function, and the apparent diffusion coefficient can be expressed as  $D = 1.5 \times 10^{-6} \exp(-0.45 \text{ eV}/kT)$ . The <sup>2</sup>H density near the surface is much higher than that of acceptors for temps below 250°C (presumably because of preferential formation of H<sub>2</sub> pair formation), and approaches the density of acceptors at

250°C. In n<sup>+</sup>-GaSb, the surface density of <sup>2</sup>H was significantly lower than in p<sup>+</sup>-GaSb. The depth of the <sup>2</sup>H profile is greater, and the form of the decay is better described by an exponential (Fig. 2). This behavior was previously observed for H in InP and explained by supposition that H readily complexes with acceptors, but that its interaction with donors is inefficient.<sup>16</sup> Such an explanation also seems plausible for GaSb. The effective diffusion coefficient for n<sup>+</sup>-GaSb can be described by:  $D = 3.4 \times 10^{-5} \exp(-0.55 \text{eV}/kT)$ .

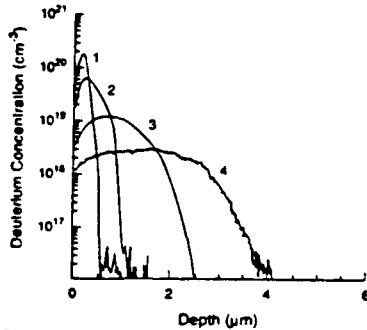


Fig. 1. <sup>2</sup>H profiles (SIMS) in p<sup>+</sup>-GaSb(Zn); 1-100, 2-150, 3-200 4-250°C; exposure time 0.5h

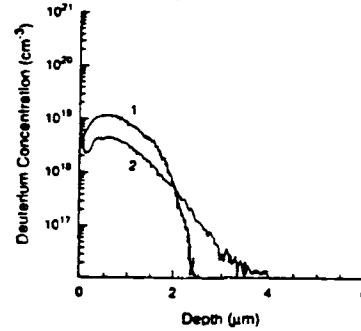


Fig. 2. <sup>2</sup>H profiles (SIMS) in p<sup>+</sup>-GaSb (Zn) (1) and in n<sup>+</sup>-GaSb(Te) (2); treated at 200°C

In undoped p-GaSb, the H density is approx. three times less than in p<sup>+</sup>-GaSb and is close to the density in n- and n<sup>+</sup>-GaSb (which do not differ). One explanation is that H in GaSb is a donor with energy level close to the valence band edge. In p<sup>+</sup>-GaSb, H is positively charged at the temperatures of hydrogenation, whereas in undoped GaSb and in n-GaSb, it is neutral. If this is true, the H donor level should lie at  $\sim E_v + 0.1 \text{eV}$ , the position that coincides with that of Fermi level pinning at the surface of GaSb.<sup>14,16,17</sup> The H level in GaSb is within 0.2eV of the position that is calculated using the vacuum reference level pinning model.<sup>18</sup> Electrical measurements indicate that there is a symmetry in acceptor and donor passivation in GaSb. As shown in Fig. 3, there is more than a two-fold decrease in the hole density in the first 0.5 μm of the heavily Si-doped p<sup>+</sup>-GaSb sample, whereas in the n<sup>+</sup>-GaSb sample, the concentration profile before and after H treatment remains constant. From the amount of passivation observed for the heavily doped p<sup>+</sup>-GaSb sample in Fig. 3, it would be expected that more lightly doped samples would be rendered highly resistive. However, measurements on the lightly Be-doped epitaxial sample (Fig. 4) show that the density decrease is not large; rather the density changes in lightly doped GaSb are comparable with those in lightly doped n-GaSb(Te), in which a decrease from

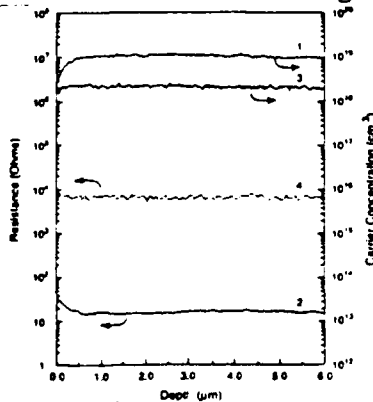


Fig. 3. Carrier density (1,3) and SRP (2,4) in p<sup>+</sup>-GaSb (1,2) and n<sup>+</sup>-GaSb (3,4) after H treatment at 150°C

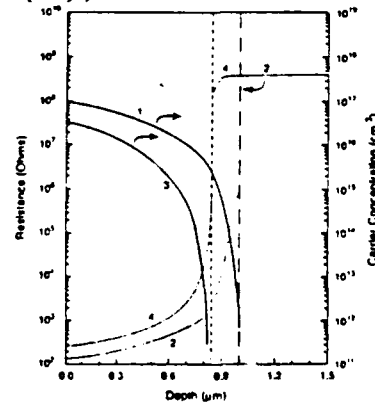


Fig. 4. Carrier density (1,3) and SRP (2,4) in p-GaSb/SI GaAs before (1,2) and after (3,4) H treatment at 150°C

2 to  $1 \times 10^{17} \text{ cm}^{-3}$  was measured using C-V, possibly because H in n- and lightly doped p-GaSb is neutral and the passivation efficiency is not so high as in the case of Coulombic attraction between charged acceptors and H ions. The effect observed in the case of p<sup>+</sup>-GaSb is probably passivation and not compensation, as confirmed by van der Pauw measurements on the p<sup>+</sup>-GaSb(Be)/SI GaAs epitaxial structures, which have shown a density decrease from 1 to  $0.6 \times 10^{19} \text{ cm}^{-3}$  and mobility increases from 100 to  $180 \text{ cm}^2/\text{Vs}$  as a result of H treatment at  $150^\circ\text{C}$ . DLTS shows the presence, in n-GaSb, of an electron trap with an apparent ionization energy  $0.25\text{eV}$  and density near  $10^{15} \text{ cm}^{-3}$ . As a result of H treatment at  $150^\circ\text{C}$ , the density of this trap decreases by six. From measurement of the PL band in p<sup>+</sup>-GaSb at room temperature, H treatment causes a five-fold increase in the intensity of this band, presumably because of passivation of the nonradiative recombination centers. Similar changes were measured for n<sup>+</sup>-, n-, and p-GaSb. Annealing of a passivated Au/n-GaSb Schottky diode at  $250^\circ\text{C}$  for 0.5h caused the complete recovery of the free electron density and to the nearly total recovery of the density of deep electron traps. In p<sup>+</sup>-GaSb, complete recovery of the hole density occurred after a  $300^\circ\text{C}$ , 0.5h anneal, and that anneal also restored to a large extent the density of nonradiative centers in p-type material.

The lifetime in n-InSb was measured before and after hydrogenation at  $150^\circ\text{C}$ , using a contactless method in which the sample is excited by a  $\text{CO}_2$  laser and the diffraction pattern for  $10.6\text{-}\mu\text{m}$  light is measured. Depth profiles were obtained by varying the excitation laser wavelength and therefore the absorption depth. The results indicate that passivation is occurring to a depth of about  $9 \mu\text{m}$ . However, SIMS depth profiling of these samples indicates that H has not penetrated more than  $0.5 \mu\text{m}$  (with a density greater than  $3 \times 10^{16} \text{ cm}^{-3}$ ). Therefore, we tentatively conclude that the H at the surface provides a sink for defects (or that H at a density less than  $3 \times 10^{16} \text{ cm}^{-3}$  in the bulk produces the observed effect). These observations are under further study. In separate experiments,  $^2\text{H}$  was implanted into GaSb at room temperature and into InSb at  $80\text{K}$  (liquid nitrogen temperature), and the depth profiles of  $^2\text{H}$  were measured using SIMS for samples unannealed and annealed at temperatures from  $100$  to  $350^\circ\text{C}$ . Figure 5 shows H redistribution toward the GaSb surface through the layer damaged by the implant and deeper into the GaSb not damaged by the implant. Figure 6 shows redistribution of H deeper into the bulk of the InSb sample. Redistribution deeper into the bulk is greater for InSb ( $\sim 50\mu\text{m}$  for the  $175^\circ\text{C}$  anneal) than for GaSb ( $\sim 5\mu\text{m}$ ).

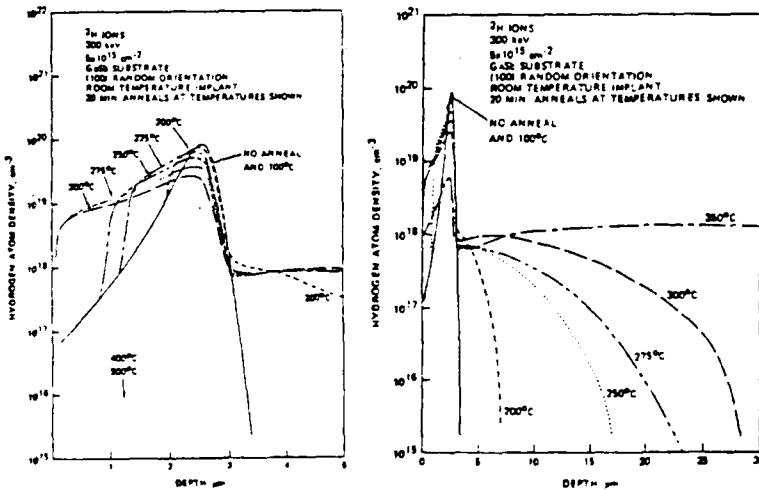


Fig. 5. SIMS depth profiles for  $^2\text{H}$  implanted into GaSb and annealed

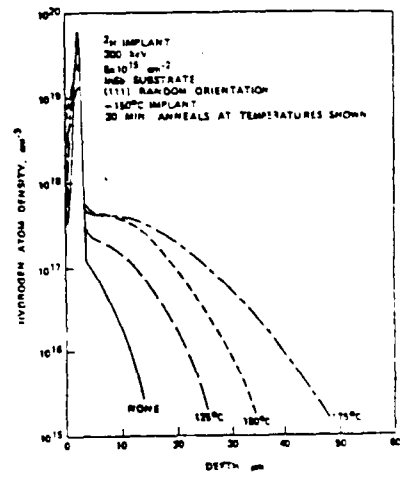


Fig. 6. SIMS depth profiles for  $^2\text{H}$  implanted into InSb and annealed

DISCUSSION AND CONCLUSIONS: Passivation of GaSb seems to be of less practical importance because the degree to which shallow acceptors can be passivated is not so high as in InP,<sup>19,20</sup> making it difficult to use H passivation to produce high resistivity GaSb layers. There does not exist a wide window in the annealing temperatures of deep and shallow defects that would make it possible to improve recombination characteristics of GaSb without changing the density of free carriers necessary for the operation of electronic devices, as is the case for GaAs.<sup>3</sup> The extrapolation schemes for the behavior of H in III-V materials proposed in ref. 16, crude as they may seem, do give an estimate of H behavior in unmeasured materials. One implication is that in AlGaAsSb quaternaries lattice matched to GaSb and used for optical confinement in DH lasers,<sup>8,9</sup> higher resistivities should result from H treatment because the H<sup>+</sup> level would lie near the middle of the gap and because the gap is near the band gap of InP,<sup>8,9</sup> making it possible to use these passivated layers for current confinement as in AlGaAs<sup>21</sup> or in InGaAsP.<sup>22</sup>

ACKNOWLEDGMENTS: It is a pleasure to thank Dr. A.G. Braginskaya of the Institute of Rare Metals in Moscow for some of the GaSb samples used in this work. The work at CMU was supported in part by NSF Grant ECS 8915034. The SIMS work was supported by the Army Research Office.

#### References

1. S.J. Pearton, J.W. Corbett, and T.S. Shi, Appl. Phys. **A43**, 153 (1987)
2. J. Chevallier, M. Aucourturier, Ann. Rev. Mater. Sci. **18**, 219 (1988)
3. A.Y. Polyakov, A.V. Pakhomov, M.V. Tishkin, E.M. Omeljanovsky, in SI III-V Materials, Eds. A.G. Milnes and C.J. Milner [Hilger, NY, 1990] p.247
4. A.Y. Polyakov, A.V. Pakhomov, M.V. Tishkin, Solid St. Comm. **74**, 711 (1990)
5. Y.M. Dellesasse, I. Szafranek, Y.N. Baillargeon, N. El-Zein, N. Holonyak, G.E. Stillman, K.Y. Cheng, J. Appl. Phys. **68**, 5866 (1990)
6. M. Mizuta, Y. Mochizuki, N. Takadoh, K. Akasaka, J. Appl. Phys. **66**, 891 (1989)
7. C. Caneau, A.K. Srivastava, A.G. Dentai, J.L. Zyskind, M.A. Pollack, Electron. Lett. **21**, 815 (1985)
8. A.E. Bochkarev, L.M. Dolginov, A.E. Drakin, L.V. Druzhinina, P.G. Eliseev, B.W. Sverdlov, Sov. J. Quantum Electr. **15**, 869 (1985)
9. S.J. Pearton, W.C. Dautremont-Smith, J. Chevallier, et al., J. Appl. Phys. **59**, 2821 (1986)
10. J.M. Zavada, H.A. Jenkinson, R.G. Sarkis, R.G. Wilson, J. Appl. Phys. **58**, 3731 (1985)
11. R.G. Wilson, F.A. Stevie, and C.W. Magee, Secondary Ion Mass Spectrometry, [Wiley, NY, 1990]
12. R.J. Hillard, H.L. Berkowitz, R.G. Mazur, P. Rai-Choudhury, Solid State Technol. **32**, 119 (1989)
13. R.J. Hillard, H.L. Berkowitz, J.M. Heddleson, R.G. Mazur, P. Rai-Choudhury III-V Rev. **3**, N4-5 (1990)
14. A.Y. Polyakov, M. Stam, A.G. Milnes, A.T. Schlesinger, in the abstracts of Electron Materials Conference, Colorado, 26 (1991)
15. W.C. Dautremont-Smith, J. Lopata, S.J. Pearton, et al. J. Appl. Phys. **66**, 1993 (1989)
16. E.M. Omeljanovsky, A.V. Pakhomov, A.Y. Polyakov, Phys. Lett. **A141**, 75 (1989)
17. N. Hasegawa, in SI III-V Materials, Eds. N. Kukimoto and S. Miyazawa [Ohmsha/North Holland, Tokyo/Amsterdam, 1986] p.471
18. M.J. Caldas, A. Fazzio, A. Zunger, Appl. Phys. Lett. **45**, 671 (1984)
19. J. Chevallier, A. Jalil, B. Theys, et al., Mater. Sci. Forum **38-41**, Ed. G. Ferenzi [Trans. Tech. Public., Switzerland, 1988] p.991
20. E.M. Omeljanovsky, A.V. Pakhomov, A.Y. Polyakov, *ibid.*, p.1063
21. G.S. Jackson, N. Pan, M.S. Feng, G.E. Stillman, N. Holonyak, R.D. Burnham, Appl. Phys. Lett. **51**, 1629 (1989)
22. C. Kazmierski, B. Theys, B. Rose, et al., Electron. Lett. **25**, 1433 (1989)

INCORPORATION OF HYDROGEN IN II-VI EPITAXIAL  
LAYERS GROWN BY MOCVD

Y. MARFAING, L. SVOB, H. DUMONT, E. RZEPKA, D. BALLUTAUD  
R. DRUILHE, C. GRATTEPAIN

Laboratoire de Physique des Solides de Bellevue  
CNRS, 1 Place A. Briand F-92195 MEUDON-CEDEX, France

Some properties of hydrogen in II-VI compounds (CdTe, ZnTe) have been previously studied using proton implantation and annealing under H<sub>2</sub> as hydrogenation techniques [1]. We report here several observations about the hydrogen incorporation which occurs during the growth of epitaxial layers by MOCVD.

In common MOCVD techniques the source of hydrogen is twofold : first the carrier gas H<sub>2</sub> which is the main gaseous component in the reactor, second the hydrogen liberated by the pyrolysis of organometallic molecules. It is often difficult to separate these two effects.

The first experiments we report concern the growth of Cd<sub>x</sub>Hg<sub>1-x</sub>Te alloys (x 0.3) by the Interdiffused Multilayer Process at 365°C. The substrate was GaAs (100) covered by a CdZnTe-ZnTe buffer layer. The precursors were Dimethylcadmium, Diisopropyltellurium and elemental mercury. The SIMS profile of Fig. 1 shows a uniform concentration of hydrogen (  $1.5 \times 10^{17} \text{ cm}^{-3}$ ) in the CdHgTe layer. At least a part of this hydrogen comes from the carrier gas as demonstrated in a subsidiary experiment : another sample was grown using a mixture H<sub>2</sub> + D<sub>2</sub> as the carrier gas during a fraction of the growth time ; SIMS analysis shows the corresponding incorporation of deuterium in the material (Fig. 2).

The hydrogen incorporation rate depends on temperature and material doping. Fig. 3 shows that the concentration of hydrogen in CdTe increases by about seven times when the growth temperature decreases from 250°C to 200°C. The effect of doping was revealed by growing an As-doped CdTe layer at 365°C on an undoped CdTe/ZnTe buffer layer and a GaAs substrate. Arsenic was introduced during growth through the decomposition of AsH<sub>3</sub>. The SIMS profiles

in Fig. 4 yield a higher hydrogen concentration in the doped layer compared to the undoped one. The formation of As-H complexes might be anticipated.

The incorporation of hydrogen from the metalorganic precursors was established by performing the growth of ZnTe at 400°C under either H<sub>2</sub> or He carrier gas. The precursors were Diethylzinc and Diethyltellurium. The comparison of the SIMS profiles in Fig. 5 reveals a higher hydrogen concentration in the material when He is used as the carrier gas. Under these conditions a larger carbon incorporation also occurs. The parallel evolution of C and H points out to the introduction of C-H complexes originating from the decomposition of organic molecules.

At last hydrogen effusion experiments have been carried out on CdTe and ZnTe layers grown in H<sub>2</sub> or He carrier gas. Preliminary results yield additional information on the relative quantity of hydrogen incorporated in these different samples.

[1] L. SVOB, A. HEURTEL, Y. MARFAING, J. Crystal Growth 101 (1990) 709 and references therein.

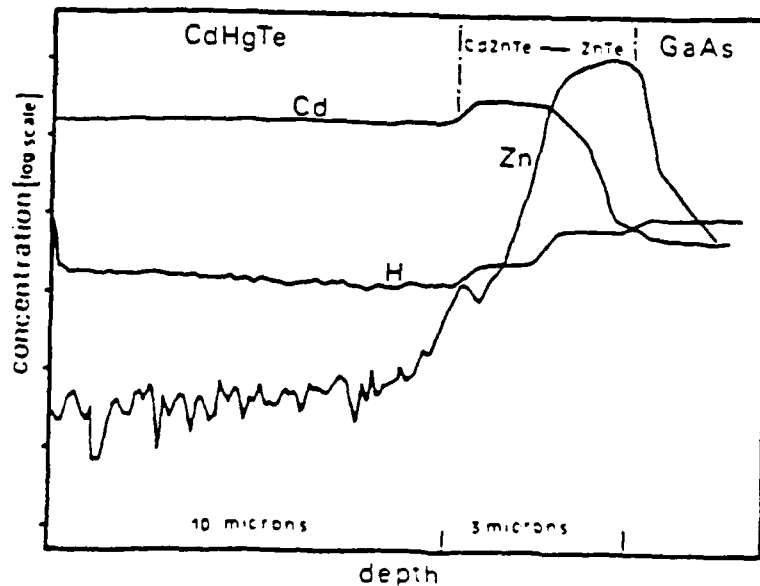


Fig. 1 - The hydrogen concentration profile in a Cd<sub>0.29</sub>Hg<sub>0.71</sub>Te layer grown by the IMP method at 365°C on a CdZnTe-ZnTe graded buffer.

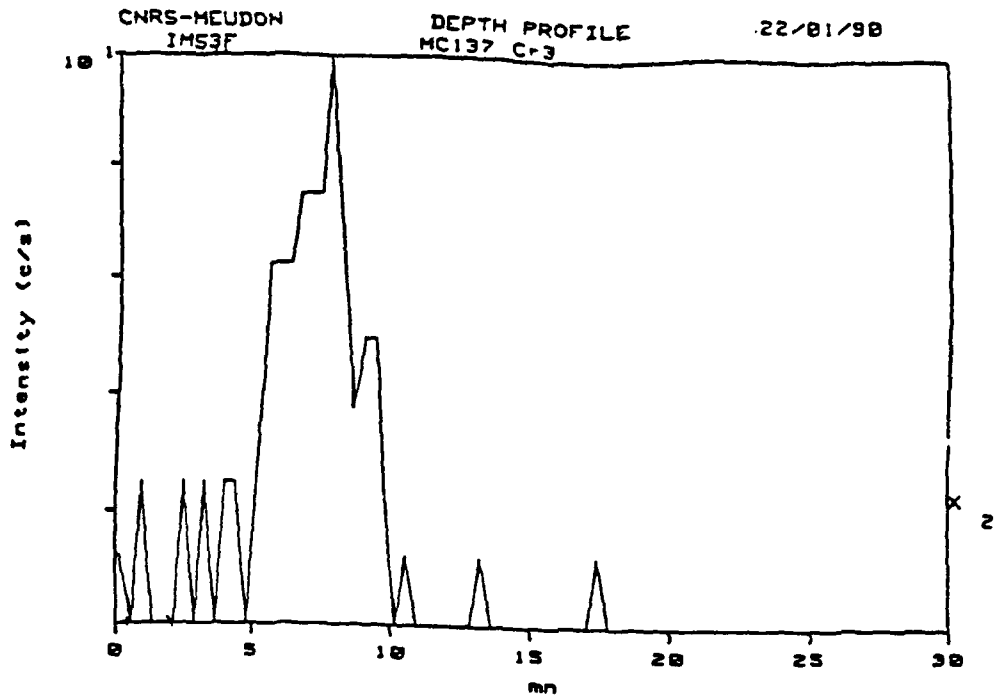


Fig. 2 - SIMS profile of deuterium in a CdHgTe layer grown by MOCVD using a carrier gas containing D<sub>2</sub>.

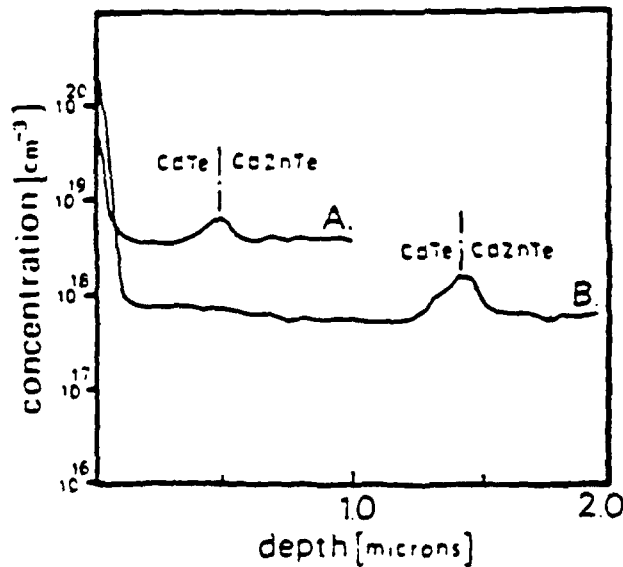


Fig. 3 - Influence of the temperature of growth on the hydrogen concentration in MOCVD grown CdTe layers : A.T = 200°C ; B.T = 250°C.

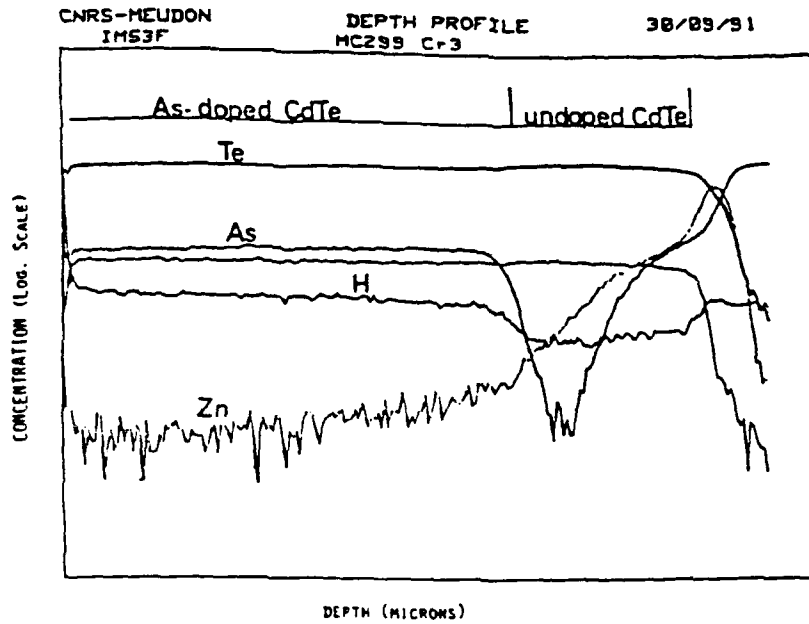


Fig. 4 - SIMS profiles of the constituting elements in an As-doped CdTe layer grown by MOCVD on a undoped CdTe layer and a GaAs substrate with ZnTe buffer.

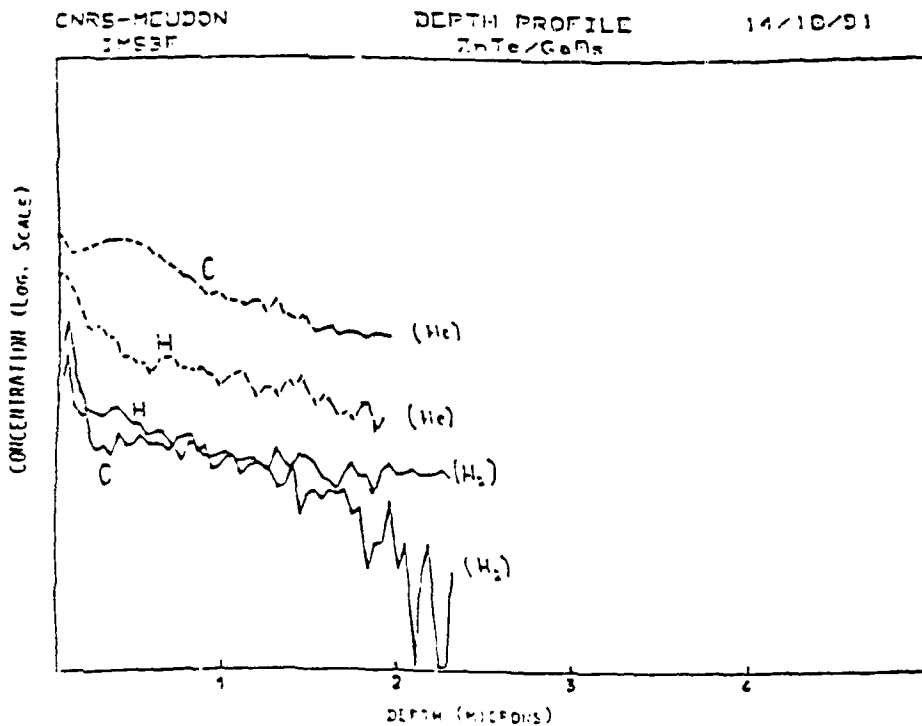


Fig. 5 - SIMS profiles of hydrogen and carbon in two ZnTe layers grown by MOCVD using H<sub>2</sub> and He as carrier gas respectively.

## Comments on Hydrogen in Natural Diamond

B. Dischler

Fraunhofer-Institut für Angewandte Festkörperphysik,  
Tullastrasse 72, D-7800 Freiburg, F.R. Germany

Hydrogen or muonium in diamond has been the subject of experimental [1,2] and theoretical [3] investigations. It is now established that hydrogen and anomalous muonium occupy the bond-centered interstitial (BCI) site in diamond [3]. Eight years ago, when the first detailed infrared absorption spectra were published [1,2], several exceptional features in the spectra were noticed but the natural interpretation by the special properties of the BCI site could not be given at that time. In figure 1 and in table I results from the literature [1,2] are reproduced. In the infrared absorption spectrum broad bands from the first ( $< 1333 \text{ cm}^{-1}$ ), second ( $< 2666 \text{ cm}^{-1}$ ), and third ( $< 4000 \text{ cm}^{-1}$ ) order lattice phonon absorption can be seen on which five sharp local vibrational mode (LVM) absorption lines (see table I) are superimposed. An interesting feature is a weak shoulder on the  $3107 \text{ cm}^{-1}$  line, located at  $3098 \text{ cm}^{-1}$  and arising from  $^{13}\text{C-H}$  [2].

It is reported that some 50 type Ia diamonds all showed the hydrogen LVM spectrum [2]. Detailed measurements showed good correlation between the intensities of the five lines, which evidently arise from a single center [1]. Two exceptional features were noticed for the hydrogen LVM lines in diamond [1]: (i) The frequencies are 5 % higher than expected for ( $\text{sp}^3$ ) C-H vibrations [4,5]. (ii) The intensities of the overtone and combination lines are very high (up to 15 % of the fundamental I) and the anharmonic frequency shifts are relatively large (0.3 to 1.1 %).

The BCI site of hydrogen in diamond provides a natural explanation for the unusual spectrum: (i) The C-H bond length is shorter than in molecules and larger force constants can be expected. (ii) The energy potential surface on which the interstitial hydrogen can move is known to be complex and not of the harmonic type [3]. It should be emphasized that only one bending vibration is observed. This indicates  $\text{C}_{3v}$  symmetry and an on-axis position of the hydrogen along the C-H-C bond in contrast to an off-axis position with  $\text{C}_{2v}$  symmetry and two bending vibrations. The observed line widths (see table I) are larger than for hydrogen in other crystals ( $0.015 - 1.0 \text{ cm}^{-1}$ ). They show very little temperature dependence in the range  $4 < T < 500 \text{ K}$  [1]. This is indicative of inhomogeneous broadening which is expected because the large lattice relaxation around the BCI site [3] makes the center sensitive to nearby lattice imperfections. Note that in a-C:H the hydrogen lines have a temperature independent width of  $75 \text{ cm}^{-1}$  [4].

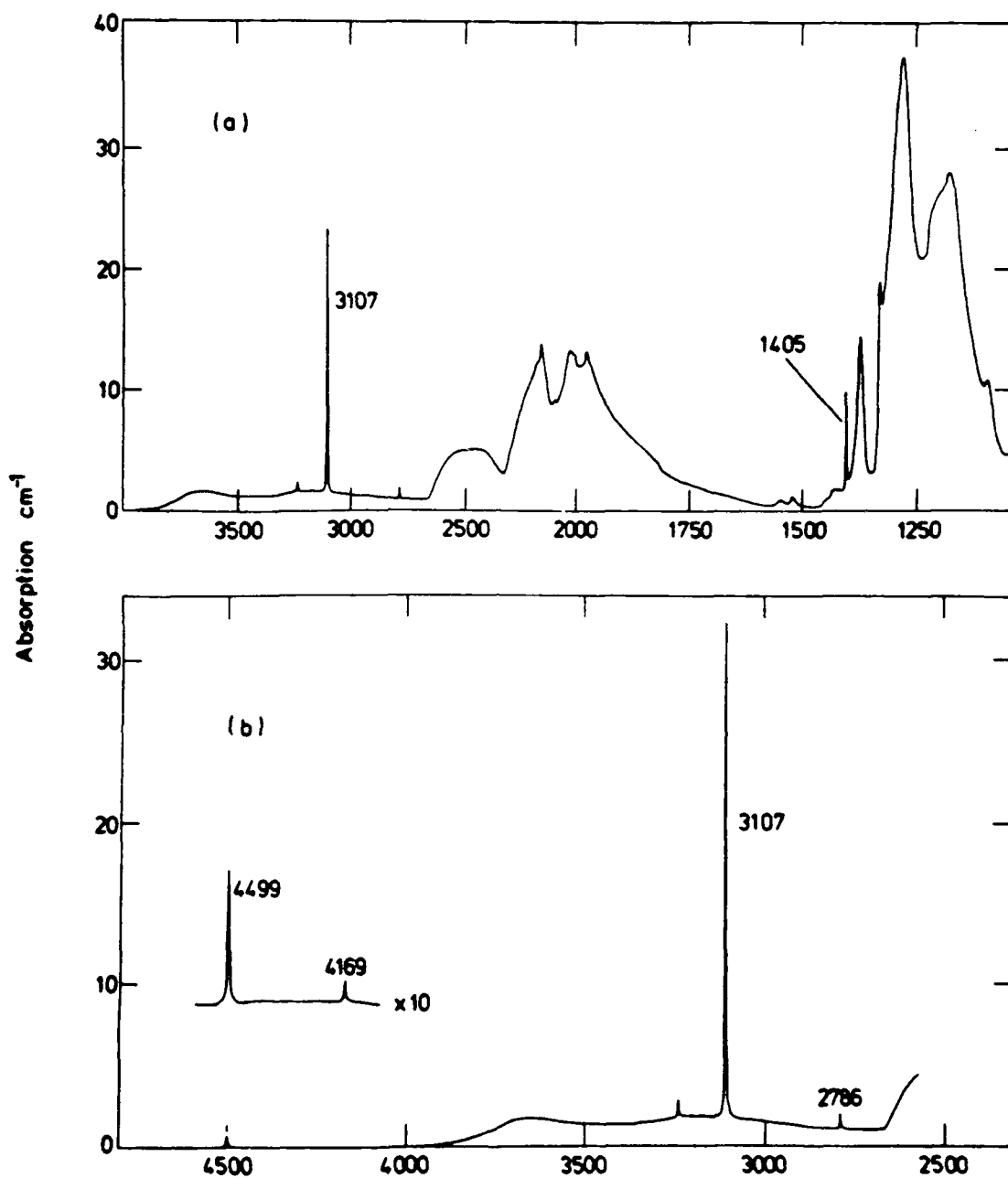


Fig. 1. Absorption lines from hydrogen in diamond measured at 300 K with (a) a standard double beam spectrometer and (b) with a monochromator [1].

Table I

Hydrogen LVM lines observed in natural diamond [1,2] and comparison with amorphous hydrogenated carbon (a-C:H) [4] and a molecule [5].

frequency (cm <sup>-1</sup> )	width (cm <sup>-1</sup> )	intensity ( % )	assignment	corresp. frequency ( cm <sup>-1</sup> )	
				a-C:H	CHD <sub>3</sub>
1405	1.5	20	$\omega_{\text{bend}}$	1370	1299
2786	2.5	3	$2 \omega_{\text{bend}}$	—	—
3098	-	1.4	$\omega_{\text{stretch}}(^{13}\text{C-H})$	—	—
3107	2.9	100	$\omega_{\text{stretch}}(^{12}\text{C-H})$	2920	2992
4169	4.4	0.6	$3 \omega_{\text{bend}}$	—	—
4499	4.8	5	$\omega_{\text{stretch}} + \omega_{\text{bend}}$	—	—

Table II

Analysis of <sup>13</sup>C-H versus <sup>12</sup>C-H isotopic shift in diamond using Eq.(1)

model	$\sigma$	k (10 <sup>6</sup> cm <sup>-2</sup> amu)	rel. intensity (%)
C-H-C (BCI)	0.24	8.9	2.2
C-H	0.99	8.2	1.1

The frequency and intensity of the shoulder at 3098 cm<sup>-1</sup> have been reported and it was assigned to the <sup>13</sup>C-H bond (1.1 % isotopic abundance) [2]. The isotopic frequency shift can be calculated by the familiar formula for LVM vibrations [6,7]:

$$\omega^2 = k \left[ \frac{1}{m} + \frac{1}{\sigma M} \right]. \quad (1)$$

Here  $k$  is the force constant,  $m$  the impurity mass,  $M$  the nearest neighbour mass and  $\sigma$  is an adjustable parameter. Most of the empirical  $\sigma$  values for LVM are between 0.5 and 3.0 [8], while the "ideal" value is  $\sigma = 1$  ( diatomic molecule or lattice TO mode). Inserting the experimental frequencies (3107.1 and 3097.8 cm<sup>-1</sup>) into Eq. (1) yields the  $\sigma$  values and force constants listed in table II. The first line applies to the BCI hydrogen with ligand masses of 24 and 25 while the second line applies if the hydrogen is bonded to one carbon only, as assumed previously [2]. Small  $\sigma$  values are indicative of a ligand relaxation away from the impurity [8], therefore the value 0.24 in table II appears very reasonable for BCI hydrogen. The relative intensity of the shoulder is difficult to determine [2] but the calculated value of 2.2 % is compatible with the observed spectrum. It is interesting to compare the force constants in table II: For the BCI model it is 8.5 % higher because of the larger ligand mass.

During the last years great activities to grow chemical vapour deposited (CVD) diamond have developed [9]. These CVD diamonds contain several percent of hydrogen but the LVM lines from BCI hydrogen are completely missing [10]. Instead C-H stretch absorption spectra similar to those from a-C:H [4] are observed. The question arises whether the different sites for hydrogen in natural or CVD diamond are caused by the different growth conditions or by the different time scales involved.

#### References:

- [1] G. Davies, A.T. Collins and P. Spear, *Solid State Commun.* **49**, 433 (1984).
- [2] G.S. Woods and A.T. Collins, *J. Phys. Chem. Solids* **44**, 471 (1983).
- [3] T.L. Estle, S. Estreicher and D.S. Marynick, *Phys. Rev. Letters* **58**, 1547 (1987) and references therein.
- [4] B. Dischler, in: *Amorphous Hydrogenated Carbon Films*, P. Koidl and P. Oelhafen, eds. (*Proc. Europ. Mat. Rec. Soc. Vol. 17, Les Edit. de Physique, Paris, 1987*) p. 189.
- [5] G. Herzberg, "Molecular Spectra II: Infrared and Raman Spectra of Polyatomic Molecules", (Van Nostrand, Princeton, N.J., 1945).
- [6] R. C. Newman, "Infrared Studies of Crystal Defects" (Taylor & Francis, London, 1973).
- [7] B. Dischler, F. Fuchs and H. Seelewind, *Physica B* **170**, 245 (1991).
- [8] B. Dischler, unpublished.
- [9] J.C. Angus and C.C. Hayman, *Science* **241**, 913 (1988).
- [10] Ch. Wild, N. Herres, J. Wsgner, P. Koidl and T.R. Anthony, *Proc. 1st Int. Symp. on Diamond and diamond-like Films*, ed. J.P. Dismukes, *Electrochem. Soc. Proc.* **89-12** (1989) p.283 and references therein.

## **<sup>2</sup>D INTERACTION WITH ION IMPLANTED AND ANNEALED GALLIUM ARSENIDE**

D.K. Sadana, J.P. de Souza, E.D. Marshall and F. Cardone  
IBM T.J. Watson Research Center  
Yorktown Heights, NY 10598

and

K.M. Jones and M.M. Aljassim  
Solar Energy Research Institute  
Golden, CO 80401

A detailed study of <sup>2</sup>D diffusion from a <sup>2</sup>D plasma into semi-insulating undoped and bulk Si-doped GaAs, and Si<sup>+</sup>, Mg<sup>+</sup> and Be<sup>+</sup> implanted/annealed GaAs was conducted. The GaAs samples were exposed to a <sup>2</sup>D plasma at 300 °C for 15 minutes in a PlasmaTherm system. The samples experienced an additional heat treatment at 300°C for 15 minutes while the plasma chamber was being flushed with N<sub>2</sub>. The following summarises our observations.

**Bulk GaAs :** Figure 1 shows <sup>2</sup>D profiles in semi-insulating undoped,  $2 \times 10^{17} \text{ cm}^{-3}$  and  $2 \times 10^{18} \text{ cm}^{-3}$  Si-doped GaAs. The doped samples showed <sup>2</sup>D levels in proportion to the doping concentrations to depths of  $\approx 0.2 - 0.3 \mu\text{m}$  extending from the the surface. The <sup>2</sup>D level in the undoped sample was  $\lesssim 3 \times 10^{16} \text{ cm}^{-3}$  near the surface and decreased gradually to SIMS detection limit at  $0.3-0.4 \mu\text{m}$ .

**Implanted But Unannealed GaAs :** Figure 2 shows the SIMS profiles of <sup>2</sup>D in GaAs samples implanted with 30 keV Si in the dose range of  $1 - 10 \times 10^{13} \text{ cm}^{-2}$ . High concentrations ( $\approx 10^{20} \text{ cm}^{-3}$ ) of <sup>2</sup>D accumulated in the implanted region. Deeper diffusion of the <sup>2</sup>D occurred in the low dose implanted ( $\lesssim 10^{13} \text{ cm}^{-2}$ ) samples compared to that in the high dose samples. Similar <sup>2</sup>D diffusion behavior was observed for Si<sup>+</sup> and Mg<sup>+</sup> implantations conducted at higher energies (upto 150 keV). Above a certain threshold implant dose which depended on the implant energy, <sup>2</sup>D profiles in all the implanted samples became identical and looked similar to that shown in Fig 2c. In other words, the <sup>2</sup>D distribution had no correspondence with the damage distribution in the implanted region. Similar dose dependence of the <sup>2</sup>D diffusion was further confirmed in Be<sup>+</sup> implanted GaAs samples which were implanted at 5-60 keV in the dose range of  $10^{13} - 5 \times 10^{14} \text{ cm}^{-2}$ . It should noted that none of the implants produced any amorphous layer in the GaAs. The anomaly between the expected damage and observed <sup>2</sup>D distributions in the high dose implanted samples (such as those in Fig 2) occurs because the samples experience  $\geq 30$  minutes anneal at 300 °C during the <sup>2</sup>D plasma experiment. During this time, partial recrystallization of the implantation induced damage can occur. The <sup>2</sup>D distribution in Figs 2b presumably represents the residual damage distribution in the high dose implanted samples.

**Implanted and Annealed GaAs:** Strong n but weak p-carrier passivation was observed when Si<sup>+</sup> and Mg<sup>+</sup> implanted/rapid thermally annealed (850 °C/10s) GaAs samples were exposed to the <sup>2</sup>D plasma. Based on the Hall data from 30 keV /  $4.5 \times 10^{13} \text{ cm}^{-2}$  and 120 keV /  $1.0 \times 10^{14} \text{ cm}^{-2}$  Si<sup>+</sup> implanted samples, the passivation effect was more pronounced ( $\geq 80\%$ ) for the shallow implant compared to the deep implant ( $\approx 50\%$ ). In contrast, in the 120 keV /  $1.0 \times 10^{14} \text{ cm}^{-2}$  Mg<sup>+</sup> implanted/RTA samples no significant passivation occurred after the plasma exposure. In both the Si<sup>+</sup> and Mg<sup>+</sup> implanted/annealed samples XTEM revealed a similar damage distribution, i.e., a discrete layer of dislocation loops centered around the mean projected range of the ion (Figs 3 and 4). The <sup>2</sup>D interaction with the loops was also found to be anomalous. The concentration of the <sup>2</sup>D in the implanted region in the case of Mg<sup>+</sup> was an order of magnitude higher than that in the case of Si<sup>+</sup> (Fig 4b). The <sup>2</sup>D distribution in the Si<sup>+</sup> implanted sample closely resembled with that of the n-carrier profile of the sample (Fig 3ii). In the Mg<sup>+</sup> implanted sample <sup>2</sup>D profile showed no resemblance with the p-carrier profile. Furthermore,  $\geq 80\%$  of the <sup>2</sup>D diffused away from the Si implanted/RTA samples during a heat treatment at 350 °C after the plasma exposure and this was accompanied by reactivation of the n-carriers. However, the <sup>2</sup>D in the Mg implanted/RTA samples remained pinned in the implanted region even after a heat treatment of 850 °C/10s.

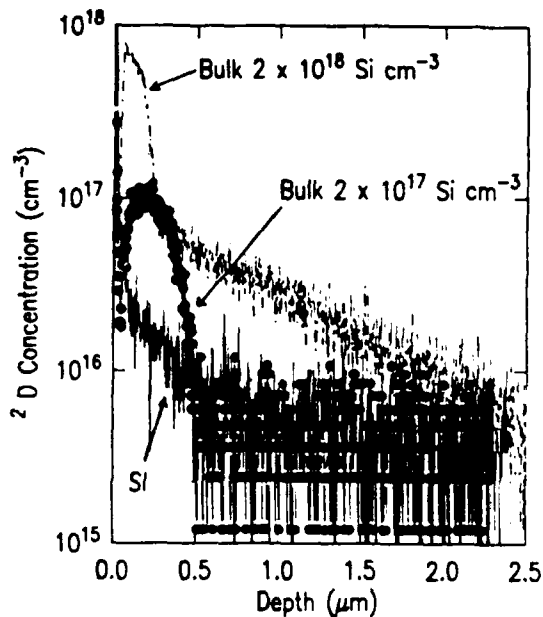


FIG. 1.  $^2\text{D}$  SIMS profiles in undoped and bulk Si-doped GaAs after the  $^2\text{D}$  plasma exposure.

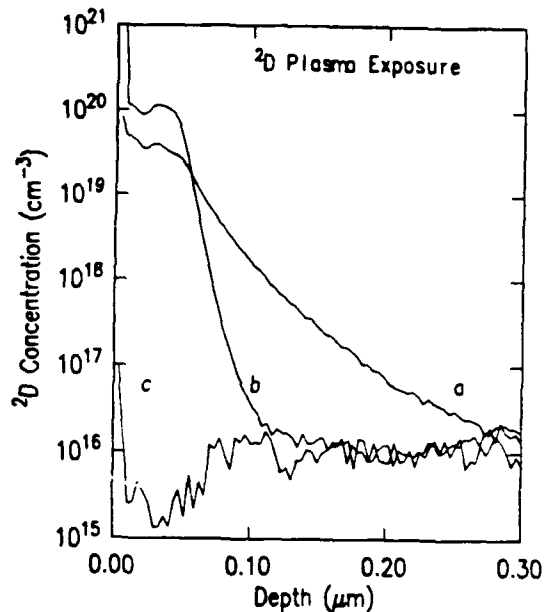


FIG. 2.  $^2\text{D}$  SIMS profiles in the GaAs samples with (a)  $\text{Si}^+$ , 30 keV,  $1.0 \times 10^{13} \text{ cm}^{-2}$ , (b)  $\text{Si}^+$ , 30 or 120 keV,  $1.0 \times 10^{13} \text{ cm}^{-2}$ , and (c) no implant (virgin). All samples were unannealed.

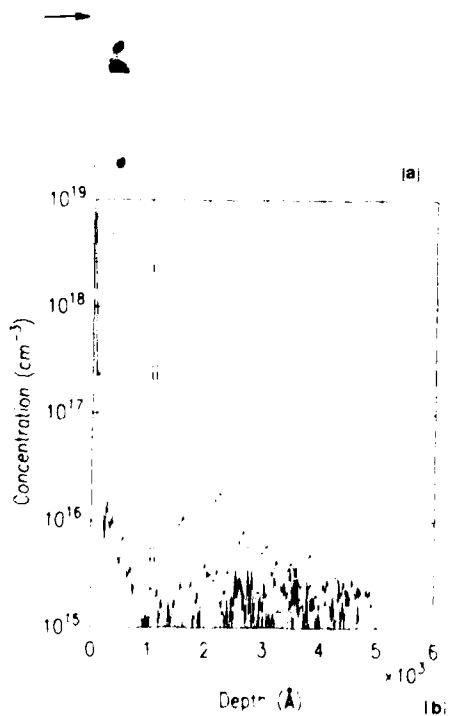


FIG. 3. GaAs sample implanted with  $^{29}\text{Si}$ , 30 keV,  $4.5 \times 10^{13} \text{ cm}^{-2}$  and subsequently annealed at  $850^\circ\text{C}/10\text{s}$ . (a) an XTEM micrograph showing the distribution of dislocation loops, (b) the corresponding SIMS profiles of  $^{29}\text{Si}$  (i) and  $^2\text{D}$  (ii) from the sample, and  $^2\text{D}$  profile after a  $350^\circ\text{C}/10\text{min}$  anneal (iii).

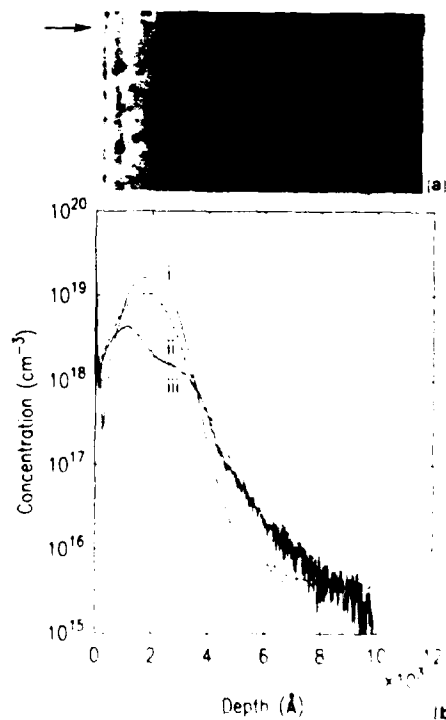


FIG. 4. GaAs sample implanted with Mg, 120 keV,  $1.0 \times 10^{13} \text{ cm}^{-2}$  and subsequently annealed at  $850^\circ\text{C}/10\text{s}$ . (a) an XTEM micrograph showing the distribution of dislocation loops and (b) the corresponding SIMS profiles of  $^2\text{D}$  (i) and Mg (ii) from the annealed sample. Also included in (b) is the Mg profile (iii) from the unannealed sample.

**OPTICAL WAVEGUIDES in GaAs CRYSTALS FORMED BY HYDROGEN INTERACTIONS**

J. M. ZAVADA, Army Research Office, RTP, NC, USA

B. L. WEISS, I. V. BRADLEY, University of Surrey, Guildford, GU2 5XH, UK

B. THEYS, J. CHEVALLIER, R. RAHBI, CNRS-LPSB, Meudon, France

R. ADDINALL, R. C. NEWMAN, IRC-Semiconductor Materials,  
Imperial College, London, SW7 2BZ, UK

H. A. JENKINSON, Army ARDEC, Dover, NJ, USA

In general, the effect of charge carriers in a semiconductor crystal is to lower the refractive index and to increase the optical absorption at frequencies below the absorption edge of the material. Optical waveguides based on carrier reduction have been studied for a number of years and experiments have shown good agreement with models based on a Drude term for the carrier contribution to the refractive index. Garmire et al. reported the use of proton implantation in bulk, Si-doped, n-type GaAs crystals to form such optical waveguides [1]. They observed that after implantation optical losses were very high, in excess of 200 Db/cm, and attributed these losses to damage effects. These losses could be reduced by thermal annealing to levels on the order of 3 Db/cm. However, the damage caused by ion implantation has been a major concern in the formation of carrier reduced waveguides and thermal annealing procedures have not always been reproducible.

Several years ago Chevallier et al. reported that atomic hydrogen in n-type GaAs can passivate Si donors leading to measurable electrical changes [2]. Since then a number of experiments have established that either atomic hydrogen (H) or atomic deuterium (D) is able to passivate a variety of shallow donors and acceptors in crystalline GaAs and other III-V semiconductors [3]. Attempts have been made to utilize this passivation technique in the processing of field effect transistors as well as laser structures. The changes in the optical properties of doped semiconductors due to the introduction of atomic hydrogen are not as well established.

Plasma hydrogenation of GaAs wafers is a relatively simple process that is compatible with conventional masking techniques. The damage to the GaAs crystal as a result of plasma exposure is expected to be significantly less than that due to ion implantation. Consequently, plasma hydrogenation of GaAs crystals may be a useful method for fabricating optical waveguides provided that appropriate optical effects can be achieved.

In this presentation we describe the results of several experiments concerning the changes produced in the refractive index of Si doped, p-type GaAs epilayers after exposure to a deuterium plasma. The epilayers used in these experiments were grown on n<sup>+</sup>-GaAs crystal substrates using conventional, slow-cooling, liquid phase epitaxy (LPE). Under such growth conditions, material grown below a certain critical temperature is p-type. The total concentration of Si atoms in the epilayers was

approximately  $2 \times 10^{19} \text{ cm}^{-3}$  and the conductivity at the surface was p-type with the carrier level at  $7 \times 10^{18} \text{ cm}^{-3}$ . Due to the LPE growth technique, the surfaces of the epilayers were not very smooth and subsequent efforts were required to remove the surface imperfections.

Two attempts were made to passivate the surface regions through plasma treatment. In the first case, the epilayer samples were polished prior to plasma treatment using a mechanical technique to obtain a smooth surface for the optical measurements. The resulting surface had good optical quality but microscopic damage and defects could not be avoided. Three such samples were exposed to a capacitive RF deuterium plasma with a power density of  $0.18 \text{ W cm}^{-2}$  for a period of ninety minutes. Processing temperatures were chosen to produce passivated layers similar to those that had been previously investigated using SIMS and electrical measurements [4]. This attempt was not successful and the samples failed to show the existence of passivated surface regions. In the second case, the epilayer samples were treated with a chemical etch to remove the surface imperfections. While the overall surface smoothness of these samples was not as good as in the first case, these samples did exhibit passivated surface regions.

Infrared reflectivity measurements were made on both sets of samples. With the first set of samples, the ones polished using a mechanical method, no regular fringe pattern could be discerned in the spectra. Based on these measurements, it was concluded that the passivation of the acceptors was weak and did not extend very deep into the samples.

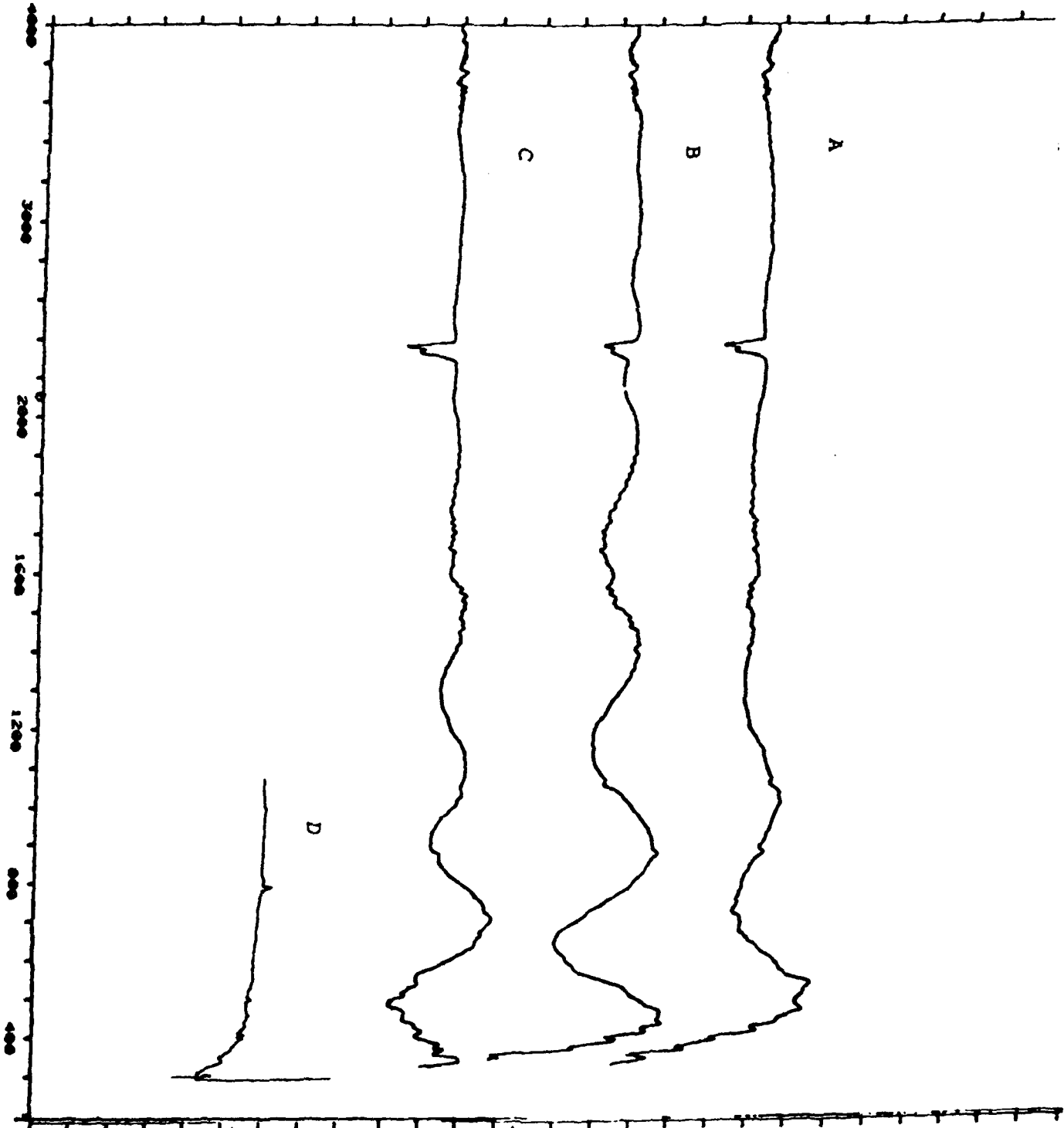
The second set of samples (A, B, C), the ones treated with a chemical etch, provided a definite set of fringes, as shown in Fig. 1. From the fringe patterns the thicknesses of the passivated layers in the three samples were calculated to be 2.7, 2.9 and 4.0  $\mu\text{m}$ . The degree of passivation in these samples was estimated by comparing the spectra with a computer simulation. The fringe amplitudes in the plasma-treated samples were about half of the corresponding ones in the simulation indicating that nearly 60% of the acceptors had been passivated.

Secondary ion mass spectrometry (SIMS) analyses were performed on the samples after the reflectivity measurements. The SIMS D depth profiles for the first set of samples showed that there was a large accumulation of D at the surface. Apparently, the mechanical polishing introduced numerous microscopic surface defects which formed trapping centers for the migrating atomic D and impeded the atoms from penetrating deeper into the epilayer. Deuterium that did pass through the surface damage region formed a plateau at a concentration comparable to the carrier level.

The SIMS D depth profiles for the samples prepared with the chemical etching method did not display any major accumulation at the surface and the depth of their plateaux are in good agreement with prior results [4]. The plateau concentrations were at the carrier level in these samples and the measured depths were 2.15, 2.80 and 3.80  $\mu\text{m}$ . These depths compare reasonably well with the thicknesses determined by infrared reflectivity, except for sample A. This sample, which had the poorest surface quality, showed very few fringes in its reflectivity spectrum.

The samples of the first set were below the cut-off condition and no attempt was made to couple laser radiation into these epilayers.

REFLECTIVITY  
(ARB. UNITS)



Following the reflectivity measurements, samples from the second set were cleaved to provide specimens with smooth end-faces for laser coupling experiments.

Waveguide losses were measured at wavelengths of 1.15 and 1.523  $\mu\text{m}$  for both TE and TM polarizations, using low power, stabilised HeNe lasers. Each of the samples in the second set provided light confinement at the shorter wavelength of 1.15  $\mu\text{m}$ . While both TE and TM modes were observed, waveguide losses were high. As expected, these losses were observed to decrease with increasing processing temperatures due to an associated increase in the passivated layer thickness. Losses in sample C, which contained a 4  $\mu\text{m}$  thick passivated layer, were on the order of 35 dB/cm for either the TE or TM mode which is considerably less than that reported for unannealed, proton implanted samples [1].

These experiments represent the first successful effort to form optical waveguides in III-V compound semiconductors using plasma passivation of dopant atoms. The D plasma treatment of Si-doped, p-GaAs has been shown to yield passivated surface regions of sufficient thickness and with large enough increases in the refractive index to guide laser radiation at wavelengths of 1.15 and 1.523  $\mu\text{m}$ . The optical changes can be measured by infrared reflectivity and correlate well with SIMS D depth profiles. The data from these two measurements can be effectively utilized to predict the waveguide characteristics of the passivated regions.

#### ACKNOWLEDGEMENTS

Portions of this work were supported by the European Research Office of the US Army and by the UK Science and Engineering Research Council. The authors wish to thank M. C. Boissy (R. T. C. Caen, France) for the samples used in this study and C. Grattepain (CNRS-Meudon) for performing the SIMS measurements.

#### REFERENCES

- [1] E. Garmire, H. Stoll, A. Yariv and R. G. Hunsperger, *Appl. Phys. Lett.* 21 87 (1982).
- [2] J. Chevallier, W. C. Dautrement-Smith, C. W. Tu and S. J. Pearton, *Appl. Phys. Lett.* 47 108 (1985).
- [3] J. Chevallier, B. Clerjaud and B. Pajot, in Hydrogen in Semiconductors, J. I. Pankove and N. M. Johnson (Eds.), "Semiconductors and Semimetals" (Academic Press Inc., Orlando, 1990).
- [4] J. Chevallier, B. Pajot, A. Jalil, R. Mostefaoui, R. Rahbi and M. C. Boissy, *Mat. Res. Soc. Symp.*, Vol. 104 337 (1988).

## **HYDROGEN PLASMA DEVICES FABRICATION AND PERFORMANCE**

**N. NG CHING HING, E. CONSTANT, P. GODTS**

**Centre Hyperfréquences et Semiconducteurs, U.A CNRS N°287  
Université des Sciences et Techniques de Lille Flandres Artois  
59655 VILLENEUVE D'ASCQ CEDEX - France**

### **ABSTRACT**

When n-type GaAs and AlGaAs are exposed to a hydrogen plasma, the free carrier concentration drops down and this is accompanied by an increase in resistance. In this paper we will describe the use of these phenomena in the technological process of field-effect-transistors : MESFET, TEGFET and MISFET, and also for the realization of IMPATT and Avalanche diodes. In the first part, the use of hydrogen passivation in the realization of these devices will be described and the performances will be discussed. In the second part, we will show the perspective of hydrogen plasma in circuit design. Lastly, the different problems that still have to be solved will be presented.

*(Extended Abstract for the Workshop on Hydrogen Migration and the Stability of Hydrogen Related Complexes in Crystalline Semiconductors, Horben bei Freiburg, Germany, 3 - 6 November 1991)*

## **Thermal Effusion as an Analytical Tool for Hydrogen Bonding in Crystalline Silicon and Germanium**

M. Stutzmann, E. Bustarret<sup>1)</sup>, J.-B. Chevrier<sup>2)</sup>, P. de Mierry<sup>3)</sup>

Max-Planck-Institut für Festkörperforschung, Heisenbergstr. 1, D-7000 Stuttgart 80,  
Germany

<sup>1)</sup> CNRS-LEPES, POB 166X, F-38042 Grenoble, France

<sup>2)</sup> Lab. Phys. Interfaces et Couches Minces, Ecole Polytechnique, F-91128 Palaiseau, France

<sup>3)</sup> Lab. Phys. Solides, CNRS, F-92195 Meudon, France

Thermally programmed desorption of hydrogen (or deuterium) from hydrogenated semiconductor surfaces or hydrogenated thin films of amorphous semiconductors has been widely used to study the different thermal stability of hydrogen in these materials. Thus, hydrogenated Si(111) surfaces as a function of hydrogen coverage show two effusion maxima at  $\approx 350^\circ\text{C}$  and  $\approx 500^\circ\text{C}$  assigned to di- and monohydride bonding configurations, respectively [1]. Also, a quite detailed understanding of hydrogen binding and diffusion energies in hydrogenated amorphous silicon has been obtained via effusion studies [2]. Here, we apply this technique to hydrogen-plasma-treated crystalline silicon and germanium with different doping levels and types of dopants, exposed to a D or H plasma at different temperatures.

Thermal desorption of deuterium from plasma-exposed crystalline silicon occurs at three distinct temperatures:  $\approx 350^\circ\text{C}$ ,  $\approx 450^\circ\text{C}$ , and  $\approx 500^\circ\text{C}$ . The corresponding bonding states of H or D have been assigned to surface dihydrides, interstitial molecules, and surface or bulk monohydrides [3]. The relative fractions of the different bonding states are found to depend strongly on a number of parameters [3,4]: (i) bulk doping level and type of dopant (ii) sample temperature during plasma treatment (iii) post-passivation anneals (iv)

pre- and post-passivation surface etching (v) pre-existing defects (e.g. dislocations, ion bombardment). Figures 1 - 3 show the dependence of the effusion spectra on the plasma-passivation temperature for *p*-type, intrinsic, and *n*-type silicon. The main features are the increase of the monohydride peak with increasing temperature for *n*-type Si, the changes in the effusion peak position of *p*-type Si for temperatures above 200°C, and the decrease of the total amount of evolved deuterium in intrinsic material with increasing temperature.

Apart from the characteristic temperature,  $T_M$ , of the effusion peaks for a fixed heating rate, information about the thermal stability of the different hydrogen configurations can be obtained from the dependence of the peak temperature on the linear heating rate,  $\beta = dT/dt$ , which is commonly used in effusion experiments. An example of this dependence for *p*-type silicon is shown in Fig. 4. Quantitative estimates for the desorption activation energy,  $E_D$ , can be deduced from a plot of  $\ln(\beta/T_M^2)$  versus  $1/T_M$ , giving values of  $E_D = 0.75$  eV and  $E_D = 1.4$  eV for the low and high temperature effusion peaks in Fig. 4.

Fig. 5 summarizes the effects of chemical etching on the effusion spectra of undoped *c*-Si which was treated in a  $D_2$ - plasma at 300°C. Without chemical etching, the effusion of  $D_2$ -molecules ( $m=4$ ) occurs in a single peak at about 450°C. Chemical etching after plasma passivation greatly reduces this effusion peak, showing that most of the deuterium was concentrated in a thin surface layer, in agreement with SIMS depth profiles. Etching prior to passivation, on the other hand increases the solubility of D, most likely because of the creation of additional surface defects capable of forming strong Si-D bonds. Also shown in Fig. 5 is the effusion of HD ( $m=3$ ) molecules. These are formed when evolved deuterium atoms react with residual hydrogen and can be used to address the question of atomic deuterium desorption.

Finally, we present in Fig. 6 the effusion spectra of  $D_2$  from plasma-treated *p*-type germanium, which occurs at lower temperatures compared to silicon (100-400°C versus 300-600°C). Contrary to *p*-type silicon, the total amount of deuterium desorbed from *p*-type germanium decreases strongly with increasing plasma treatment temperature, and resembles more the behavior observed for undoped silicon. This finding will be discussed in comparison to the low efficiency for shallow acceptor passivation in *p*-type germanium.

## References

1. G. Schulze, M. Henzler, Surf. Sci. **3**, 1 (1972).
2. W. Beyer, Physica B **170**, 105 (1991).
3. M. Stutzmann, M.S. Brandt, J. Appl. Phys. **68**, 1406 (1990).
4. M. Stutzmann, J.-B. Chevrier, C.P. Herrero, A. Breitschwerdt, Appl. Phys. A **53**, 47 (1991).

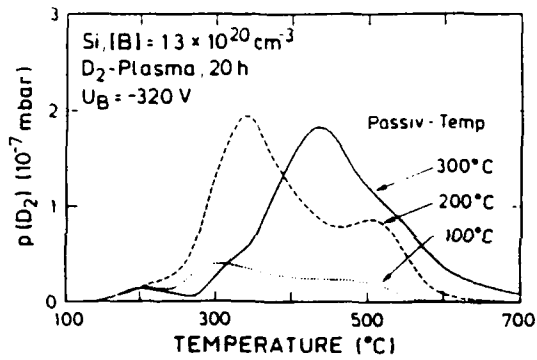


Fig.1: Deuterium effusion spectra for p-type silicon plasma-passivated at different temperatures.

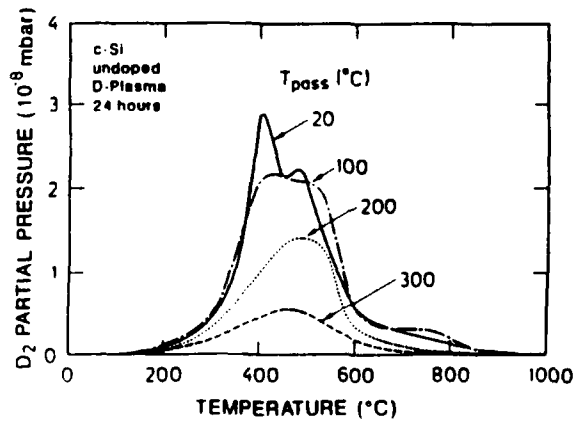


Fig.2: Same as Fig.1, but for undoped Si.

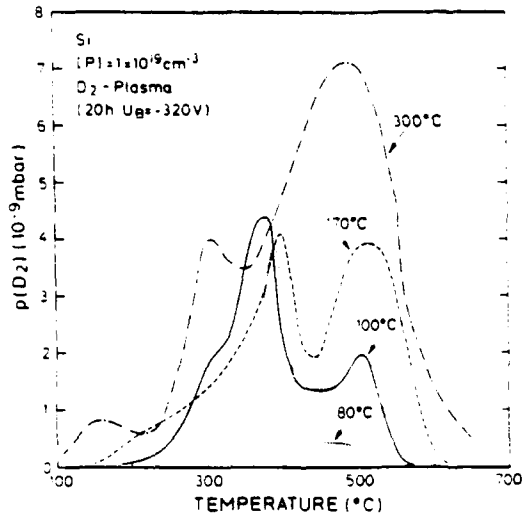


Fig. 3: Same as Fig. 1, but for n-type silicon.

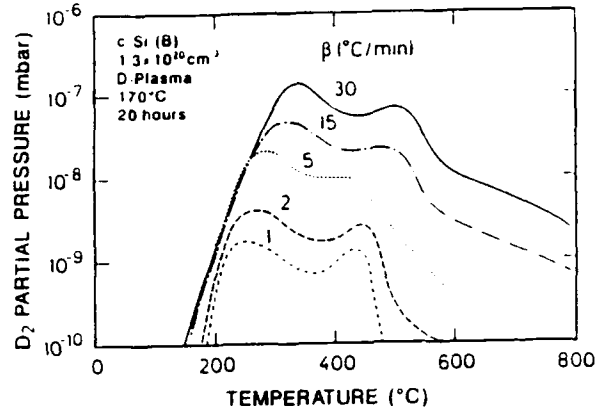


Fig. 4: Deuterium effusion spectra of p-type Si measured with different heating rates,  $\beta$ .

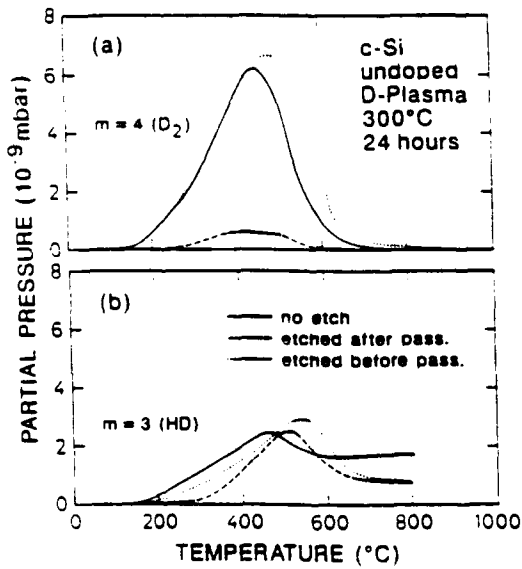


Fig. 5: Influence of chemical etching on the effusion spectra of  $D_2$  and HD molecules in undoped Si.

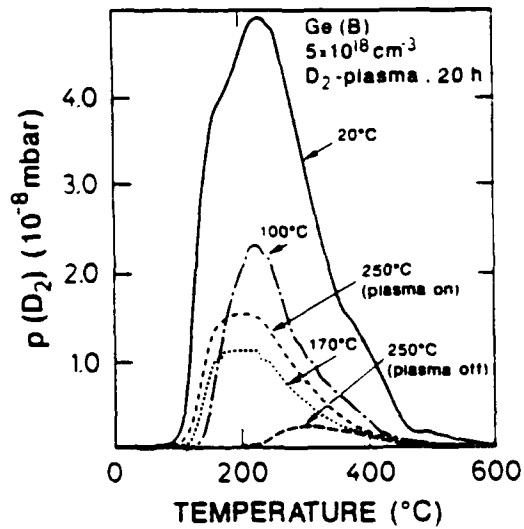


Fig. 6: Deuterium effusion of p-type germanium.

## Hydrogenation of SiGe/Si Layered Structures

K. L. Wang, V. Arbet-Engels, J. S. Park, and M. A. Kallel

Device Research Laboratory, University of California, Los Angeles, CA 90024

### Summary

#### Hydrogenated $\text{Si}_m\text{Ge}_n$ Superlattices

The concept of zone folding in 1974 by Gnutzmann et al. [1] indicates that the minimum of the conduction band of an indirect bandgap semiconductor can be folded back to the  $\Gamma$  point through the use of an artificial periodicity. However, with the growth of alternate Si and Ge layers to form a superlattice (SL), no experimental evidence of direct band gap transitions has been demonstrated. At UCLA, we have investigated the effect of hydrogen passivation on the photoluminescence (PL) spectra of Si-rich SL's. These SL's were grown at low temperature by molecular beam epitaxy (MBE). The structure consists of a 2  $\mu\text{m}$  thick  $\text{Si}_{1-x}\text{Ge}_x$  relaxed buffer layer on which the SL is grown. The SL is made of 80 periods of  $m$  Si monolayers and  $n$  Ge monolayers and is symmetrically strained with the average Ge concentration in the superlattice matched to that in the buffer layer. Transmission electron micrographs (TEM) show layered SL's with a low dislocation density. However, due to its strain relaxation, the buffer contains a high density of misfit dislocations located near the Si/ $\text{Si}_{1-x}\text{Ge}_x$  interface. A typical PL spectrum of a  $16 \times 4$  ( $m \times n$ ) SL is shown in Fig. 1, along with the PL spectra of the passivated sample under different hydrogenation conditions. For the as-grown sample, we observe the transverse optical (TO) phonon assisted boron bound exciton luminescence line at 1.093 eV, a sharp peak at 1.023 eV and a broad spectrum or background luminescence at lower energies attributed to point defects and dislocations in the buffer layer [2]. After passivation, only two well defined peaks remain from the original spectrum. The broad background luminescence almost completely disappears and a new line at 0.962 eV, a 61 meV lower in energy than the narrow line, emerges. This line corresponds to the phonon replica of the 1.023 eV peak. The main peak is seen to have its apparent intensity slightly reduced upon hydrogenation. Nevertheless, after subtracting the background PL signal from the as-grown spectrum, the relative intensity of the sharp peak is in fact increased. It can be seen more obviously on Fig 2 where we show the PL spectra

of a  $12 \times 4$  SL for both the as-grown and H-annealed cases. The phonon replica with an energy difference of 58 meV ( $12 \times 4$ ) from the main feature is well resolved following the hydrogen treatment. The increase in PL intensity upon passivation is attributed to a reduction of the density of recombination centers due to defects, leading to an improved yield or intensity of the superlattice peaks. In order to investigate the re-activation of the passivated defects, we annealed the samples in  $N_2$  at  $350^\circ\text{C}$ ,  $450^\circ\text{C}$ , and  $550^\circ\text{C}$  for time periods of 30 min. The spectra are shown in Fig. 3 for the  $16 \times 4$  SL. For the three temperatures, we observe a decrease in the PL intensity peak at 1.023 eV. The resurgence of the background luminescence does not permit the identification of the phonon replica. The broad background luminescence signal does not completely recover after annealing. However,  $N_2$  annealing has probably a dominant effect on the luminescence even if most of the passivated defects are reactivated after  $N_2$  annealing above  $400^\circ\text{C}$ .

This result demonstrated that hydrogenation is selective means in distinguishing defect- and band gap-related luminescence signals.

### Hydrogenation of $\delta$ -doped Si Layers

The hydrogen compensation and the neutralization of acceptors by atomic hydrogen have been exploited for new device applications. Towards this goal, the effect of hydrogen passivation on intersubband absorption of boron  $\delta$ -doped Si layers was also investigated. The samples used in this study consist of a sequence of 35 Å heavily boron doped Si layers followed by a 300 Å undoped Si spacers, repeated ten times [3]. The structures are grown in a Si MBE chamber on a  $p^-$  substrate which is used in order to reduce free carrier absorption from the substrate. Two samples, A and B, are doped to the densities of  $4 \times 10^{20} \text{ cm}^{-3}$  and  $7 \times 10^{19} \text{ cm}^{-3}$ , respectively. The measured absorption spectra of sample A versus the photon energy after several different hydrogenation time periods (10, 30, 60, and 90 min.) are shown on Fig. 4. The absorption peak originates from transitions between the holes subbands in the  $\delta$ -doped potential well. After a H plasma exposition for 60 min, the peak intensity decreases by approximately 30 %. In addition, the absorption spectra shifts to lower energies as the hydrogenation time period is increased. The shift to the lower energy side is due to a decrease of the active dopant density in the  $\delta$ -layers, resulting in a shallower potential well. This assertion is supported by the observation of the absorption spectra of sample B with a lower doping

density shown on Fig. 5. After only ten minutes of H exposition, the absorbance decreases considerably. These observations suggest that the H atoms are trapped with the acceptors and neutralize the holes, effectively reducing the doping concentration, and that the transition energy is a function of the density of only those acceptors which are not bounded to H atoms in the potential wells. After a hydrogenation for 90 minutes, no detectable absorption is measured for both samples but a new peak at about 230 meV (or  $1870\text{ cm}^{-1}$ ) emerges. This peak may be ascribed to the Si-H stretching motion of the B-H complex [4] and thus confirms the passivation of the boron atoms. This statement was directly supported by SIMS analysis where perfect correlation between H and B atoms was observed. In order to study the re-activation of the passivated acceptors, we annealed the samples in a  $\text{N}_2$  backfilled standard furnace at  $300\text{ }^\circ\text{C}$  for several time periods. The resulting spectra are shown on Fig. 6. Upon annealing, the absorption peak increases and the energy transition shifts to the higher energy side, towards its initial value. The dissociation of the B-H complexes occurs during the annealing and the H atoms subsequently outdiffuse from the sample. The dissociation activation energy was estimated using a simple first order kinetics model. We obtained an activation energy of  $1.9 \pm 0.1\text{ eV}$ , about  $0.2\text{ eV}$  higher than those reported for 3-dimensional (3-D) systems. The 2-D system in our case may account for the difference from the 3-D case. More work needs to be done to assess the difference in activation energy between the  $\delta$ -doped Si layers and bulk Si.

In conclusion, atomic hydrogen is shown to alter the effective dopant density in  $\delta$ -doped Si multiple quantum wells. These results may be used to tailor intersubband absorption process. In addition, the deactivation of specific layered regions may be of interest for the isolation of quantum devices.

**Acknowledgement:** The work was in part supported by ARO.

## References

- [1] U. Gnutzmann and K. Clausecker. *Appl. Phys.*, 3, 9, 1974.
- [2] R. Sauer, J. Weber, J. Stolz, E. R. Weber, K.-H. Küsters, and H. Alexander. *Appl. Phys. A*, 36, 1, 1985.
- [3] J. S. Park, R. P. G. Karunasiri, Y. J. Mii and K. L. Wang. *Appl. Phys. Lett.*, 58(10), 1083, 1991.
- [4] J. I. Pankove, P. J. Zanzucchi, C. W. Magee, and G. Lucovsky. *Appl. Phys. Lett.*, 46(4), 421, 1985.

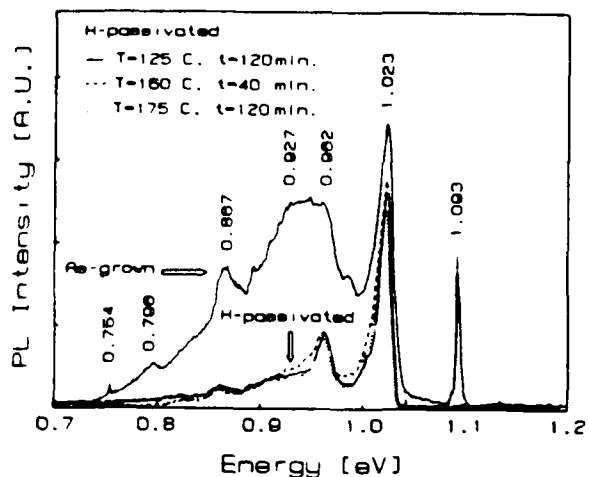


FIG. 1 As-grown and hydrogenated photoluminescence spectra of a  $16 \times 4$  superlattice. Hydrogenated spectra for three different temperatures and times are represented:  $125^\circ\text{C}$  for 20 min,  $160^\circ\text{C}$  for 40 min, and  $175^\circ\text{C}$  for 120 min.

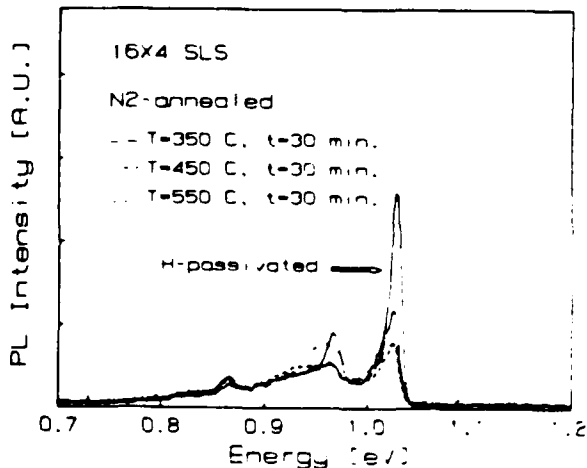


FIG. 3 Annealed spectrum of a  $16 \times 4$  superlattice to remove H. Three different annealing conditions are used:  $350^\circ\text{C}$  for 30 min,  $450^\circ\text{C}$  for 30 min, and  $550^\circ\text{C}$  for 30 min. Also, the passivated spectrum is plotted for comparison.

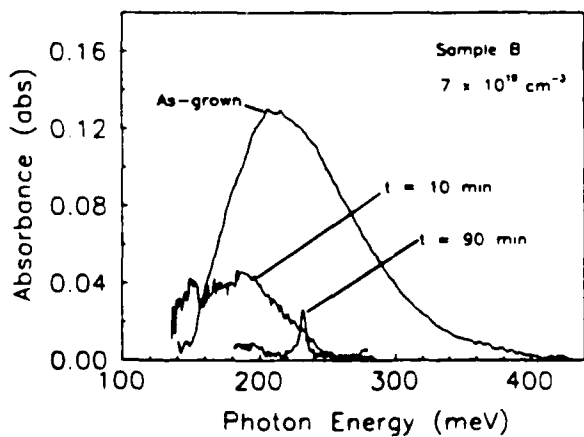


Fig. 5 Absorption spectra for sample B taken after different hydrogenation time periods.

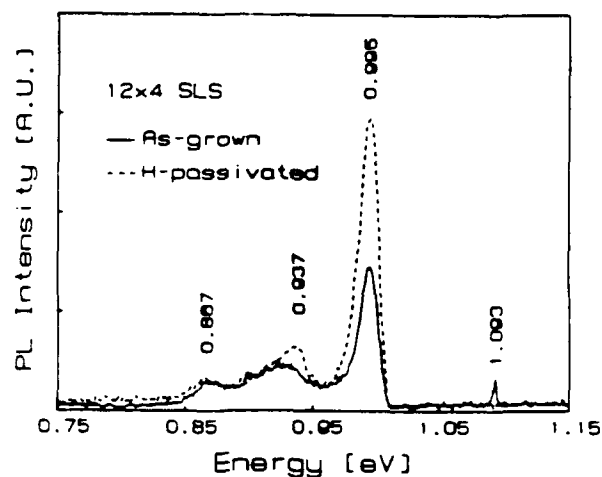


FIG. 2 As-grown and hydrogenated photoluminescence spectra of a  $12 \times 4$  superlattice. The superlattice was passivated for 120 min at  $175^\circ\text{C}$ .

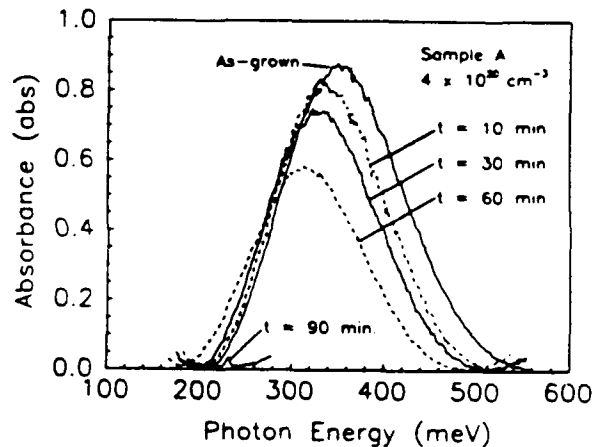


Fig. 4 Absorption spectra for sample A taken after different hydrogenation time periods.

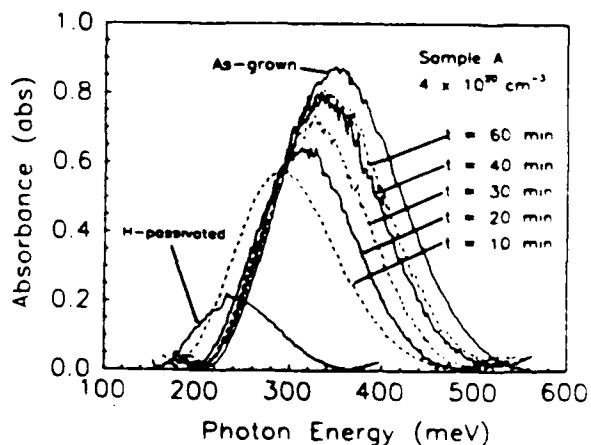


Fig. 6 Absorption spectra for sample A taken after different periods.

EFFECTS OF HYDROGEN ON THE PHOTOLUMINESCENCE OF Si-DOPED  
GaAs/AlGaAs MULTIPLE QUANTUM WELLS

F. VOILLOT, N. LAURET, INSA, Toulouse, France

R. G. WILSON, Hughes Research Labs, Malibu, CA, USA

J. M. ZAVADA, Army Research Office, RTP, NC, USA

B. THEYS, CNRS-LPSB, Meudon, France

By now it is well known that atomic hydrogen is able to passivate shallow impurities in crystalline semiconductors [1]. Hydrogen neutralization of donor and acceptor atoms has been exploited for new device applications including field effect transistors and solid state lasers. Passivation of deep levels by hydrogenation has also been observed and leads to an increase in luminescence efficiency in InP compounds [2]. However, the effects of hydrogen on the electronic and optical properties of two dimensional systems, such as multiple quantum wells (MQW) and superlattices (SL), has received attention only recently. Studies on the photoluminescence properties of GaSb/AlSb MQW [3] and SiGe SL [4] have been made and indicate a similar improvement in the luminescence signal. The purpose of the present work is to extend these results by investigating the effect of hydrogen on the optical properties of Si-doped GaAs/AlGaAs MQW structures.

In these experiments a set of GaAs/AlGaAs MQW samples grown by molecular beam epitaxy (MBE) have been studied. Here we report the results from two samples in this set. Each sample was grown on a semi-insulating GaAs substrate beginning with an undoped GaAs epilayer about 250 nm thick. The MQW structure consisted of alternated layers of AlGaAs barriers, with Al mole content of 0.3, and GaAs wells. The thickness of the barriers  $L_b$  was 12.5 nm and that of the wells  $L_z$  was 15 nm. The cycle was repeated 63 times to produce a MQW region approximately  $1.73 \mu\text{m}$  thick and capped with a GaAs layer. A Si doping spike was introduced during MBE growth in the wells for sample #324 and both in the wells and barriers for sample #325. The doping spike was about 5 nm thick with a doping level of  $5 \times 10^{15} \text{ cm}^{-3}$ .

The photoluminescence (PL) characteristics of similar samples have been previously reported by Shanabrook and Comas [5]. They found that the binding energies of the donor impurities increased due to the spatial confinement and reached a maximum when the dopant spike was located at the center of the well. PL measurements that were made of the current samples showed good agreement with the prior results.

Each sample was broken into smaller pieces and specimens were exposed to a RF deuterium plasma operating at low power density ( $0.04 \text{ W cm}^{-2}$ ) in order to limit irradiation damage. Two different hydrogenation conditions were studied. The first one, D1193, was for 90 min exposure with the samples at  $240^\circ\text{C}$ , the second, D1189, for 360 min exposure with the samples at  $200^\circ\text{C}$ .

Photoluminescence (PL) measurements on the hydrogenated samples and on their untreated partners were made at 4.2 K using the 700 nm line of a pyridine II dye laser that was pumped by an Ar cw laser operating at 514 nm. The luminescence was dispersed by a 0.85 m double spectrometer at a spectral resolution of 0.4 meV and detected by a cooled GaAs cathode PMT. The excitation power was varied from  $20 \text{ mW cm}^{-2}$  to  $20 \text{ W cm}^{-2}$ .

Typical spectra before and after the two hydrogenation treatments for samples #324 are shown in Fig.1. The excitation power was changed to separate the effect of hydrogen on the impurity related line, that saturates at high excitation power, from the free exciton line that does not. In most of the samples, some changes in the peak position were observed, probably due to inhomogeneity either in the average well thickness or the Al content in the barriers. In some cases, Fig. 1b, we observed the exciton lines of the GaAs buffer layer which indicates that deuterium has reached the buffer layer and has improved its optical quality too.

One of the main results from the PL measurements is that there is a decrease in the FWHM of the free exciton line from 9 meV to 5 meV at high excitation power. This effect is due to a reduction in the low energy side of the peak, which is particularly noticeable at low excitation power where the contributions of the free exciton and the impurity related peaks are more clearly separated. There is also an inversion of the ratio of the free exciton line to the impurity related line, which again is more visible at low excitation power. Furthermore, we observe an increase in the intensity of the exciton line after hydrogenation. This effect is much larger in the case of the D1189 hydrogenation which was done at a lower temperature.

Secondary ion mass spectrometry (SIMS) measurements of the MQW samples were made following the PL measurements. A CAMECA IMS-3f machine was used and D, Al, Si depth distributions were obtained. The absolute D concentration was determined using a  $\text{D}^+$  implanted GaAs sample as a standard. The error on the D concentration is estimated to be about 20% and the uncertainty in the microprofilometer measured depth is 7%. SIMS depth profiles for sample #324 are shown in Fig. 2. For the low temperature hydrogenation, D1189, the D level is almost constant throughout the MQW region at a level of  $4 \times 10^{18} \text{ cm}^{-3}$ . The D profile in the substrate is similar to those generally observed in diffusion of hydrogen in GaAs [1] except for a large accumulation of D at the buffer layer/substrate interface. Such an accumulation of diffusing D has been previously observed in D implanted MQW structures [6]. With the high

temperature hydrogenation, D1193, we observe a diffusion profile for D, at a lower concentration, in the MQW region as well as in the GaAs buffer. An accumulation of D is also found at the buffer/substrate interface in this sample.

In conclusion, we have observed in our GaAs/AlGaAs MQW samples optical changes similar to those reported in the GaSb/AlSb MQW and SiGe SL studies. There is an increase in the luminescence efficiency and a diminution of impurity related peaks. This process could be used as a method to improve the quality of the MQW structures for device applications. After hydrogenation there is a large, narrow free exciton PL peak which is generally regarded as the signature of a good quality sample material. Our experiments also point out the problem of proper hydrogenation conditions. Changes in these conditions can drastically alter the D diffusion profiles. So, while initial concentrations and location of impurities are important parameters, the time and temperature of hydrogenation, as seen in our results, need to be selected carefully.

#### ACKNOWLEDGMENT

The authors wish to thank J. Comas (NIST, Gaithersburg, MD) for the MQW samples used in this study.

#### REFERENCES

- [1] J. Chevallier, B. Clerjaud and B. Pajot, in Hydrogen in Semiconductors, J. I. Pankove and N. M. Johnson (Eds.), "Semiconductors and Semimetals" (Academic Press Inc., Orlando, 1990).
- [2] V. Swaminathan, J. Lopata, S. E. G. Slusky, W. C. Dautremont-Smith, and S. J. Pearton, Defect Control in Semiconductors (K. Sumino, ed.) 879 (1990).
- [3] M. Capizzi, C. Coluzza, A. Forchel, and A. Frova, Superlatt. and Microstructures 5, 297 (1989).
- [4] V. Arbet-Engels, M. A. Kallel, and K. L. Wang, submitted to Appl. Phys. Lett. (1991).
- [5] B. V. Shanabrook and J. Comas, Surface Sci. 142, 504 (1984).
- [6] J. M. Zavada, R. G. Wilson and J. Comas, J. Appl. Phys. 65, 1968 (1989).

324

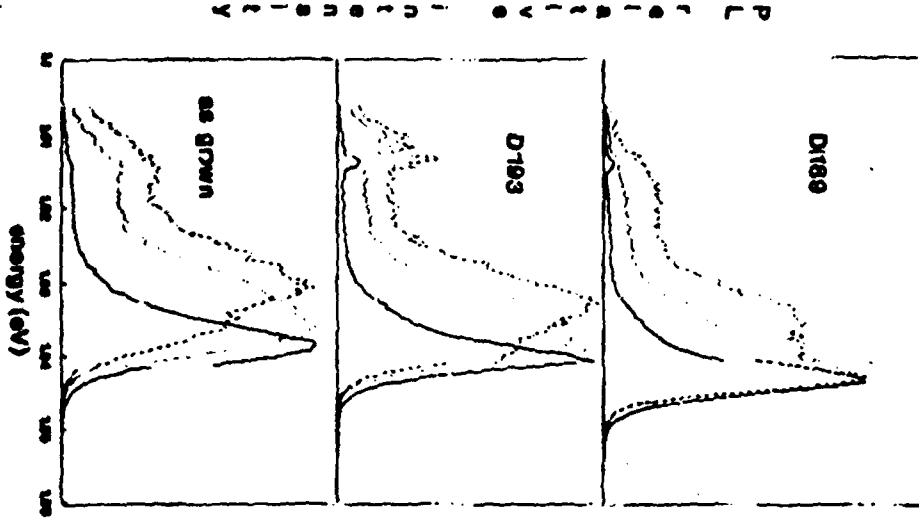


Figure 1

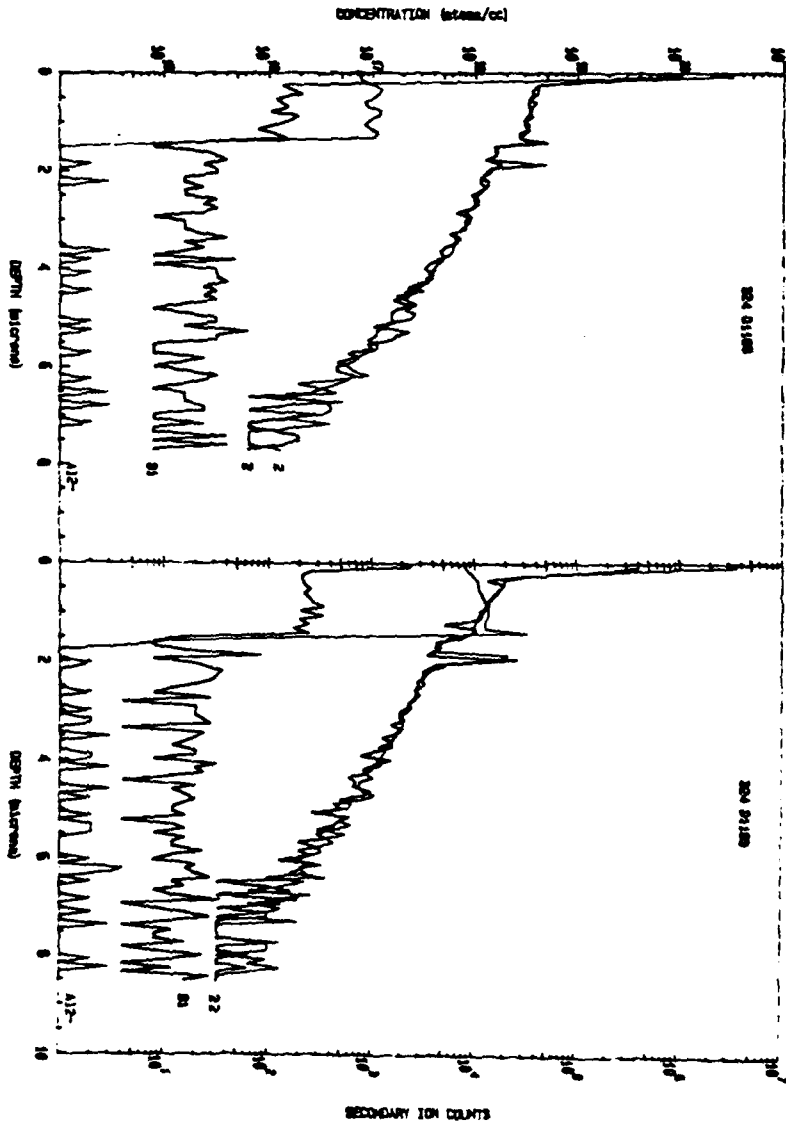


Figure 2

AUTHOR INDEX

Abernathy C. R.	1	Machayekhi B.	58
Achtziger N.	37	Magerle R.	33
Addinall R.	81	Maier M.	5
Aljassim M. M.	79	Marfaing Y.	71
Amore Bonapasta A.	53	Marshall E. D.	79
Arbet-Engels V.	90	Mathiot D.	54
Bachem K. H.	5	McQuaid S. A.	42
Ballutaud D.	71	Meng Xian-ti	20
Bao X. J.	67	Milnes A. G.	67
Baurichter A.	37	Newman R. C.	42, 81
Bech Nielsen B.	16	Ng Chung Hing N.	85
Bernauer M.	13	Oberg S.	9, 10
Binns M. J.	42	Pajot B.	30, 31
Bonde Nielsen K.	16	Park J. S.	90
Bradley I. V.	81	Pearton S. J.	1, 67
Bustarret E.	86	Pensl G.	26
Cardone F.	79	Pfeiffer W.	33
Chevallier J.	58, 81	Polyakov A. Y.	67
Chevrier J.-B.	86	Porte C.	63
Clerjaud B.	63	Prescha Th.	46
Constant E.	85	Pross P.	33
Corbett J. W.	24	Rahbi R.	81
Côte D.	63	Rai-Choudhuri P.	67
Darwich R.	30, 31	Rzepka E.	71
Deák P.	24	Sadana D. K.	79
Deicher M.	33	Schlesinger T. E.	67
de Mierry P.	86	Seager C. H.	61
de Souza J. P.	79	Skudlik H.	33
Dischler B.	75	Snyder L. C.	24
Druilhe R.	71	Song C.	30, 31
Dumont H.	71	Stam M.	67
Endrös A. L.	13	Stavola M.	1
Forkel D.	37	Stolz P.	26
Gebhard M.	37	Stutzmann M.	86
Godts P.	85	Svob L.	71
Grattepain C. M.	58, 71	Theys B.	58, 81, 94
Hahn W.-S.	63	Tucker J. H.	42
Heinrich M.	24	Ulrici W.	63
Hillard R. J.	67	Umerski A.	9
Hobson W. S.	1	Van de Walle C.	41
Holm B.	16	Vogt B.	37
Jenkinson H. A.	81	Voillot F.	94
Johnson N. M.	50	Wagner J.	5
Jones K. M.	79	Wang K. L.	90
Jones R.	9, 10	Wasik D.	63
Kallel M. A.	90	Weber J.	46
Keller R.	33	Weiss B. L.	81
Kozuch D. M.	1	Wichert Th.	33
Lang M.	26	Wilson R. G.	67, 94
Lauret N.	94	Witthuhn W.	37
Lauterbach Th.	5	Zavada J. M.	67, 81, 94
Leitch A. W. R.	46	Zundel T.	46